

Demystifying Variational Diffusion Models

Fabio De Sousa Ribeiro

Imperial College London

f.de-sousa-ribeiro@imperial.ac.uk

Ben Glocker

Imperial College London

b.glocker@imperial.ac.uk

Contents

1	Introduction	2
2	Latent Variable Models	4
2.1	Variational Autoencoder	5
2.2	Hierarchical Latent Variable Models	8
2.3	Generative Feedback	10
2.4	Top-down Inference	12
2.5	The W[H]ole Problem	15
3	Variational Diffusion Models	16
3.1	Forward Process: Gaussian Diffusion	20
3.2	Linear Gaussian Transitions	23
3.3	The Top-down Posterior	24
3.4	Reverse Process: Discrete-Time Generative Model	28
3.5	Generative Transitions	30
3.6	Variational Lower Bound	31
3.7	Estimator of the Discrete-Time Diffusion Loss	34
3.8	Reverse Process: Continuous-Time Generative Model	36
3.9	On Infinite Depth	37
3.10	Estimator of the Continuous-Time Diffusion Loss	39

4 Understanding Diffusion Objectives	42
4.1 Model Parameterizations	44
4.2 Translating Loss Parameterizations	52
4.3 Invariance to the Noise Schedule	55
4.4 Weighted Diffusion Loss	57
4.5 Noise Schedule Density	59
4.6 Importance Sampling Distribution	61
4.7 ELBO with Data Augmentation	64
5 Discussion & Outlook	71
Acknowledgements	77
 Appendices	 78
A Notation & Extras	79
A.1 Notation	79
A.2 Learning the Noise Schedule	82
A.3 Numerically Stable Primitives	83
A.4 Equivalence of Diffusion Specifications	87
References	89

Demystifying Variational Diffusion Models

Fabio De Sousa Ribeiro¹ and Ben Glocker²

¹*Imperial College London; f.de-sousa-ribeiro@imperial.ac.uk*

²*Imperial College London; b.glocker@imperial.ac.uk*

ABSTRACT

Despite the growing interest in diffusion models, gaining a deep understanding of the model class remains an elusive endeavour, particularly for the uninitiated in non-equilibrium statistical physics. Thanks to the rapid rate of progress in the field, most existing work on diffusion models focuses on either applications or theoretical contributions. Unfortunately, the theoretical material is often inaccessible to practitioners and new researchers, leading to a risk of superficial understanding in ongoing research. Given that diffusion models are now an indispensable tool, a clear and consolidating perspective on the model class is needed to properly contextualize recent advances in generative modelling and lower the barrier to entry for new researchers. To that end, we revisit predecessors to diffusion models like hierarchical latent variable models and synthesize a holistic perspective using only directed graphical modelling and variational inference principles. The resulting narrative is easier to follow as it imposes fewer prerequisites on the average reader relative to the view from non-equilibrium thermodynamics or stochastic differential equations.

1

Introduction

A generative model is a simulation of a data-generating process. Understanding the true generative process of data is valuable as it naturally reveals the causal relationships in the world. These causal relationships are advantageous as they tend to generalize more effectively to new situations than mere correlations, which may be spurious and unreliable. Generative modelling typically consists of using data from observations of \mathbf{x} to estimate the marginal distribution $p(\mathbf{x})$. Knowing $p(\mathbf{x})$ facilitates many useful tasks, such as: (i) sample generation, (ii) density estimation, (iii) compression, (iv) data imputation, (v) model selection, etc. As $p(\mathbf{x})$ is typically unknown and/or intractable, we often have to approximate it with a model $p_{\theta}(\mathbf{x}) \approx p(\mathbf{x})$, by optimizing some parameters θ . Although various generative modelling strategies exist, diffusion models (Sohl-Dickstein et al., 2015; Ho et al., 2020) have emerged as the latest dominant paradigm. With that said, gaining a deep understanding of the model class remains an elusive endeavour, particularly for the uninitiated in non-equilibrium statistical physics.

Thanks to the rapid rate of progress in the field, existing work on diffusion models focuses on either applications or theoretical contributions. However, research material on diffusion is often inaccessible to

practitioners and new researchers. Given that diffusion models are now an indispensable tool, we argue that a clear, consolidating perspective on the model class is needed to properly contextualize recent advances in generative modelling and lower the barrier to entry. To that end, we revisit predecessors to diffusion models like hierarchical latent variable models (HLVMs) (Salimans et al., 2015; Valpola, 2015; Sønderby et al., 2016), and synthesize a holistic perspective using *only* directed graphical modelling and variational inference principles. The resulting narrative is easier to follow as it imposes fewer prerequisites on the reader relative to the view from non-equilibrium thermodynamics (Sohl-Dickstein et al., 2015) or stochastic differential equations (SDEs) (Song et al., 2021b,a). Other variational perspectives on diffusion have been studied (Huang et al., 2021; Kingma et al., 2021; Vahdat et al., 2021), but their expositions are optimized for technical and empirical contributions to the model class rather than accessibility. A notable exception is the technical review by Luo (2022); however, our account is far more comprehensive, covers a lot more recent material, and is more mathematically consistent with the seminal works in the field (Kingma et al., 2021; Kingma and Gao, 2023).

We begin our exposition by revisiting deep latent variable models (Kingma and Welling, 2013; Rezende et al., 2014) and their hierarchical counterparts (§2). We then highlight the difficulties with bottom-up inference procedures for even modestly deep hierarchies and present a compelling argument in favour of the *top-down* hierarchical model using a concept called *generative feedback* (§2.3). This contrasts with prior work (Burda et al., 2015; Luo, 2022), which offers an incomplete efficiency-based view. We then show that the top-down hierarchy is ubiquitous in both classical HLVMs (Valpola, 2015; Sønderby et al., 2016; Kingma et al., 2016) and diffusion models. We explain how both model classes share optimization objectives and offer an intuitive understanding of diffusion models as a specific instantiation of HLVMs with top-down inference. In §2.5, we reproduce the *hole problem* in LVMs, explain how diffusion models overcome it by construction, and stress its importance for sample quality. In §3, we provide a comprehensive account of modern diffusion models from the top-down hierarchy perspective, and in §5, we conclude with a forward-looking discussion.

2

Latent Variable Models

A latent variable model is a statistical model that connects observable variables to a set of unobserved (i.e., latent) variables. The core assumption is that the data are generated by a random process involving these unobserved variables, which capture the underlying structure of the data. This approach often simplifies analysis by reducing data dimensionality, uncovering hidden patterns, and enhancing interpretability. Latent variable models are widely used to identify and model latent factors that influence observed phenomena, thereby improving our ability to understand, predict, and draw inferences from complex data.

A basic example of a latent variable model is the Gaussian Mixture Model (GMM), which posits that data are generated from a mixture of multiple Gaussian distributions, each representing a different latent component or cluster. The assumed data-generating process is simple: (i) a cluster (i.e., latent mixture component) is selected at random from a finite set; (ii) a data point is drawn from the corresponding Gaussian distribution. GMMs are useful density estimators as the Gaussianity assumption admits tractable closed-form solutions, enabling efficient computation of the marginal likelihood $p(\mathbf{x})$ and parameter estimation using methods like the Expectation-Maximization (EM) algorithm.

The advent of deep learning has given rise to *deep* latent variable models, which leverage neural networks to capture more complex, non-linear relationships between observed and latent variables. These models, including Variational Autoencoders (VAEs) and diffusion models, have gained prominence for their ability to model high-dimensional data, generate realistic synthetic samples, and discover intricate underlying structures in ways that traditional models previously struggled to. In the following sections, we will cover the necessary fundamentals of VAEs and hierarchical latent variable models, which will form the foundation of our exposition on variational diffusion models.

2.1 Variational Autoencoder

Variational autoencoders (Kingma and Welling, 2013) assume that data $\mathbf{x} \in \mathcal{X}^D$ are generated by some random process involving an unobserved random variable $\mathbf{z} \in \mathcal{Z}^K$. The generative process is straightforward:

- (i) sample a latent variable from a prior distribution $\mathbf{z} \sim p(\mathbf{z})$;
- (ii) sample an observation from a conditional distribution $\mathbf{x} \sim p(\mathbf{x} \mid \mathbf{z})$.

If we choose \mathbf{z} to be a discrete random variable and $p(\mathbf{x} \mid \mathbf{z})$ to be a Gaussian distribution, then $p(\mathbf{x})$ is a Gaussian mixture. If we instead choose \mathbf{z} to be a continuous random variable, then the marginal distribution of \mathbf{x} represents an *infinite* mixture of Gaussians, and is given by marginalizing out the latent variable: $p(\mathbf{x}) = \int p(\mathbf{x}, \mathbf{z}) d\mathbf{z}$.

For complicated non-linear likelihood functions, where $p(\mathbf{x} \mid \mathbf{z})$ is parameterized by a deep neural network for example, integrating out the latent variable \mathbf{z} to compute $p(\mathbf{x})$ has no analytic solution, so we must rely on approximations. A straightforward Monte Carlo approximation of $p(\mathbf{x})$ is certainly possible:

$$p(\mathbf{x}) = \mathbb{E}_{\mathbf{z} \sim p(\mathbf{z})} [p(\mathbf{x} \mid \mathbf{z})] \approx \frac{1}{N} \sum_{i=1}^N p(\mathbf{x} \mid \mathbf{z}_i), \quad \mathbf{z}_1, \dots, \mathbf{z}_N \stackrel{\text{iid}}{\sim} p(\mathbf{z}), \quad (2.1)$$

but is subject to the *curse of dimensionality*, since the number of samples needed to properly cover the latent space grows exponentially with the dimensionality of the latent variable \mathbf{z} .

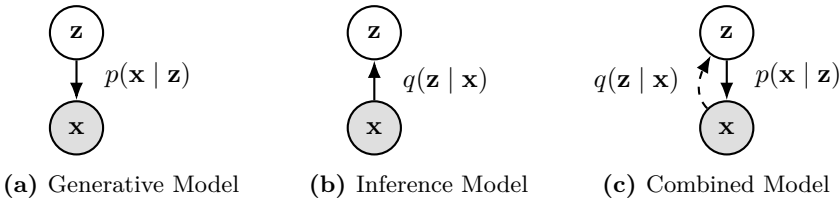


Figure 2.1: Probabilistic graphical model of a latent variable model (e.g. variational autoencoder). Directed arrows represent the assumed flow of conditional dependencies or causal influence between variables.

Alternatively, we can turn to *variational* methods, which pose probabilistic inference as an optimization problem (Jordan et al., 1999). The first thing to note is that the intractability of $p(\mathbf{x})$ is related to the intractability of the true posterior over the latent variable $p(\mathbf{z} | \mathbf{x})$ through a basic identity:

$$p(\mathbf{x}) = \frac{p(\mathbf{x} | \mathbf{z})p(\mathbf{z})}{p(\mathbf{z} | \mathbf{x})}, \quad \text{where} \quad p(\mathbf{z} | \mathbf{x}) = \frac{p(\mathbf{x} | \mathbf{z})p(\mathbf{z})}{\int p(\mathbf{x} | \mathbf{z})p(\mathbf{z}) d\mathbf{z}}. \quad (2.2)$$

Using a complicated neural network-based likelihood renders the integral on the right-hand side (RHS) intractable. To estimate $p(\mathbf{x})$ we can approximate the true posterior $p(\mathbf{z} | \mathbf{x})$ via a parametric inference model $q(\mathbf{z} | \mathbf{x})$ of our choice, such that $q(\mathbf{z} | \mathbf{x}) \approx p(\mathbf{z} | \mathbf{x})$. Learning a single function with shared variational parameters ϕ to map each datapoint \mathbf{x} to a posterior distribution $q(\mathbf{z} | \mathbf{x})$ is known as *amortized inference*. Alternatively, optimizing distinct variational parameters for each individual datapoint \mathbf{x} is equally valid, more expressive, but much less efficient, as it typically involves a per-datapoint optimization loop known as *coordinate-ascent* variational inference.

We may optionally write $q_\phi(\mathbf{z} | \mathbf{x})$ and $p_\theta(\mathbf{x} | \mathbf{z})$ to explicitly state that these are parametric distributions realized by an encoder-decoder setup with variational parameters ϕ and model parameters θ . The typical VAE setup specifies a prior $p(\mathbf{z})$ with no learnable parameters, and it is often chosen to be standard Gaussian: $p(\mathbf{z}) = \mathcal{N}(\mathbf{z}; \mathbf{0}, \mathbf{I})$. It is important to note that unlike the latent variable(s) \mathbf{z} which are *local*, the parameters $\{\phi, \theta\}$ are *global* since they are shared for all datapoints.

To improve our approximation, we would like to minimize the Kullback-Leibler (KL) divergence $\arg \min_{q(\mathbf{z} | \mathbf{x})} D_{\text{KL}}(q(\mathbf{z} | \mathbf{x}) \| p(\mathbf{z} | \mathbf{x}))$

(see [Rezende \(2018\)](#) to learn why), but it is not possible do so directly as we do not have access to the true posterior $p(\mathbf{z} \mid \mathbf{x})$ for evaluation.

VAEs maximise the Variational Lower Bound (VLB) of $\log p(\mathbf{x})$:

$$D_{\text{KL}}(q(\mathbf{z} \mid \mathbf{x}) \parallel p(\mathbf{z} \mid \mathbf{x})) = \int q(\mathbf{z} \mid \mathbf{x}) \log \frac{q(\mathbf{z} \mid \mathbf{x})}{p(\mathbf{z} \mid \mathbf{x})} d\mathbf{z} \quad (2.3)$$

$$= \mathbb{E}_{q(\mathbf{z} \mid \mathbf{x})} \left[\log q(\mathbf{z} \mid \mathbf{x}) - \log \frac{p(\mathbf{x}, \mathbf{z})}{p(\mathbf{x})} \right] \quad (2.4)$$

$$= \mathbb{E}_{q(\mathbf{z} \mid \mathbf{x})} [\log q(\mathbf{z} \mid \mathbf{x}) - \log p(\mathbf{x}, \mathbf{z})] + \log p(\mathbf{x}) \quad (2.5)$$

$$= -\text{VLB}(\mathbf{x}) + \log p(\mathbf{x}), \quad (2.6)$$

now adding $\text{VLB}(\mathbf{x})$ to both sides reveals:

$$D_{\text{KL}}(q(\mathbf{z} \mid \mathbf{x}) \parallel p(\mathbf{z} \mid \mathbf{x})) + \text{VLB}(\mathbf{x}) = \log p(\mathbf{x}) \quad (2.7)$$

$$\implies \text{VLB}(\mathbf{x}) \leq \log p(\mathbf{x}), \quad (2.8)$$

as $D_{\text{KL}}(q(\mathbf{z} \mid \mathbf{x}) \parallel p(\mathbf{z} \mid \mathbf{x})) \geq 0$ by Gibbs' inequality. Hence, maximizing the VLB implicitly minimizes the KL divergence of $q(\mathbf{z} \mid \mathbf{x})$ from the true posterior $p(\mathbf{z} \mid \mathbf{x})$ as desired. The VLB is also known as the Evidence Lower BOund (ELBO) since $p(\mathbf{x})$ is called the *evidence*. The form of the VLB typically optimized by VAEs is:

$$\text{VLB}(\mathbf{x}) = \mathbb{E}_{q(\mathbf{z} \mid \mathbf{x})} \left[\log \frac{p(\mathbf{x}, \mathbf{z})}{q(\mathbf{z} \mid \mathbf{x})} \right] \quad (2.9)$$

$$= \mathbb{E}_{q(\mathbf{z} \mid \mathbf{x})} [\log p(\mathbf{x} \mid \mathbf{z})] + \mathbb{E}_{q(\mathbf{z} \mid \mathbf{x})} \left[\log \frac{p(\mathbf{z})}{q(\mathbf{z} \mid \mathbf{x})} \right] \quad (2.10)$$

$$= \mathbb{E}_{q(\mathbf{z} \mid \mathbf{x})} [\log p(\mathbf{x} \mid \mathbf{z})] - D_{\text{KL}}(q(\mathbf{z} \mid \mathbf{x}) \parallel p(\mathbf{z})), \quad (2.11)$$

which amounts to maximizing the expected likelihood $p(\mathbf{x} \mid \mathbf{z})$ of observing \mathbf{x} under our approximate posterior $q(\mathbf{z} \mid \mathbf{x})$, regularized by the KL divergence of $q(\mathbf{z} \mid \mathbf{x})$ from the prior $p(\mathbf{z})$.

If we let \mathcal{D} be a dataset of i.i.d. data, then $\text{VLB}(\mathcal{D}) = \sum_{\mathbf{x} \in \mathcal{D}} \text{VLB}(\mathbf{x})$. Finally, we can use stochastic variational inference ([Hoffman et al., 2013](#)) and the *reparameterization trick* ([Kingma and Welling, 2013](#); [Rezende et al., 2014](#)) to *jointly* optimize the VLB w.r.t. the model parameters θ , and variational parameters ϕ . For more details on this procedure, the reader may refer to [Kingma et al. \(2019\)](#) and [Blei et al. \(2017\)](#).

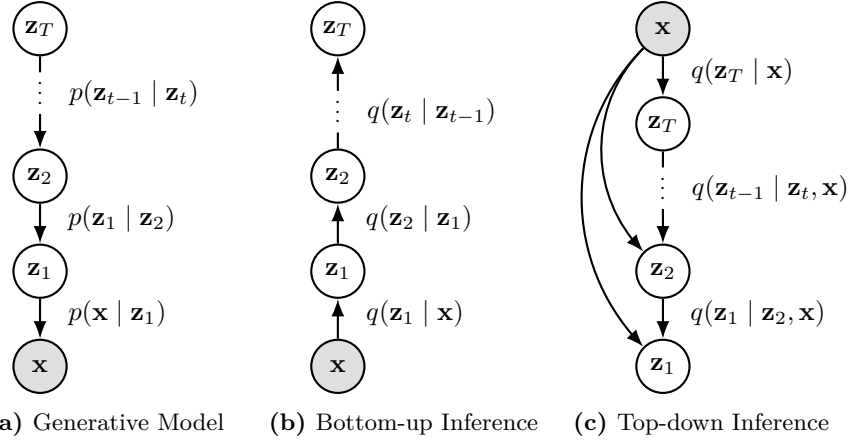


Figure 2.2: Hierarchical latent variable graphical models. (a) The generative model $p(\mathbf{x}, \mathbf{z}_{1:T})$ of a hierarchical VAE with T latent variables is a Markov chain. (b) The standard *bottom-up* inference model $q(\mathbf{z}_{1:T} | \mathbf{x})$ of a hierarchical VAE is a Markov chain in the reverse direction. (c) The *top-down* inference model follows the same topological ordering of the latent variables as the generative model. Notably, this top-down structure is also used to specify diffusion models. However, in diffusion models the posterior $q(\mathbf{z}_{1:T} | \mathbf{x})$ is tractable due to Gaussian conjugacy, which enables us to specify the *generative* model transitions as $p(\mathbf{z}_{t-1} | \mathbf{z}_t) = q(\mathbf{z}_{t-1} | \mathbf{z}_t, \mathbf{x} = \hat{\mathbf{x}}_\theta(\mathbf{z}_t; t))$, where the data \mathbf{x} is replaced by an image denoising model $\hat{\mathbf{x}}_\theta(\mathbf{z}_t; t)$.

2.2 Hierarchical Latent Variable Models

A hierarchical VAE is a deep latent variable model comprised of a hierarchy of $T \geq 2$ latent variables $\mathbf{z}_1, \mathbf{z}_2, \dots, \mathbf{z}_T$. Introducing additional (auxiliary) latent variables significantly improves the flexibility and expressivity of both inference and generative models (Salimans et al., 2015; Ranganath et al., 2016; Maaløe et al., 2016).

The joint distribution $p(\mathbf{x}, \mathbf{z}_{1:T})$ specifying a generative model of \mathbf{x} is a variational Markov chain:

$$\mathbf{z}_T \rightarrow \mathbf{z}_{T-1} \rightarrow \mathbf{z}_{T-2} \rightarrow \dots \rightarrow \mathbf{z}_1 \rightarrow \mathbf{x}, \quad (2.12)$$

defined as:

$$p(\mathbf{x}, \mathbf{z}_{1:T}) = p(\mathbf{z}_T)p(\mathbf{z}_{T-1} | \mathbf{z}_T) \cdots p(\mathbf{z}_1 | \mathbf{z}_2)p(\mathbf{x} | \mathbf{z}_1) \quad (2.13)$$

$$= p(\mathbf{z}_T) \left[\prod_{t=2}^T p(\mathbf{z}_{t-1} \mid \mathbf{z}_t) \right] p(\mathbf{x} \mid \mathbf{z}_1). \quad (2.14)$$

The approximate posterior $q(\mathbf{z}_{1:T} \mid \mathbf{x})$ is also a Markov chain but in the reverse (bottom-up) direction:

$$\mathbf{z}_T \leftarrow \mathbf{z}_{T-1} \leftarrow \mathbf{z}_{T-2} \leftarrow \cdots \leftarrow \mathbf{z}_1 \leftarrow \mathbf{x}, \quad (2.15)$$

which is defined as:

$$q(\mathbf{z}_{1:T} \mid \mathbf{x}) = q(\mathbf{z}_1 \mid \mathbf{x})q(\mathbf{z}_2 \mid \mathbf{z}_1)q(\mathbf{z}_3 \mid \mathbf{z}_2) \cdots q(\mathbf{z}_T \mid \mathbf{z}_{T-1}) \quad (2.16)$$

$$= q(\mathbf{z}_1 \mid \mathbf{x}) \prod_{t=2}^T q(\mathbf{z}_t \mid \mathbf{z}_{t-1}). \quad (2.17)$$

The marginal likelihood $p(\mathbf{x})$ is obtained by marginalizing out the latent variables:

$$p(\mathbf{x}) = \int p(\mathbf{x} \mid \mathbf{z}_1)p(\mathbf{z}_1) d\mathbf{z}_1, \quad (2.18)$$

where

$$p(\mathbf{z}_t) = \int p(\mathbf{z}_t \mid \mathbf{z}_{t+1})p(\mathbf{z}_{t+1}) d\mathbf{z}_{t+1}, \quad \text{for } t = 1, \dots, T-1. \quad (2.19)$$

Like the standard non-hierarchical case, the model is fit by maximizing the VLB of $\log p(\mathbf{x})$, but now includes additional terms specifying the assumed factorization of the latent variables:

$$\log p(\mathbf{x}) \geq \text{VLB}(\mathbf{x}) = \mathbb{E}_{q(\mathbf{z}_{1:T} \mid \mathbf{x})} \left[\log \frac{p(\mathbf{x}, \mathbf{z}_{1:T})}{q(\mathbf{z}_{1:T} \mid \mathbf{x})} \right]. \quad (2.20)$$

In the following sections, we explore both practical and theoretical challenges in using the aforementioned objective for training HLVMs – particularly under bottom-up inference – and introduce a new perspective using a concept we call *generative feedback*, which augments the commonly cited but incomplete efficiency-based view.

2.3 Generative Feedback

Burda et al. (2015) and Sønderby et al. (2016) both found that hierarchical latent variable models with purely bottom-up inference are typically not capable of utilizing more than two layers of latent variables. This often manifests as *posterior collapse*, whereby the posterior distribution collapses to a standard Gaussian prior, failing to learn meaningful representations and effectively deactivating latent variables. Generally speaking, having a learnable inference network can destabilize training by creating asynchronous learning dynamics with the generator, often leading to posterior collapse due to a constantly shifting target.

To better understand why bottom-up inference is challenging for even modestly deep hierarchies, we start by noting the asymmetry between the associated generative and inference models in Equations 2.14 and 2.17 respectively. Burda et al. (2015); Sohl-Dickstein et al. (2015) point this out as a source of difficulty in training the inference model efficiently, since there is no way to express each term in the VLB as an expectation under a distribution over a single latent variable. Luo (2022); Bishop and Bishop (2023) present a similar efficiency-based argument against bottom-up inference in hierarchical latent variable models.

We claim that efficiency-based arguments paint an incomplete picture; the main reason one should avoid bottom-up inference is the lack of direct *feedback* from the generative model. To show why generative feedback is important, we stress that the purpose of the inference model is to perform *Bayesian inference* at any given layer in the hierarchy. Concretely, its job is to compute the posterior distribution $q(\mathbf{z}_t | \mathbf{x})$ over each latent variable \mathbf{z}_t by:

$$q(\mathbf{z}_t | \mathbf{x}) = \frac{p(\mathbf{x} | \mathbf{z}_t)p(\mathbf{z}_t)}{p(\mathbf{x})} \quad (2.21)$$

$$\propto p(\mathbf{x} | \mathbf{z}_t) \int p(\mathbf{z}_t | \mathbf{z}_{t+1})p(\mathbf{z}_{t+1}) d\mathbf{z}_{t+1}, \quad (2.22)$$

which clearly shows that each posterior $q(\mathbf{z}_t | \mathbf{x})$ is not only proportional to the current layer's prior $p(\mathbf{z}_t)$ but also depends on the layer above's $p(\mathbf{z}_{t+1})$, and so on, following the reverse of the generative Markov chain, as specified in Equation 2.14.

Therefore, it stands to reason that interleaving feedback from each transition in the generative model into each respective transition in the inference model can align the inference network with the generative model and improve the inference procedure. To that end, we can take Equation 2.22 and rewrite the posterior distribution over each \mathbf{z}_t such that it contains a more explicit dependency on \mathbf{z}_{t+1} :

$$q(\mathbf{z}_t \mid \mathbf{z}_{t+1}, \mathbf{x}) = \frac{p(\mathbf{x} \mid \mathbf{z}_t, \mathbf{z}_{t+1})p(\mathbf{z}_t \mid \mathbf{z}_{t+1})}{p(\mathbf{x} \mid \mathbf{z}_{t+1})} \quad (2.23)$$

$$= \frac{p(\mathbf{x} \mid \mathbf{z}_t)p(\mathbf{z}_t \mid \mathbf{z}_{t+1})}{p(\mathbf{x} \mid \mathbf{z}_{t+1})} \cdot \frac{p(\mathbf{z}_{t+1})}{p(\mathbf{z}_t)}, \quad (2.24)$$

where the likelihood term $p(\mathbf{x} \mid \mathbf{z}_t, \mathbf{z}_{t+1})$ simplifies to $p(\mathbf{x} \mid \mathbf{z}_t)$ due to the conditional independence relation $\mathbf{x} \perp\!\!\!\perp \mathbf{z}_{t+1} \mid \mathbf{z}_t$ specified by the generative Markov chain. Now simply re-anchoring the time indices from t and $t + 1$ to $t - 1$ and t , respectively, reveals:

$$q(\mathbf{z}_{t-1} \mid \mathbf{z}_t, \mathbf{x}) = \frac{p(\mathbf{x} \mid \mathbf{z}_{t-1})p(\mathbf{z}_{t-1} \mid \mathbf{z}_t)p(\mathbf{z}_t)}{p(\mathbf{x}, \mathbf{z}_t)} \quad (2.25)$$

$$\propto p(\mathbf{x} \mid \mathbf{z}_{t-1})p(\mathbf{z}_{t-1} \mid \mathbf{z}_t)p(\mathbf{z}_t). \quad (2.26)$$

The posterior $q(\mathbf{z}_{t-1} \mid \mathbf{z}_t, \mathbf{x})$ now follows the same topological ordering of the latent variables as the prior $p(\mathbf{z}_{t-1} \mid \mathbf{z}_t)$, and it coincides with the *top-down* inference model in HVAEs (Sønderby et al., 2016; Kingma et al., 2016). Figure 2.2 shows how this top-down structure compares to the bottom-up approach. An added benefit of the top-down approach is that the generative model can also receive data-dependent feedback from the inference procedure, which can be beneficial in practice.

Ladder Networks. Valpola (2015); Rasmus et al. (2015) were, to the best of our knowledge, the first to introduce such lateral feedback connections between the inference and generative paths in hierarchical latent variable models. They called their denoising autoencoder a *ladder network* (see Figure 2.3), which later inspired the ladder VAE (Sønderby et al., 2016). Valpola (2015) argue that incorporating lateral feedback connections enables the higher layers to learn abstract invariant representations as they no longer have to retain all the details about the

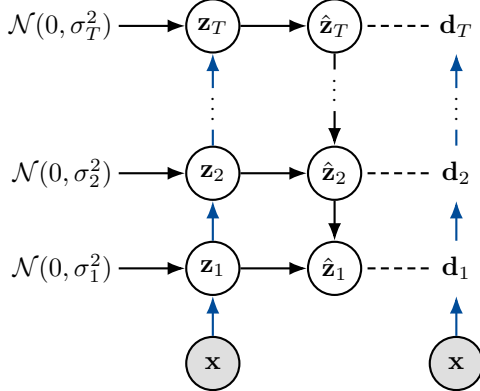


Figure 2.3: A Ladder Network. The latent variables $\mathbf{z}_1, \mathbf{z}_2, \dots, \mathbf{z}_T$ are noisy representations of \mathbf{x} , and $\mathbf{d}_1, \mathbf{d}_2, \dots, \mathbf{d}_T$ are clean representations; both sets are produced by a shared encoder (blue arrows). The variables $\hat{\mathbf{z}}_1, \hat{\mathbf{z}}_2, \dots, \hat{\mathbf{z}}_T$ are outputs of denoising functions where $\hat{\mathbf{z}}_t = g_t(\mathbf{z}_t, \hat{\mathbf{z}}_{t+1})$. Notice how $g_t(\cdot)$ receives both bottom-up and top-down information. The dashed horizontal lines denote local cost functions used to minimize $\|\hat{\mathbf{z}}_t - \mathbf{d}_t\|_2^2$. The main difference compared to denoising diffusion models is that here the denoising targets \mathbf{d}_t are learned representations of \mathbf{x} rather than fixed, increasingly noisier versions of \mathbf{x} .

input. Concretely, as depicted in Figure 2.3, each denoised variable $\hat{\mathbf{z}}_t := g_t(\mathbf{z}_t, \hat{\mathbf{z}}_{t+1})$ is computed using a denoising function $g_t(\cdot)$ which receives bottom-up feedback from \mathbf{z}_t and top-down feedback from $\hat{\mathbf{z}}_{t+1}$. For further discussion please refer to §3.

2.4 Top-down Inference

The joint approximate posterior $q(\mathbf{z}_{1:T} \mid \mathbf{x})$ can be alternatively factorized into the *top-down* inference model (Sønderby et al., 2016; Kingma et al., 2016). As mentioned in Section 2.3, the top-down inference model follows the same topological ordering of the latent variables as the generative model, that is:

$$q(\mathbf{z}_{1:T} \mid \mathbf{x}) = q(\mathbf{z}_T \mid \mathbf{x})q(\mathbf{z}_{T-1} \mid \mathbf{z}_T, \mathbf{x}) \cdots q(\mathbf{z}_1 \mid \mathbf{z}_2, \mathbf{x}) \quad (2.27)$$

$$= q(\mathbf{z}_T \mid \mathbf{x}) \prod_{t=2}^T q(\mathbf{z}_{t-1} \mid \mathbf{z}_t, \mathbf{x}). \quad (2.28)$$

Variants of the top-down inference model have featured in much deeper state-of-the-art HVAEs for sample generation (Maaløe et al., 2019; Vahdat and Kautz, 2020; Child, 2020; Shu and Ermon, 2022) and approximate counterfactual inference (De Sousa Ribeiro et al., 2023; Monteiro et al., 2022). As we will show, the top-down hierarchical latent variable model serves as the basis for parameterizing diffusion models.

Variational Lower Bound. For now, we derive the corresponding VLB to obtain a concrete optimization objective: $\text{VLB}(\mathbf{x})$

$$\text{VLB}(\mathbf{x}) = \mathbb{E}_{q(\mathbf{z}_{1:T}|\mathbf{x})} \left[\log \frac{p(\mathbf{x}, \mathbf{z}_{1:T})}{q(\mathbf{z}_{1:T} | \mathbf{x})} \right] \quad (2.29)$$

$$= \mathbb{E}_{q(\mathbf{z}_{1:T}|\mathbf{x})} \left[\log \frac{p(\mathbf{z}_T)p(\mathbf{x} | \mathbf{z}_1) \prod_{t=2}^T p(\mathbf{z}_{t-1} | \mathbf{z}_t)}{q(\mathbf{z}_T | \mathbf{x}) \prod_{t=2}^T q(\mathbf{z}_{t-1} | \mathbf{z}_t, \mathbf{x})} \right] \quad (2.30)$$

$$\begin{aligned} &= \mathbb{E}_{q(\mathbf{z}_{1:T}|\mathbf{x})} \left[\log p(\mathbf{x} | \mathbf{z}_1) + \log \frac{p(\mathbf{z}_T)}{q(\mathbf{z}_T | \mathbf{x})} \right. \\ &\quad \left. + \sum_{t=2}^T \log \frac{p(\mathbf{z}_{t-1} | \mathbf{z}_t)}{q(\mathbf{z}_{t-1} | \mathbf{z}_t, \mathbf{x})} \right] \end{aligned} \quad (2.31)$$

$$\begin{aligned} &= \mathbb{E}_{q(\mathbf{z}_1|\mathbf{x})} [\log p(\mathbf{x} | \mathbf{z}_1)] + \mathbb{E}_{q(\mathbf{z}_T|\mathbf{x})} \left[\log \frac{p(\mathbf{z}_T)}{q(\mathbf{z}_T | \mathbf{x})} \right] \\ &\quad + \sum_{t=2}^T \mathbb{E}_{q(\mathbf{z}_{t-1}, \mathbf{z}_t|\mathbf{x})} \left[\log \frac{p(\mathbf{z}_{t-1} | \mathbf{z}_t)}{q(\mathbf{z}_{t-1} | \mathbf{z}_t, \mathbf{x})} \right] \end{aligned} \quad (2.32)$$

$$\begin{aligned} &= \mathbb{E}_{q(\mathbf{z}_1|\mathbf{x})} [\log p(\mathbf{x} | \mathbf{z}_1)] + \mathbb{E}_{q(\mathbf{z}_T|\mathbf{x})} \left[\log \frac{p(\mathbf{z}_T)}{q(\mathbf{z}_T | \mathbf{x})} \right] \\ &\quad + \sum_{t=2}^T \mathbb{E}_{q(\mathbf{z}_t|\mathbf{x})} \left[\mathbb{E}_{q(\mathbf{z}_{t-1}|\mathbf{z}_t, \mathbf{x})} \left[\log \frac{p(\mathbf{z}_{t-1} | \mathbf{z}_t)}{q(\mathbf{z}_{t-1} | \mathbf{z}_t, \mathbf{x})} \right] \right] \end{aligned} \quad (2.33)$$

$$\begin{aligned} &= \mathbb{E}_{q(\mathbf{z}_1|\mathbf{x})} [\log p(\mathbf{x} | \mathbf{z}_1)] - D_{\text{KL}}(q(\mathbf{z}_T | \mathbf{x}) \parallel p(\mathbf{z}_T)) \\ &\quad - \sum_{t=2}^T \mathbb{E}_{q(\mathbf{z}_t|\mathbf{x})} [D_{\text{KL}}(q(\mathbf{z}_{t-1} | \mathbf{z}_t, \mathbf{x}) \parallel p(\mathbf{z}_{t-1} | \mathbf{z}_t))]. \end{aligned} \quad (2.34)$$

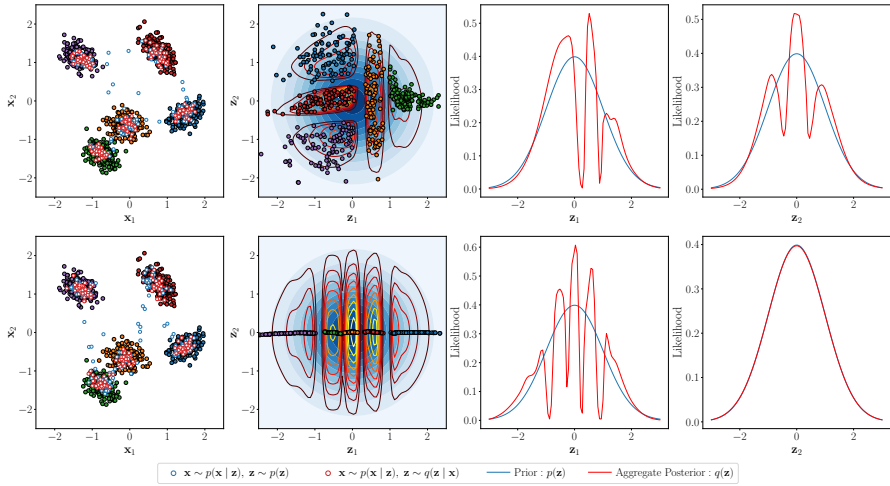


Figure 2.4: Demonstration of the ‘hole problem’. Results are from a single stochastic layer VAE trained on a 2D toy dataset with five clusters. The latent variable \mathbf{z} is also 2-dimensional for illustration purposes. The leftmost column shows the dataset, overlaid with reconstructed datapoints (red border) and random samples from the generative model (blue border). The remaining columns show the assumed prior $p(\mathbf{z}) = \mathcal{N}(\mathbf{z}; \mathbf{0}, \mathbf{I})$ (blue contours) overlaid with the aggregate posterior $q(\mathbf{z}) = \sum_{i=1}^N q(\mathbf{z} | \mathbf{x}_i)/N$. As shown, there are regions with high density under the prior which are assigned low density under the aggregate posterior. This affects the quality of the random samples since we are likely to sample from regions in $p(\mathbf{z})$ not covered by the data. Further, the bottom row shows a common occurrence in VAEs where latent variable(s) are not activated/used at all by the model, in this case, \mathbf{z}_2 was not used.

It is well worth dedicating some time to understanding the details of the above derivation and the resulting expression, as it is the *exact* objective optimized by diffusion models as well.

One thing to notice is that it comprises the familiar trade-off between minimizing input reconstruction error and keeping the hierarchical approximate posterior $q(\mathbf{z}_{1:T} | \mathbf{x})$ close to the hierarchical prior $p(\mathbf{z}_{1:T})$. In contrast to standard VAEs, the prior in HVAEs is typically learned from data rather than being fixed, as this affords greater flexibility and allows us to match the data distribution much more easily (Kingma et al., 2016; Hoffman and Johnson, 2016; Tomczak and Welling, 2018).

2.5 The W[H]ole Problem

A primary issue with VAEs is the so-called *hole problem* (Rezende and Viola, 2018). The hole problem refers to the often observed mismatch between the so-called aggregate posterior $q(\mathbf{z})$ and the prior $p(\mathbf{z})$ over the latent variables (Makhzani et al., 2015; Hoffman and Johnson, 2016).

The aggregate posterior is simply the average posterior distribution over the dataset $\mathcal{D} = \{\mathbf{x}_i\}_{i=1}^N$, that is:

$$q(\mathbf{z}) = \int q(\mathbf{z} \mid \mathbf{x}) p_{\mathcal{D}}(\mathbf{x}) d\mathbf{x}, \quad p_{\mathcal{D}}(\mathbf{x}) = \frac{1}{N} \sum_{i=1}^N \delta(\mathbf{x} - \mathbf{x}_i), \quad (2.35)$$

where $p_{\mathcal{D}}(\mathbf{x})$ is the *empirical distribution*, constructed by a Dirac delta function $\delta(\cdot)$ centered on each training datapoint \mathbf{x}_i . As shown in Figure 2.4, there can be regions with *high* probability density under the prior which have *low* probability density under the aggregate posterior. As a result, the quality of generated samples can be affected when the decoder receives \mathbf{z} 's sampled from regions in $p(\mathbf{z})$ which are not well-covered by the data. This phenomenon can be interpreted as a type of distribution shift/drift which occurs when sampling from the model. One possible workaround is to use $q(\mathbf{z})$ as the prior instead, however, computing $q(\mathbf{z})$ is usually computationally prohibitive in practice as it requires marginalizing out a (possibly very large) dataset.

As we will show, diffusion models circumvent the hole problem by defining the aggregate posterior to be equal to the prior by construction. This has profound implications as we can avoid drift when sampling.

3

Variational Diffusion Models

A diffusion probabilistic model (Sohl-Dickstein et al., 2015) can be understood as a hierarchical VAE with a particular choice of inference and generative model. Like HVAEs, diffusion models are deep latent variable models that maximize the variational lower bound of the log-likelihood of the data (i.e. the ELBO). Diffusion models were largely inspired by ideas from statistical physics rather than variational Bayesian methods, so they come with a different set of modelling choices, advantages and nomenclature. The general idea behind diffusion models is to define a *fixed* forward diffusion process that converts any complex data distribution into a tractable distribution, and then learn a generative model that reverses this diffusion process. Figure 3.1 compares diffusion models with (top-down inference) HVAEs and the following sections explore the details. Diffusion models have the following distinctive properties:

- (i) The joint posterior $q(\mathbf{z}_{1:T} \mid \mathbf{x})$ is fixed rather than learned from observed data;
- (ii) Each latent variable \mathbf{z}_t has the same dimensionality as \mathbf{x} ;
- (iii) The aggregate posterior $q(\mathbf{z}_T)$ is equal to the prior $p(\mathbf{z}_T)$ by construction;

- (iv) The functional form of the inference model is identical to that of the generative model. This corresponds exactly to the top-down inference model structure used in HVAEs;
- (v) A single neural network is shared across all levels of the latent variable hierarchy, and each layer can be trained independently;
- (vi) They optimize a *weighted* objective that suppresses modelling effort on imperceptible details and better aligns with human perception.

Recent model innovations (Ho et al., 2020) – along with insights from stochastic processes (Anderson, 1982) and score-based generative modelling (Hyvärinen and Dayan, 2005; Vincent, 2011; Song and Ermon, 2019; Song et al., 2021b) – have yielded a myriad of impressive synthesis results (Nichol and Dhariwal, 2021; Dhariwal and Nichol, 2021; Nichol et al., 2022; Ho et al., 2022; Rombach et al., 2022; Saharia et al., 2022; Hoogeboom et al., 2022). Kingma et al. (2021); Kingma and Gao (2023) introduced a family of diffusion-based generative models they call Variational Diffusion Models (VDMs), and showed us that:

- (i) The latent hierarchy can be made infinitely deep¹ via a continuous-time model where $T \rightarrow \infty$;
- (ii) The continuous-time VLB is invariant to the noise schedule², meaning we can learn/adapt our noise schedule such that it minimizes the variance of the resulting Monte Carlo estimator of the loss;
- (iii) Although *weighted* diffusion objectives *appear* markedly different from regular maximum likelihood training, they all implicitly optimize some instance of the ELBO;
- (iv) VDMs are capable of state-of-the-art image synthesis, showing that standard maximum likelihood-based training objectives (i.e. the ELBO) are not inherently at odds with perceptual quality.

¹This notion was concurrently explored by Song et al. (2021b); Huang et al. (2021); Vahdat et al. (2021).

²Except for the signal-to-noise ratio at its endpoints (see Section 4.3).

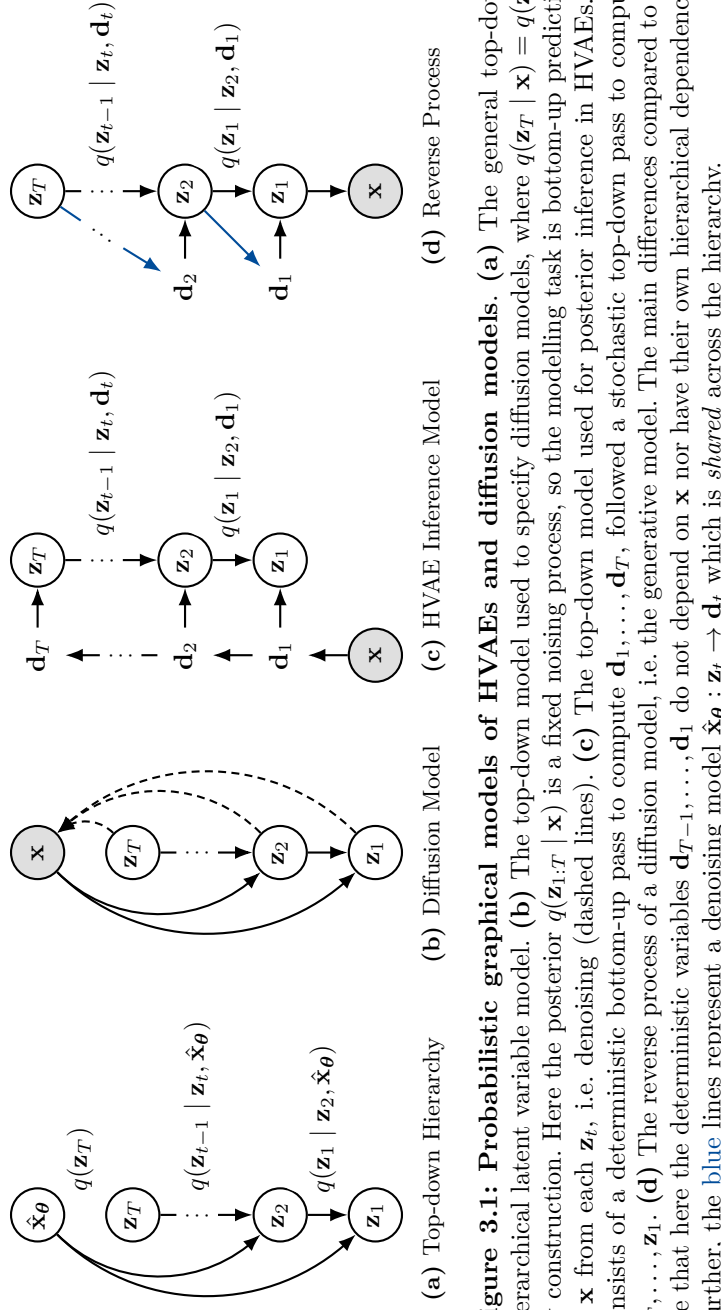


Figure 3.1: Probabilistic graphical models of HVAEs and diffusion models. (a) The general top-down hierarchical latent variable model. (b) The top-down model used to specify diffusion models, where $q(\mathbf{z}_T \mid \mathbf{x}) = q(\mathbf{z}_T)$ by construction. Here the posterior $q(\mathbf{z}_{1:T} \mid \mathbf{x})$ is a fixed noising process, so the modelling task is bottom-up prediction of \mathbf{x} from each \mathbf{z}_t , i.e. denoising (dashed lines). (c) The top-down model used for posterior inference in HVAEs. It consists of a deterministic bottom-up pass to compute $\mathbf{d}_1, \dots, \mathbf{d}_T$, followed a stochastic top-down pass to compute $\mathbf{z}_T, \dots, \mathbf{z}_1$. (d) The reverse process of a diffusion model, i.e. the generative model. The main differences compared to (c) are that here the deterministic variables $\mathbf{d}_{T-1}, \dots, \mathbf{d}_1$ do not depend on \mathbf{x} nor have their own hierarchical dependencies. Further, the blue lines represent a denoising model $\hat{\mathbf{x}}_\theta : \mathbf{z}_t \rightarrow \mathbf{d}_t$ which is *shared* across the hierarchy.

3.0.1 On Representation Learning

One important distinction to make between hierarchical VAEs and diffusion models at this stage is that the role of the latent variables $\mathbf{z}_{1:T}$ is very different from a *representation learning* perspective. In hierarchical VAEs, the posterior latents $\mathbf{z}_{1:T}$ are useful learned representations of \mathbf{x} , which *increase* in semantic informativeness w.r.t. \mathbf{x} as we go from \mathbf{z}_1 to \mathbf{z}_T . In diffusion models, the latent variables $\mathbf{z}_{1:T}$ generally have *no* semantic meaning, and they *decrease* in informativeness w.r.t. \mathbf{x} as we go from \mathbf{z}_1 to \mathbf{z}_T . This is because each \mathbf{z}_t in diffusion models is simply a noisy version of \mathbf{x} following a Gaussian diffusion process.

The latent variables $\mathbf{z}_1, \mathbf{z}_2, \dots, \mathbf{z}_T$ in ladder networks are noisy versions of the input \mathbf{x} , and the noise is additive isotropic Gaussian, like in diffusion models. However, the main difference is that each \mathbf{z}_t is a (noisy) learned representation of the input \mathbf{x} rather than simply a linear function of it, i.e.: $\mathbf{z}_t = f_t(\mathbf{z}_{t-1}) + \sigma_t \boldsymbol{\epsilon}$, where $f_t(\cdot)$ is a learned non-linear function and σ_t specifies the level of additive Gaussian noise corruption. In contrast, the diffusion process can be parameterized directly (linearly) in terms of \mathbf{x} as: $\mathbf{z}_t = \alpha_t \mathbf{x} + \sigma_t \boldsymbol{\epsilon}$. Moreover, the denoising targets also differ in that diffusion models learn to denoise the input \mathbf{x} directly or linear functions of it (i.e. via noise $\boldsymbol{\epsilon} = (\mathbf{z}_t - \alpha_t \mathbf{x})/\sigma_t$ or velocity $\mathbf{v} = \alpha_t \boldsymbol{\epsilon} - \sigma_t \mathbf{x}$ prediction), whereas ladder networks learn to denoise learned representations of the input \mathbf{d}_t given by the same non-linear functions $f_t(\cdot)$ used to define the latent variables.

The sum of the local cost functions in ladder networks is analogous to the diffusion loss – in both cases, the goal is to reconstruct the input from different noisy versions of it. However, unlike diffusion models, ladder networks focus on hierarchical representation learning rather than sample generation and it is generally not possible to evaluate each local cost function independently of the others. Nonetheless, we argue that ladder networks can serve as valuable inspiration for designing diffusion-based representation learning methods in the future.

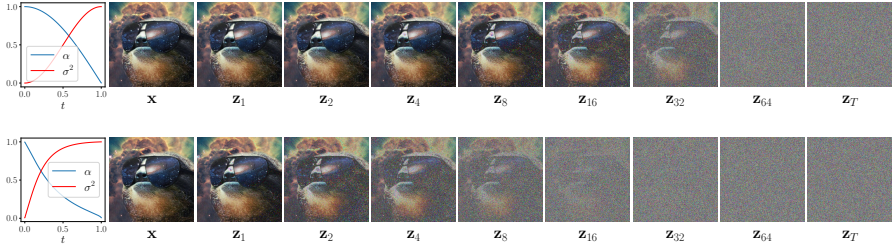


Figure 3.2: Example of a Gaussian diffusion process ($T = 100$). Showing two popular noise schedules in terms of $\{\alpha, \sigma^2\}$ as per Section 3.1. (Top) cosine (Nichol and Dhariwal, 2021); (Bottom) EDM (Karras et al., 2022).

3.1 Forward Process: Gaussian Diffusion

A *Gaussian diffusion process* gradually transforms data \mathbf{x} into random noise over time, by adding increasing amounts of Gaussian noise at each timestep $t = 0, \dots, 1$ resulting in a set of latent variables $\mathbf{z}_0, \dots, \mathbf{z}_1$ ³. Each latent variable \mathbf{z}_t is simply a noisy version of \mathbf{x} , and its distribution conditional on \mathbf{x} is given by:

$$q(\mathbf{z}_t \mid \mathbf{x}) = \mathcal{N} \left(\mathbf{z}_t; \alpha_t \mathbf{x}, \sigma_t^2 \mathbf{I} \right), \quad \mathbf{z}_t = \alpha_t \mathbf{x} + \sigma_t \boldsymbol{\epsilon}_t, \quad (3.1)$$

where $\boldsymbol{\epsilon}_t \sim \mathcal{N}(\boldsymbol{\epsilon}_t; 0, \mathbf{I})$, $\alpha_t \in (0, 1)$ and $\sigma_t^2 \in (0, 1)$ are chosen scalar valued functions of time $t \in [0, 1]$. See Figs. 3.2 & 3.3a for examples.

The key idea is to define the forward diffusion process such that the noisiest latent variable \mathbf{z}_1 at time $t = 1$ is standard Gaussian distributed: $q(\mathbf{z}_1 \mid \mathbf{x}) = \mathcal{N}(\mathbf{z}_1; 0, \mathbf{I})$, thus $q(\mathbf{z}_1 \mid \mathbf{x}) = q(\mathbf{z}_1)$. To that end, the scaling coefficients $\alpha_0 > \dots > \alpha_1$ decrease w.r.t. time t , whereas the noise variances $\sigma_0^2 < \dots < \sigma_1^2$ increase w.r.t. t . As we will show, this enables us to learn a generative Markov chain which starts from $\mathbf{z}_1 \sim q(\mathbf{z}_1)$ and reverses the forward diffusion process to obtain samples from the data distribution. The implications of this are profound; the *aggregate* posterior $q(\mathbf{z}_1)$ is equal to the prior $p(\mathbf{z}_1)$ by construction, which circumvents the *hole problem* in VAEs (see Figure 2.4). Hoffman and Johnson (2016) showed that the optimal prior is the aggregate posterior, as long as our posterior approximation is good enough.

³Without loss of generality, and for consistency with the continuous-time case where $T \rightarrow \infty$, we now denote the latent variables as $\mathbf{z}_{0:1}$ rather than $\mathbf{z}_{1:T}$.

3.1.1 Variance Preserving Process

A *variance-preserving* (VP) diffusion process is achieved by solving for the value of α_t such that the variance of the respective latent variable $\mathbb{V}[\mathbf{z}_t]$ is equal to the variance of the input data $\mathbb{V}[\mathbf{x}]$. This can be important from a modelling perspective, as adding increasing amounts of noise to the input alters its statistics and can affect learning.

We can begin by first applying some basic properties of *variance* to simplify $\mathbb{V}[\mathbf{z}_t]$ as follows:

$$\mathbb{V}[\mathbf{z}_t] = \mathbb{V}[\alpha_t \mathbf{x} + \sigma_t \boldsymbol{\epsilon}_t] \quad (3.2)$$

$$= \mathbb{V}[\alpha_t \mathbf{x}] + \mathbb{V}[\sigma_t \boldsymbol{\epsilon}_t] \quad (3.3)$$

$$= \alpha_t^2 \mathbb{V}[\mathbf{x}] + \sigma_t^2 \mathbb{V}[\boldsymbol{\epsilon}_t] \quad (3.4)$$

$$= \alpha_t^2 \mathbb{V}[\mathbf{x}] + \sigma_t^2, \quad (3.5)$$

since $\mathbb{V}[\boldsymbol{\epsilon}_t] = 1$ by definition. Taking the result and solving for α_t yields

$$\alpha_t^2 \mathbb{V}[\mathbf{x}] + \sigma_t^2 = \mathbb{V}[\mathbf{x}] \quad (3.6)$$

$$\alpha_t^2 = \frac{\mathbb{V}[\mathbf{x}] - \sigma_t^2}{\mathbb{V}[\mathbf{x}]} \quad (3.7)$$

$$\implies \mathbb{V}[\mathbf{z}_t] = \mathbb{V}[\mathbf{x}] \iff \alpha_t^2 = 1 - \frac{\sigma_t^2}{\mathbb{V}[\mathbf{x}]}, \quad (3.8)$$

which further simplifies to $\alpha_t^2 = 1 - \sigma_t^2$ as long as our input data is standardized (i.e. $\mathbb{V}[\mathbf{x}] = 1$).

Choosing diffusion processes is a fairly deep research topic with significant practical implications. We have decided to cover VP processes only, as they are the most widely used in practice as of the time of this writing and can be relatively straightforward to understand. Furthermore, all other types of forward processes can be converted to a VP process without loss of generality. For more information on variance-exploding processes, for example, please refer to [Song et al. \(2021b\)](#). For details on learning the noise schedule from data see [Appendix A.2](#).

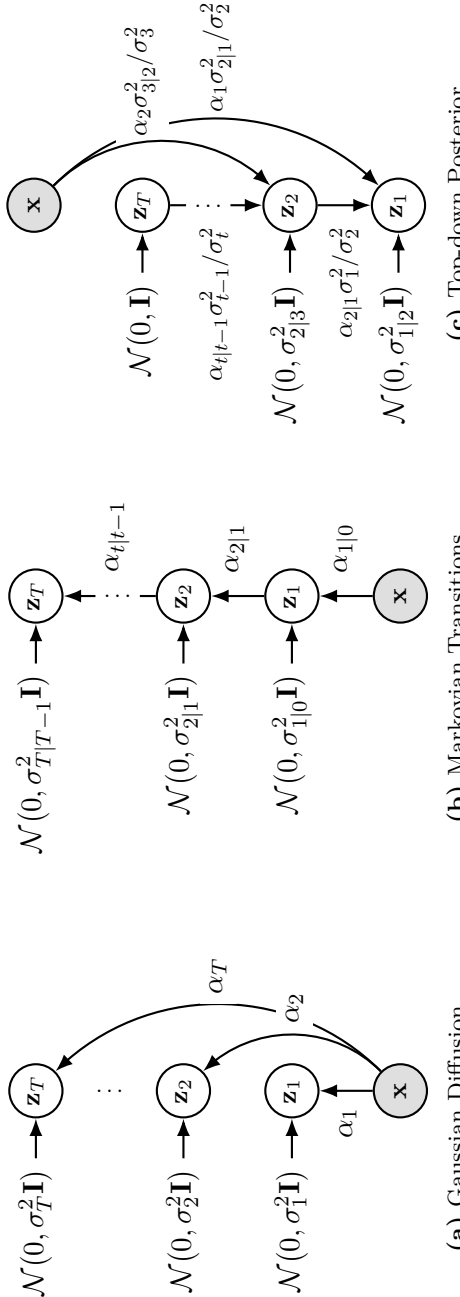


Figure 3.3: Graphical model(s) describing a discrete-time Gaussian diffusion process (T timesteps in total).

(a) Parameterization of the forward process in terms of the conditionals $q(\mathbf{z}_t \mid \mathbf{x})$ (ref. Section 3.1). Each latent variable \mathbf{z}_t is a noisy version of \mathbf{x} given by: $\mathbf{z}_t = \alpha_t \mathbf{x} + \sigma_t \epsilon_t$, and $\epsilon_t \sim \mathcal{N}(0, \mathbf{I})$. (b) Markov chain formed by a sequence of transition distributions $q(\mathbf{z}_t \mid \mathbf{z}_{t-1})$ (ref. Section 3.2). Each latent variable is given by: $\mathbf{z}_t = \alpha_{t|t-1} \mathbf{z}_{t-1} + \sigma_{t|t-1} \epsilon_t$, with parameters $\alpha_{t|t-1} := \alpha_t / \alpha_{t-1}$ and $\sigma_{t|t-1}^2 := \sigma_t^2 - \alpha_{t|t-1}^2 \sigma_{t-1}^2$. (c) The top-down posterior is tractable due to Gaussian conjugacy: $q(\mathbf{z}_{t-1} \mid \mathbf{z}_t, \mathbf{x}) \propto q(\mathbf{z}_t \mid \mathbf{z}_{t-1})q(\mathbf{z}_{t-1} \mid \mathbf{x})$ (ref. Section 3.3), where $q(\mathbf{z}_{t-1} \mid \mathbf{x})$ acts as a Gaussian prior and $q(\mathbf{z}_t \mid \mathbf{z}_{t-1})$ as a Gaussian likelihood. This top-down posterior is used to specify the *generative* model transitions as $p(\mathbf{z}_{t-1} \mid \mathbf{z}_t) = q(\mathbf{z}_{t-1} \mid \mathbf{z}_t, \mathbf{x} = \hat{\mathbf{x}}_{\theta}(\mathbf{z}_t; t))$, where the data \mathbf{x} is replaced by a learnable denoising model $\hat{\mathbf{x}}_{\theta}(\mathbf{z}_t; t)$.

3.2 Linear Gaussian Transitions

The conditional distribution of \mathbf{z}_t given a preceding latent variable \mathbf{z}_s , for any timestep $s < t$, is given by:

$$q(\mathbf{z}_t | \mathbf{z}_s) = \mathcal{N} \left(\mathbf{z}_t; \alpha_{t|s} \mathbf{z}_s, \sigma_{t|s}^2 \mathbf{I} \right), \quad \mathbf{z}_t = \alpha_{t|s} \mathbf{z}_s + \sigma_{t|s} \boldsymbol{\epsilon}_t, \quad (3.9)$$

where $\boldsymbol{\epsilon}_t \sim \mathcal{N}(\boldsymbol{\epsilon}_t; 0, \mathbf{I})$, thereby forming a Markov chain:

$$\mathbf{z}_1 \leftarrow \mathbf{z}_{(T-1)/T} \leftarrow \mathbf{z}_{(T-2)/T} \leftarrow \cdots \leftarrow \mathbf{z}_0 \leftarrow \mathbf{x}. \quad (3.10)$$

Figure 3.3b provides an example. In the continuous-time case where $T \rightarrow \infty$, each transition is w.r.t. an infinitesimal change in time dt .

The transition distribution $q(\mathbf{z}_t | \mathbf{z}_s)$ is useful for computing closed-form expressions for the parameters of the posterior $q(\mathbf{z}_s | \mathbf{z}_t, \mathbf{x})$, which defines our *reverse-process*, i.e. the generative model (c.f. Section 3.3). Let's focus on deriving $\alpha_{t|s}$ first. By construction, we know that each \mathbf{z}_t is given by:

$$\mathbf{z}_t = \alpha_t \mathbf{x} + \sigma_t \boldsymbol{\epsilon}_t = \alpha_t \left(\frac{\mathbf{z}_s - \sigma_s \boldsymbol{\epsilon}_s}{\alpha_s} \right) + \sigma_t \boldsymbol{\epsilon}_t, \quad (3.11)$$

since $\mathbf{x} = (\mathbf{z}_s - \sigma_s \boldsymbol{\epsilon}_s) / \alpha_s$ for any $s < t$. The conditional mean of $q(\mathbf{z}_t | \mathbf{z}_s)$ is then readily given by:

$$\mathbb{E}[\mathbf{z}_t | \mathbf{z}_s] = \alpha_t \left(\frac{\mathbf{z}_s - \sigma_s \mathbb{E}[\boldsymbol{\epsilon}_s]}{\alpha_s} \right) + \sigma_t \mathbb{E}[\boldsymbol{\epsilon}_t] \quad (3.12)$$

$$= \frac{\alpha_t}{\alpha_s} \mathbf{z}_s \quad (\text{since } \mathbb{E}[\boldsymbol{\epsilon}_t] = 0, \forall t) \quad (3.13)$$

$$=: \alpha_{t|s} \mathbf{z}_s. \quad (3.14)$$

To compute a closed-form expression for the variance $\sigma_{t|s}^2$ of the transition distribution $q(\mathbf{z}_t | \mathbf{z}_s)$, we can start by rewriting the equation for \mathbf{z}_t in terms of the preceding latent \mathbf{z}_s as follows:

$$\mathbf{z}_t = \alpha_{t|s} \mathbf{z}_s + \sigma_{t|s} \boldsymbol{\epsilon}_t \quad (3.15)$$

$$= \frac{\alpha_t}{\alpha_s} (\alpha_s \mathbf{x} + \sigma_s \boldsymbol{\epsilon}_s) + \sigma_{t|s} \boldsymbol{\epsilon}_t \quad (\text{substitute } \alpha_{t|s}, \mathbf{z}_s) \quad (3.16)$$

$$= \alpha_t \mathbf{x} + \frac{\alpha_t}{\alpha_s} \sigma_s \boldsymbol{\epsilon}_s + \sigma_{t|s} \boldsymbol{\epsilon}_t \quad (3.17)$$

$$\implies \sigma_t \epsilon_t = \frac{\alpha_t}{\alpha_s} \sigma_s \epsilon_s + \sigma_{t|s} \epsilon_t. \quad (\text{since } \mathbf{z}_t = \alpha_t \mathbf{x} + \sigma_t \epsilon_t) \quad (3.18)$$

The above implication allows us to compute the variance $\sigma_{t|s}^2$ straightforwardly. Firstly, recall that variance is invariant to changes in a location parameter, therefore: $\mathbb{V}[cX] = c^2 \mathbb{V}[X]$ for some constant c and random variable X . Secondly, the variance of a sum of n independent random variables is simply the sum of their variances: $\mathbb{V}[\sum_{i=1}^n X_i] = \sum_{i=1}^n \mathbb{V}[X_i]$. Using these two properties we show that:

$$\mathbb{V}[\sigma_t \epsilon_t] = \mathbb{V}\left[\frac{\alpha_t}{\alpha_s} \sigma_s \epsilon_s + \sigma_{t|s} \epsilon_t\right] \quad (3.19)$$

$$\sigma_t^2 \mathbb{V}[\epsilon_t] = \left(\frac{\alpha_t}{\alpha_s}\right)^2 \sigma_s^2 \mathbb{V}[\epsilon_s] + \sigma_{t|s}^2 \mathbb{V}[\epsilon_t] \quad (3.20)$$

$$\sigma_t^2 = \left(\frac{\alpha_t}{\alpha_s}\right)^2 \sigma_s^2 + \sigma_{t|s}^2 \quad (3.21)$$

$$\sigma_{t|s}^2 = \sigma_t^2 - \left(\frac{\alpha_t}{\alpha_s}\right)^2 \sigma_s^2. \quad (3.22)$$

3.3 The Top-down Posterior

Since the forward process is a Markov chain, the joint distribution of any two latent variables \mathbf{z}_t and \mathbf{z}_s where $t > s$ factorizes as: $q(\mathbf{z}_s, \mathbf{z}_t | \mathbf{x}) = q(\mathbf{z}_t | \mathbf{z}_s)q(\mathbf{z}_s | \mathbf{x})$. Using Bayes' theorem, it is then possible to derive closed-form expressions for the parameters of the posterior distribution $q(\mathbf{z}_s | \mathbf{z}_t, \mathbf{x})$, which is itself Gaussian due to conjugacy, where $q(\mathbf{z}_s | \mathbf{x})$ acts as a Gaussian prior and $q(\mathbf{z}_t | \mathbf{z}_s)$ a Gaussian likelihood:

$$q(\mathbf{z}_s | \mathbf{z}_t, \mathbf{x}) = \mathcal{N}\left(\mathbf{z}_s; \boldsymbol{\mu}_Q(\mathbf{z}_t, \mathbf{x}; s, t), \sigma_Q^2(s, t)\mathbf{I}\right), \quad (3.23)$$

$$\mathbf{z}_s = \boldsymbol{\mu}_Q(\mathbf{z}_t, \mathbf{x}; s, t) + \sigma_Q(s, t)\boldsymbol{\epsilon}_t, \quad (3.24)$$

with $\boldsymbol{\epsilon}_t \sim \mathcal{N}(\boldsymbol{\epsilon}_t; 0, \mathbf{I})$. In the following, we will derive closed-form expressions for the posterior parameters $\boldsymbol{\mu}_Q(\mathbf{z}_t, \mathbf{x}; s, t)$ and $\sigma_Q^2(s, t)$ in detail. For a graphical model of the posterior see Figure 3.3c.

Before proceeding, we note that this posterior distribution will be instrumental in defining our generative model (i.e. the reverse process) as explained later on in Section 3.4. Furthermore, notice that the posterior

$q(\mathbf{z}_s \mid \mathbf{z}_t, \mathbf{x})$ coincides with the *top-down* inference model specification of a hierarchical VAE.

For simplicity, let D denote the dimensionality of \mathbf{z}_t , satisfying $\dim(\mathbf{z}_t) = \dim(\mathbf{x}), \forall t$. Furthermore, recall that our covariance matrix of choice is isotropic/spherical: $\sigma_Q^2 \mathbf{I}$. The posterior is then given by

$$q(\mathbf{z}_s \mid \mathbf{z}_t, \mathbf{x}) = \frac{q(\mathbf{z}_t \mid \mathbf{z}_s)q(\mathbf{z}_s \mid \mathbf{x})}{q(\mathbf{z}_t \mid \mathbf{x})} \quad (3.25)$$

$$\propto q(\mathbf{z}_t \mid \mathbf{z}_s)q(\mathbf{z}_s \mid \mathbf{x}) \quad (3.26)$$

$$= \mathcal{N}(\mathbf{z}_t; \alpha_{t|s}\mathbf{z}_s, \sigma_{t|s}^2 \mathbf{I}) \cdot \mathcal{N}(\mathbf{z}_s; \alpha_s \mathbf{x}, \sigma_s^2 \mathbf{I}) \quad (3.27)$$

$$= \prod_{i=1}^D \frac{1}{\sigma_{t|s} \sqrt{2\pi}} \exp \left\{ -\frac{1}{2\sigma_{t|s}^2} (\mathbf{z}_{t,i} - \alpha_{t|s}\mathbf{z}_{s,i})^2 \right\} \quad (3.28)$$

$$\cdot \prod_{i=1}^D \frac{1}{\sigma_s \sqrt{2\pi}} \exp \left\{ -\frac{1}{2\sigma_s^2} (\mathbf{z}_{s,i} - \alpha_s \mathbf{x}_i)^2 \right\} \quad (3.29)$$

$$\propto \prod_{i=1}^D \exp \left\{ -\frac{1}{2\sigma_{t|s}^2} (\mathbf{z}_{t,i} - \alpha_{t|s}\mathbf{z}_{s,i})^2 \right\} \cdot \prod_{i=1}^D \exp \left\{ -\frac{1}{2\sigma_s^2} (\mathbf{z}_{s,i} - \alpha_s \mathbf{x}_i)^2 \right\} \quad (3.30)$$

$$= \prod_{i=1}^D \exp \left\{ -\frac{1}{2\sigma_{t|s}^2} (\mathbf{z}_{t,i}^2 - 2\mathbf{z}_{t,i}\alpha_{t|s}\mathbf{z}_{s,i} + \alpha_{t|s}^2 \mathbf{z}_{s,i}^2) \right\} \quad (3.31)$$

$$- \frac{1}{2\sigma_s^2} (\mathbf{z}_{s,i}^2 - 2\mathbf{z}_{s,i}\alpha_s \mathbf{x}_i + \alpha_s^2 \mathbf{x}_i^2) \Big\} \quad (3.32)$$

$$= \prod_{i=1}^D \exp \left\{ -\frac{1}{2} \left[\frac{\mathbf{z}_{t,i}^2 - 2\mathbf{z}_{t,i}\alpha_{t|s}\mathbf{z}_{s,i} + \alpha_{t|s}^2 \mathbf{z}_{s,i}^2}{\sigma_{t|s}^2} \right. \right. \quad (3.33)$$

$$\left. \left. + \frac{\mathbf{z}_{s,i}^2 - 2\mathbf{z}_{s,i}\alpha_s \mathbf{x}_i + \alpha_s^2 \mathbf{x}_i^2}{\sigma_s^2} \right] \right\} \quad (3.34)$$

$$= \prod_{i=1}^D \exp \left\{ -\frac{1}{2} \left[\mathbf{z}_{s,i}^2 \left(\frac{\alpha_{t|s}^2}{\sigma_{t|s}^2} + \frac{1}{\sigma_s^2} \right) - 2\mathbf{z}_{s,i} \left(\frac{\alpha_{t|s}\mathbf{z}_{t,i}}{\sigma_{t|s}^2} + \frac{\alpha_s \mathbf{x}_i}{\sigma_s^2} \right) \right] \right\} \quad (3.35)$$

$$+ \frac{\mathbf{z}_{t,i}^2}{\sigma_{t|s}^2} + \frac{\alpha_s^2 \mathbf{x}_i^2}{\sigma_s^2} \Bigg] \Bigg\}. \quad (3.36)$$

The next step is to ‘match the moments’ from Equation (3.36) with what we expect to see in a Gaussian distribution, i.e. something of the form:

$$\mathcal{N}(x; \mu, \sigma^2) \propto \exp \left\{ -\frac{x^2}{2\sigma^2} + \frac{\mu x}{\sigma^2} - \frac{\mu^2}{2\sigma^2} \right\}. \quad (3.37)$$

This exercise yields closed-form expressions for the parameters of the posterior distribution as desired. Without loss of generality, consider the $D = 1$ dimensional case for brevity.

Matching the first term in Eq. (3.36) with $-\frac{x^2}{2\sigma^2}$ we can see that:

$$-\frac{\mathbf{z}_s^2}{2} \left(\frac{\alpha_{t|s}^2}{\sigma_{t|s}^2} + \frac{1}{\sigma_s^2} \right) \implies \frac{1}{\sigma_Q^2} = \frac{\alpha_{t|s}^2}{\sigma_{t|s}^2} + \frac{1}{\sigma_s^2}, \quad (3.38)$$

where σ_Q^2 is the variance of the posterior $q(\mathbf{z}_s \mid \mathbf{z}_t, \mathbf{x})$. Matching the second term in Eq. (3.36) with $\frac{\mu x}{\sigma^2}$ we get:

$$\mathbf{z}_s \left(\frac{\alpha_{t|s} \mathbf{z}_t}{\sigma_{t|s}^2} + \frac{\alpha_s \mathbf{x}}{\sigma_s^2} \right) \implies \frac{\boldsymbol{\mu}_Q}{\sigma_Q^2} = \frac{\alpha_{t|s} \mathbf{z}_t}{\sigma_{t|s}^2} + \frac{\alpha_s \mathbf{x}}{\sigma_s^2} \quad (3.39)$$

$$\implies \boldsymbol{\mu}_Q = \sigma_Q^2 \left(\frac{\alpha_{t|s} \mathbf{z}_t}{\sigma_{t|s}^2} + \frac{\alpha_s \mathbf{x}}{\sigma_s^2} \right), \quad (3.40)$$

where $\boldsymbol{\mu}_Q$ is the mean of the posterior $q(\mathbf{z}_s \mid \mathbf{z}_t, \mathbf{x})$.

The closed-form expressions for $\boldsymbol{\mu}_Q$, σ_Q^2 simplify quite significantly:

$$\frac{1}{\sigma_Q^2} = \frac{\sigma_s^2}{\sigma_s^2} \cdot \frac{\alpha_{t|s}^2}{\sigma_{t|s}^2} + \frac{\sigma_{t|s}^2}{\sigma_{t|s}^2} \cdot \frac{1}{\sigma_s^2} \quad (3.41)$$

$$= \frac{\alpha_{t|s}^2 \sigma_s^2 + \sigma_{t|s}^2}{\sigma_{t|s}^2 \sigma_s^2} \implies \sigma_Q^2 = \frac{\sigma_{t|s}^2 \sigma_s^2}{\alpha_{t|s}^2 \sigma_s^2 + \sigma_{t|s}^2}, \quad (3.42)$$

and for the posterior mean we then have:

$$\boldsymbol{\mu}_Q = \sigma_Q^2 \left(\frac{\alpha_{t|s} \mathbf{z}_t}{\sigma_{t|s}^2} + \frac{\alpha_s \mathbf{x}}{\sigma_s^2} \right) \quad (3.43)$$

Distribution	Mean	Covariance
$q(\mathbf{z}_t \mid \mathbf{x})$ (§3.1)	$\alpha_t \mathbf{x}$	$\sigma_t^2 \mathbf{I}$
$q(\mathbf{z}_t \mid \mathbf{z}_s)$ (§3.2)	$\alpha_{t s} \mathbf{z}_s$	$\sigma_{t s}^2 \mathbf{I}$
$q(\mathbf{z}_s \mid \mathbf{z}_t, \mathbf{x})$ (§3.3)	$\boldsymbol{\mu}_Q(\mathbf{z}_t, \mathbf{x}; s, t)$	$\sigma_Q^2(s, t) \mathbf{I}$
Parameter	Expression	
$\alpha_{t s}$	α_t / α_s	
$\sigma_{t s}^2$	$\sigma_t^2 - \alpha_{t s}^2 \sigma_s^2$	
$\boldsymbol{\mu}_Q(\mathbf{z}_t, \mathbf{x}; s, t)$	$\frac{\alpha_{t s} \sigma_s^2}{\sigma_t^2} \mathbf{z}_t + \frac{\alpha_s \sigma_{t s}^2}{\sigma_t^2} \mathbf{x}$	
$\sigma_Q^2(s, t)$	$\frac{\sigma_{t s}^2 \sigma_s^2}{\alpha_{t s}^2 \sigma_s^2 + \sigma_{t s}^2}$	

Table 3.1: Breakdown of the distributions involved in defining a typical Gaussian diffusion (LHS), along with closed-form expressions for their respective parameters (RHS). Note that s denotes a preceding timestep relative to timestep t , i.e. $s < t$. The top-down posterior distribution $q(\mathbf{z}_s \mid \mathbf{z}_t, \mathbf{x})$ is tractable due to Gaussian conjugacy: $q(\mathbf{z}_s \mid \mathbf{z}_t, \mathbf{x}) \propto q(\mathbf{z}_t \mid \mathbf{z}_s)q(\mathbf{z}_s \mid \mathbf{x})$, where $q(\mathbf{z}_s \mid \mathbf{x})$ plays the role of a conjugate (Gaussian) prior and $q(\mathbf{z}_t \mid \mathbf{z}_s)$ the plays the role of a Gaussian likelihood.

$$= \frac{\sigma_{t|s}^2 \sigma_s^2}{\alpha_{t|s}^2 \sigma_s^2 + \sigma_{t|s}^2} \cdot \frac{\sigma_s^2 \alpha_{t|s} \mathbf{z}_t + \sigma_{t|s}^2 \alpha_s \mathbf{x}}{\sigma_{t|s}^2 \sigma_s^2} \quad (3.44)$$

$$= \frac{\sigma_s^2 \alpha_{t|s} \mathbf{z}_t + \sigma_{t|s}^2 \alpha_s \mathbf{x}}{\alpha_{t|s}^2 \sigma_s^2 + \sigma_{t|s}^2} \quad (3.45)$$

$$= \frac{\alpha_{t|s} \sigma_s^2}{\alpha_{t|s}^2 \sigma_s^2 + \sigma_{t|s}^2} \mathbf{z}_t + \frac{\alpha_s \sigma_{t|s}^2}{\alpha_{t|s}^2 \sigma_s^2 + \sigma_{t|s}^2} \mathbf{x}. \quad (3.46)$$

Using the fact that $\sigma_{t|s}^2 = \sigma_t^2 - \alpha_{t|s}^2 \sigma_s^2$ as in Equation 3.22, we get the final expression:

$$\boldsymbol{\mu}_Q(\mathbf{z}_t, \mathbf{x}; s, t) = \frac{\alpha_{t|s} \sigma_s^2}{\sigma_t^2} \mathbf{z}_t + \frac{\alpha_s \sigma_{t|s}^2}{\sigma_t^2} \mathbf{x}, \quad (3.47)$$

revealing that the posterior mean $\boldsymbol{\mu}_Q$, equivalently denoted as $\boldsymbol{\mu}_Q(\mathbf{z}_t, \mathbf{x}; s, t)$

by Kingma et al. (2021), is essentially a weighted average of the conditioning set $\{\mathbf{z}_t, \mathbf{x}\}$ of the posterior distribution $q(\mathbf{z}_s \mid \mathbf{z}_t, \mathbf{x})$.

In summary, the top-down posterior distribution is given by:

$$q(\mathbf{z}_s \mid \mathbf{z}_t, \mathbf{x}) = \mathcal{N} \left(\mathbf{z}_s; \frac{\alpha_{t|s}\sigma_s^2}{\sigma_t^2} \mathbf{z}_t + \frac{\alpha_s\sigma_{t|s}^2}{\sigma_t^2} \mathbf{x}, \frac{\sigma_{t|s}^2\sigma_s^2}{\alpha_{t|s}^2\sigma_s^2 + \sigma_{t|s}^2} \mathbf{I} \right) \quad (3.48)$$

$$= \mathcal{N} \left(\mathbf{z}_s; \boldsymbol{\mu}_Q(\mathbf{z}_t, \mathbf{x}; s, t), \sigma_Q^2(s, t) \mathbf{I} \right). \quad (3.49)$$

To conclude, Table 3.1 provides a concise breakdown of all the distributions involved in defining a Gaussian diffusion, along with the respective closed-form expressions of their parameters.

3.4 Reverse Process: Discrete-Time Generative Model

The generative model in diffusion models inverts the Gaussian diffusion process outlined in Section 3.1. In other words, it estimates the *reverse-time* variational Markov Chain relative to a corresponding *forward-time* diffusion process. An interesting aspect of VDMs is that they admit continuous-time generative models ($T \rightarrow \infty$) in a principled manner, and these correspond to the infinitely deep limit of a hierarchical VAE with a fixed encoder. We first describe the discrete-time model (finite T) (Sohl-Dickstein et al., 2015; Ho et al., 2020), as it closely relates to the material already covered, then describe the continuous-time version.

Notation. To unify the notation for both the discrete and continuous-time model versions, Kingma et al. (2021) uniformly discretize time into T segments of width $\tau = 1/T$. Each time segment corresponds to a level/step in the hierarchy of latent variables defined as follows:

$$t(i) = \frac{i}{T}, \quad s(i) = \frac{i-1}{T}, \quad (3.50)$$

where $s(i)$ precedes $t(i)$ in the timestep hierarchy, for an index i . For simplicity, we may sometimes use s and t as shorthand notation for $s(i)$ and $t(i)$ when our intentions are clear from context.

As previously mentioned, the discrete-time generative model of a variational diffusion model is identical to the hierarchical VAE's

generative model described in Section 2.2. Using the new index notation defined above, we can re-express the discrete-time generative model as:

$$p(\mathbf{x}, \mathbf{z}_{0:1}) = p(\mathbf{z}_1)p(\mathbf{z}_{(T-1)/T} \mid \mathbf{z}_T) \cdots p(\mathbf{z}_0 \mid \mathbf{z}_{1/T})p(\mathbf{x} \mid \mathbf{z}_0) \quad (3.51)$$

$$= \underbrace{p(\mathbf{z}_1)}_{\text{prior}} \underbrace{p(\mathbf{x} \mid \mathbf{z}_0)}_{\text{likelihood}} \prod_{i=1}^T \underbrace{p(\mathbf{z}_{s(i)} \mid \mathbf{z}_{t(i)})}_{\text{transitions}}. \quad (3.52)$$

This corresponds to a Markov chain:

$$\mathbf{z}_1 \rightarrow \mathbf{z}_{(T-1)/T} \rightarrow \mathbf{z}_{(T-2)/T} \rightarrow \cdots \rightarrow \mathbf{z}_0 \rightarrow \mathbf{x}, \quad (3.53)$$

which is equivalent in principle to the hierarchical VAE's Markov chain: $\mathbf{z}_T \rightarrow \mathbf{z}_{T-1} \rightarrow \cdots \rightarrow \mathbf{z}_1 \rightarrow \mathbf{x}$, for equal T .

Each component of the discrete-time generative model is defined as:

- (i) The **prior** term can be safely set to $p(\mathbf{z}_1) = \mathcal{N}(0, \mathbf{I})$ in a variance preserving diffusion process since – for small enough $\text{SNR}(t = 1)$ – the noisiest latent \mathbf{z}_1 holds almost no information about the input \mathbf{x} . In other words, this means that $q(\mathbf{z}_1 \mid \mathbf{x}) \approx \mathcal{N}(\mathbf{z}_1; 0, \mathbf{I})$ by construction, and as such there exists a distribution $p(\mathbf{z}_1)$ such that $D_{\text{KL}}(q(\mathbf{z}_1 \mid \mathbf{x}) \parallel p(\mathbf{z}_1)) \approx 0$.
- (ii) The **likelihood** term $p(\mathbf{x} \mid \mathbf{z}_0)$ factorizes over the number of elements D (e.g. pixels) in \mathbf{x} , \mathbf{z}_0 as:

$$p(\mathbf{x} \mid \mathbf{z}_0) = \prod_{i=1}^D p(x^{(i)} \mid z_0^{(i)}), \quad (3.54)$$

such as a product of (potentially discretized) Gaussian distributions. This distribution could conceivably be modelled autoregressively, but there is little advantage in doing so, as \mathbf{z}_0 (the least noisy latent) is almost identical to \mathbf{x} by construction. This means that $p(\mathbf{x} \mid \mathbf{z}_0) \approx q(\mathbf{x} \mid \mathbf{z}_0)$ for sufficiently large $\text{SNR}(t = 0)$. Intuitively, since \mathbf{z}_0 is almost equal to \mathbf{x} by construction, modelling $p(\mathbf{z}_0)$ is practically equivalent to modelling $p(\mathbf{x})$, so the likelihood term $p(\mathbf{x} \mid \mathbf{z}_0)$ is typically omitted, as learning $p(\mathbf{z}_0 \mid \mathbf{z}_{1/T})$ has proven to be sufficient in practice.

(iii) The **transition** conditional distributions $p(\mathbf{z}_s \mid \mathbf{z}_t)$ are defined to be the same as the top-down posteriors $q(\mathbf{z}_s \mid \mathbf{z}_t, \mathbf{x})$ presented in Section 3.3, but with the observed data \mathbf{x} replaced by the output of a time-dependent *denoising* model $\hat{\mathbf{x}}_\theta(\mathbf{z}_t; t)$, that is:

$$p(\mathbf{z}_s \mid \mathbf{z}_t) = q(\mathbf{z}_s \mid \mathbf{z}_t, \mathbf{x} = \hat{\mathbf{x}}_\theta(\mathbf{z}_t; t)). \quad (3.55)$$

The role of the denoising model is to predict \mathbf{x} from each of its noisy versions \mathbf{z}_t in turn. There are three different interpretations of this component of the generative model, as we describe next.

3.5 Generative Transitions

The conditional distributions of the generative model are given by:

$$p(\mathbf{z}_s \mid \mathbf{z}_t) = \mathcal{N} \left(\mathbf{z}_s; \boldsymbol{\mu}_\theta(\mathbf{z}_t; s, t), \sigma_Q^2(s, t) \mathbf{I} \right) \quad (3.56)$$

where $\sigma_Q^2(s, t)$ is the posterior variance we derived in Equation 3.22, and $\boldsymbol{\mu}_\theta(\mathbf{z}_t; s, t)$ is analogous to the posterior mean we derived in Equation 3.47, that is:

$$q(\mathbf{z}_s \mid \mathbf{z}_t, \mathbf{x}) = \mathcal{N} \left(\mathbf{z}_s; \boldsymbol{\mu}_Q(\mathbf{z}_t, \mathbf{x}; s, t), \sigma_Q^2(s, t) \mathbf{I} \right), \quad (3.57)$$

where the posterior mean is given by

$$\boldsymbol{\mu}_Q(\mathbf{z}_t, \mathbf{x}; s, t) = \frac{\alpha_{t|s} \sigma_s^2}{\sigma_t^2} \mathbf{z}_t + \frac{\alpha_s \sigma_{t|s}^2}{\sigma_t^2} \mathbf{x}. \quad (3.58)$$

The crucial difference between $\boldsymbol{\mu}_Q(\mathbf{z}_t, \mathbf{x}; s, t)$ and $\boldsymbol{\mu}_\theta(\mathbf{z}_t; s, t)$ is that, in the latter, the observed data \mathbf{x} is replaced by our image prediction model $\hat{\mathbf{x}}_\theta(\mathbf{z}_t; t)$ with parameters θ :

$$\boldsymbol{\mu}_\theta(\mathbf{z}_t; s, t) = \frac{\alpha_{t|s} \sigma_s^2}{\sigma_t^2} \mathbf{z}_t + \frac{\alpha_s \sigma_{t|s}^2}{\sigma_t^2} \hat{\mathbf{x}}_\theta(\mathbf{z}_t; t). \quad (3.59)$$

It is worth noting at this stage that there are multiple equivalent parameterizations beyond image-prediction $\hat{\mathbf{x}}_\theta(\mathbf{z}_t; t)$, e.g. noise and velocity prediction, all of which can be reparameterized to compute the posterior mean estimate $\boldsymbol{\mu}_\theta(\mathbf{z}_t; s, t)$. For consistency, we will continue to use the image-prediction version for now and provide a detailed derivation of the alternatives in Section 4.

3.6 Variational Lower Bound

The optimization objective of a discrete-time variational diffusion model is the ELBO in Equation 2.34, i.e. the same as a hierarchical VAE's with a *top-down* inference model. For consistency, we re-express the VLB here using the discrete-time index notation: $s(i) = (i-1)/T$, $t(i) = i/T$: $-\log p(\mathbf{x})$

$$\leq -\mathbb{E}_{q(\mathbf{z}_0|\mathbf{x})} [\log p(\mathbf{x} | \mathbf{z}_0)] + D_{\text{KL}}(q(\mathbf{z}_1 | \mathbf{x}) \| p(\mathbf{z}_1)) + \mathcal{L}_T(\mathbf{x}) \quad (3.60)$$

$$= -\text{VLB}(\mathbf{x}), \quad (\text{free energy}) \quad (3.61)$$

where the so-called diffusion loss $\mathcal{L}_T(\mathbf{x})$ term is given by:

$$\mathcal{L}_T(\mathbf{x}) = \sum_{i=1}^T \mathbb{E}_{q(\mathbf{z}_{t(i)}|\mathbf{x})} \left[D_{\text{KL}}(q(\mathbf{z}_{s(i)} | \mathbf{z}_{t(i)}, \mathbf{x}) \| p(\mathbf{z}_{s(i)} | \mathbf{z}_{t(i)})) \right]. \quad (3.62)$$

The remaining terms are the familiar expected reconstruction loss and KL of the posterior from the prior. For reasons explained in detail in Section 3.4 and Appendix A.3.2, under a well-specified diffusion process, these terms can be safely omitted in practice as they do not provide meaningful contributions to the diffusion loss.

3.6.1 Deriving the KL Divergence Terms

Minimizing the diffusion loss $\mathcal{L}_T(\mathbf{x})$ involves computing the (expected) KL divergence of the posterior from the prior, at each noise level. [Kingma et al. \(2021\)](#) provide a relatively detailed derivation of $D_{\text{KL}}(q(\mathbf{z}_{s(i)} | \mathbf{z}_{t(i)}, \mathbf{x}) \| p(\mathbf{z}_{s(i)} | \mathbf{z}_{t(i)}))$; we re-derive it here for completeness, whilst adding some additional instructive details to aid in understanding.

Using s and t as shorthand notation for $s(i)$ and $t(i)$, recall that the posterior is given by:

$$q(\mathbf{z}_s | \mathbf{z}_t, \mathbf{x}) = \mathcal{N} \left(\mathbf{z}_s; \boldsymbol{\mu}_Q(\mathbf{z}_t, \mathbf{x}; s, t), \sigma_Q^2(s, t) \mathbf{I} \right), \quad (3.63)$$

$$\boldsymbol{\mu}_Q(\mathbf{z}_t, \mathbf{x}; s, t) = \frac{\alpha_{t|s} \sigma_s^2}{\sigma_t^2} \mathbf{z}_t + \frac{\alpha_s \sigma_{t|s}^2}{\sigma_t^2} \mathbf{x}, \quad (3.64)$$

and since we have defined our generative model as $p(\mathbf{z}_s | \mathbf{z}_t) = q(\mathbf{z}_s | \mathbf{z}_t, \mathbf{x} = \hat{\mathbf{x}}_{\boldsymbol{\theta}}(\mathbf{z}_t; t))$ we have

$$p(\mathbf{z}_s | \mathbf{z}_t) = \mathcal{N} \left(\mathbf{z}_s; \boldsymbol{\mu}_{\boldsymbol{\theta}}(\mathbf{z}_t; s, t), \sigma_Q^2(s, t) \mathbf{I} \right), \quad (3.65)$$

$$\boldsymbol{\mu}_{\boldsymbol{\theta}}(\mathbf{z}_t; s, t) = \frac{\alpha_{t|s}\sigma_s^2}{\sigma_t^2}\mathbf{z}_t + \frac{\alpha_s\sigma_{t|s}^2}{\sigma_t^2}\hat{\mathbf{x}}_{\boldsymbol{\theta}}(\mathbf{z}_t; t). \quad (3.66)$$

Of particular importance is the fact that the variances of both $q(\mathbf{z}_s | \mathbf{z}_t, \mathbf{x})$ and $p(\mathbf{z}_s | \mathbf{z}_t)$ are equal:

$$\sigma_Q^2(s, t) = \frac{\sigma_{t|s}^2\sigma_s^2}{\alpha_{t|s}^2\sigma_s^2 + \sigma_{t|s}^2} = \frac{\sigma_{t|s}^2\sigma_s^2}{\sigma_t^2}, \quad (3.67)$$

where the result in Equation 3.22, $\sigma_{t|s}^2 = \sigma_t^2 - \alpha_{t|s}^2\sigma_s^2$, simplifies the denominator. Furthermore, both distributions have identical isotropic/spherical covariances: $\sigma_Q^2(s, t)\mathbf{I}$, which we denote as $\sigma_Q^2\mathbf{I}$ for short.

The KL divergence between D -dimensional Gaussian distributions is available in closed form, thus:

$$D_{\text{KL}}(q(\mathbf{z}_s | \mathbf{z}_t, \mathbf{x}) \| p(\mathbf{z}_s | \mathbf{z}_t)) \quad (3.68)$$

$$= \frac{1}{2} \left[\text{Tr} \left(\frac{1}{\sigma_Q^2} \mathbf{I} \sigma_Q^2 \mathbf{I} \right) - D + (\boldsymbol{\mu}_{\boldsymbol{\theta}} - \boldsymbol{\mu}_Q)^\top \frac{1}{\sigma_Q^2} \mathbf{I} (\boldsymbol{\mu}_{\boldsymbol{\theta}} - \boldsymbol{\mu}_Q) \right] \quad (3.69)$$

$$+ \log \frac{\det(\sigma_Q^2 \mathbf{I})}{\det(\sigma_Q^2 \mathbf{I})} \quad (3.70)$$

$$= \frac{1}{2} \left[D - D + \frac{1}{\sigma_Q^2} (\boldsymbol{\mu}_{\boldsymbol{\theta}} - \boldsymbol{\mu}_Q)^\top (\boldsymbol{\mu}_{\boldsymbol{\theta}} - \boldsymbol{\mu}_Q) + 0 \right] \quad (3.71)$$

$$= \frac{1}{2\sigma_Q^2} \sum_{i=1}^D (\boldsymbol{\mu}_{Q,i} - \boldsymbol{\mu}_{\boldsymbol{\theta},i})^2 \quad (3.72)$$

$$= \frac{1}{2\sigma_Q^2(s, t)} \left\| \boldsymbol{\mu}_Q(\mathbf{z}_t, \mathbf{x}; s, t) - \boldsymbol{\mu}_{\boldsymbol{\theta}}(\mathbf{z}_t; s, t) \right\|_2^2. \quad (3.73)$$

It is possible to simplify the above equation quite significantly, resulting in a short expression involving the signal-to-noise ratio of the diffused data. To that end, expressing Equation 3.73 in terms of the denoising model $\hat{\mathbf{x}}_{\boldsymbol{\theta}}(\mathbf{z}_t; t)$ we get:

$$D_{\text{KL}}(q(\mathbf{z}_s | \mathbf{z}_t, \mathbf{x}) \| p(\mathbf{z}_s | \mathbf{z}_t)) \quad (3.74)$$

$$= \frac{1}{2\sigma_Q^2(s, t)} \left\| \boldsymbol{\mu}_Q(\mathbf{z}_t, \mathbf{x}; s, t) - \boldsymbol{\mu}_{\boldsymbol{\theta}}(\mathbf{z}_t; s, t) \right\|_2^2 \quad (3.75)$$

$$= \frac{1}{2\sigma_Q^2(s, t)} \left\| \frac{\alpha_{t|s}\sigma_s^2}{\sigma_t^2} \mathbf{z}_t + \frac{\alpha_s\sigma_{t|s}^2}{\sigma_t^2} \mathbf{x} - \left(\frac{\alpha_{t|s}\sigma_s^2}{\sigma_t^2} \mathbf{z}_t + \frac{\alpha_s\sigma_{t|s}^2}{\sigma_t^2} \hat{\mathbf{x}}_{\theta}(\mathbf{z}_t; t) \right) \right\|_2^2 \quad (3.76)$$

$$= \frac{1}{2\sigma_Q^2(s, t)} \left\| \frac{\alpha_s\sigma_{t|s}^2}{\sigma_t^2} \mathbf{x} - \frac{\alpha_s\sigma_{t|s}^2}{\sigma_t^2} \hat{\mathbf{x}}_{\theta}(\mathbf{z}_t; t) \right\|_2^2 \quad (3.77)$$

$$= \frac{1}{2\sigma_Q^2(s, t)} \left(\frac{\alpha_s\sigma_{t|s}^2}{\sigma_t^2} \right)^2 \|\mathbf{x} - \hat{\mathbf{x}}_{\theta}(\mathbf{z}_t; t)\|_2^2 \quad (3.78)$$

$$= \frac{\sigma_t^2}{2\sigma_{t|s}^2\sigma_s^2} \frac{\alpha_s^2\sigma_{t|s}^4}{\sigma_t^4} \|\mathbf{x} - \hat{\mathbf{x}}_{\theta}(\mathbf{z}_t; t)\|_2^2 \quad (\text{recall } \sigma_Q^2(s, t) = (\sigma_{t|s}^2\sigma_s^2)/\sigma_t^2) \quad (3.79)$$

$$= \frac{1}{2\sigma_s^2} \frac{\alpha_s^2\sigma_{t|s}^2}{\sigma_t^2} \|\mathbf{x} - \hat{\mathbf{x}}_{\theta}(\mathbf{z}_t; t)\|_2^2 \quad (\text{exponents cancel}) \quad (3.80)$$

$$= \frac{1}{2\sigma_s^2} \frac{\alpha_s^2(\sigma_t^2 - \alpha_{t|s}^2\sigma_s^2)}{\sigma_t^2} \|\mathbf{x} - \hat{\mathbf{x}}_{\theta}(\mathbf{z}_t; t)\|_2^2 \quad (\text{recall } \sigma_{t|s}^2 = \sigma_t^2 - \alpha_{t|s}^2\sigma_s^2) \quad (3.81)$$

$$= \frac{1}{2} \frac{\sigma_s^{-2} \left(\alpha_s^2\sigma_t^2 - \alpha_s^2\frac{\alpha_t^2}{\sigma_s^2}\sigma_s^2 \right)}{\sigma_t^2} \|\mathbf{x} - \hat{\mathbf{x}}_{\theta}(\mathbf{z}_t; t)\|_2^2 \quad (3.82)$$

$$= \frac{1}{2} \frac{\alpha_s^2\sigma_t^2\sigma_s^{-2} - \alpha_t^2}{\sigma_t^2} \|\mathbf{x} - \hat{\mathbf{x}}_{\theta}(\mathbf{z}_t; t)\|_2^2 \quad (3.83)$$

$$= \frac{1}{2} \left(\frac{\alpha_s^2\sigma_t^2}{\sigma_s^2} \frac{1}{\sigma_t^2} - \frac{\alpha_t^2}{\sigma_t^2} \right) \|\mathbf{x} - \hat{\mathbf{x}}_{\theta}(\mathbf{z}_t; t)\|_2^2 \quad (3.84)$$

$$= \frac{1}{2} \left(\frac{\alpha_s^2}{\sigma_s^2} - \frac{\alpha_t^2}{\sigma_t^2} \right) \|\mathbf{x} - \hat{\mathbf{x}}_{\theta}(\mathbf{z}_t; t)\|_2^2 \quad (3.85)$$

$$= \frac{1}{2} (\text{SNR}(s) - \text{SNR}(t)) \|\mathbf{x} - \hat{\mathbf{x}}_{\theta}(\mathbf{z}_t; t)\|_2^2. \quad (3.86)$$

In words, the final expression shows that the diffusion loss, at timestep t , consists of a squared error term involving the data \mathbf{x} and the model $\hat{\mathbf{x}}_{\theta}(\mathbf{z}_t; t)$, weighted by a difference in signal-to-noise ratio at s and t .

3.7 Estimator of the Discrete-Time Diffusion Loss

For model training, we can compute the diffusion loss $\mathcal{L}_T(\mathbf{x})$ with an unbiased Monte Carlo estimator by:

(i) Using the *reparameterisation gradient estimator* (Kingma and Welling, 2013; Rezende et al., 2014) to sample $\mathbf{z}_t \sim q(\mathbf{z}_t \mid \mathbf{x})$:

$$\mathbf{z}_t = \alpha_t \mathbf{x} + \sigma_t \boldsymbol{\epsilon} := g_{\alpha_t, \sigma_t}(\boldsymbol{\epsilon}, \mathbf{x}), \quad \boldsymbol{\epsilon} \sim p(\boldsymbol{\epsilon}) = \mathcal{N}(0, \mathbf{I}). \quad (3.87)$$

(ii) Avoid computing all T loss terms by selecting a single timestep, sampled uniformly at random from $i \sim U\{1, T\}$, at each iteration.

Under the above setup, the estimator of the diffusion loss is given by:

$$\mathcal{L}_T(\mathbf{x}) = \sum_{i=1}^T \mathbb{E}_{q(\mathbf{z}_{t(i)} \mid \mathbf{x})} \left[D_{\text{KL}}(q(\mathbf{z}_{s(i)} \mid \mathbf{z}_{t(i)}, \mathbf{x}) \parallel p(\mathbf{z}_{s(i)} \mid \mathbf{z}_{t(i)})) \right] \quad (3.88)$$

$$= \sum_{i=1}^T \mathbb{E}_{q(\mathbf{z}_t \mid \mathbf{x})} [D_{\text{KL}}(q(\mathbf{z}_s \mid \mathbf{z}_t, \mathbf{x}) \parallel p(\mathbf{z}_s \mid \mathbf{z}_t))] \quad (\text{using shorthand notation } s, t) \quad (3.89)$$

$$= \sum_{i=1}^T \int \left(\frac{1}{2} (\text{SNR}(s) - \text{SNR}(t)) \|\mathbf{x} - \hat{\mathbf{x}}_{\boldsymbol{\theta}}(\mathbf{z}_t; t)\|_2^2 \right) q(\mathbf{z}_t \mid \mathbf{x}) d\mathbf{z}_t \quad (\text{from Equation 3.86}) \quad (3.90)$$

$$= \frac{1}{2} \int \left(\sum_{i=1}^T (\text{SNR}(s) - \text{SNR}(t)) \|\mathbf{x} - \hat{\mathbf{x}}_{\boldsymbol{\theta}}(g_{\alpha_t, \sigma_t}(\boldsymbol{\epsilon}, \mathbf{x}); t)\|_2^2 \right) p(\boldsymbol{\epsilon}) d\boldsymbol{\epsilon} \quad (\text{as } \mathbf{z}_t = \alpha_t \mathbf{x} + \sigma_t \boldsymbol{\epsilon}) \quad (3.91)$$

$$= \frac{1}{2} \mathbb{E}_{\boldsymbol{\epsilon} \sim \mathcal{N}(0, \mathbf{I})} \left[T \cdot \mathbb{E}_{i \sim U\{1, T\}} \left[(\text{SNR}(s) - \text{SNR}(t)) \|\mathbf{x} - \hat{\mathbf{x}}_{\boldsymbol{\theta}}(\mathbf{z}_t; t)\|_2^2 \right] \right] \quad (\text{Monte Carlo estimate}) \quad (3.92)$$

$$= \frac{T}{2} \mathbb{E}_{\boldsymbol{\epsilon} \sim \mathcal{N}(0, \mathbf{I}), i \sim U\{1, T\}} \left[(\text{SNR}(s) - \text{SNR}(t)) \|\mathbf{x} - \hat{\mathbf{x}}_{\boldsymbol{\theta}}(\mathbf{z}_t; t)\|_2^2 \right]. \quad (3.93)$$

For clarity, above we used Monte Carlo estimation and a basic identity to arrive at Equation 3.92:

$$\mathbb{E}_q [f(x)] \approx \frac{1}{T} \sum_{i=1}^T f(x_i) \implies T \cdot \mathbb{E}_q [f(x)] \approx \sum_{i=1}^T f(x_i), \quad (3.94)$$

where $x_i \sim q$ are random samples from a distribution q , which is representative of $U\{1, T\}$ in our case.

Equation 3.93 can be rewritten in terms of the more commonly used noise-prediction model $\hat{\epsilon}_{\theta}(\mathbf{z}_t; t)$ (Ho et al., 2020) as follows:

$$\begin{aligned} \mathcal{L}_T(\mathbf{x}) &= \frac{T}{2} \mathbb{E}_{\epsilon \sim \mathcal{N}(0, \mathbf{I}), i \sim U\{1, T\}} \left[(\text{SNR}(s) - \text{SNR}(t)) \right. \\ &\quad \cdot \left. \left\| \frac{\mathbf{z}_t - \sigma_t \epsilon}{\alpha_t} - \frac{\mathbf{z}_t - \sigma_t \hat{\epsilon}_{\theta}(\mathbf{z}_t; t)}{\alpha_t} \right\|_2^2 \right] \\ &\quad (\text{since } \mathbf{x} = (\mathbf{z}_t - \sigma_t \epsilon_t) / \alpha_t) \quad (3.95) \end{aligned}$$

$$= \frac{T}{2} \mathbb{E}_{\epsilon \sim \mathcal{N}(0, \mathbf{I}), i \sim U\{1, T\}} \left[(\text{SNR}(s) - \text{SNR}(t)) \left\| \frac{\sigma_t}{\alpha_t} (\hat{\epsilon}_{\theta}(\mathbf{z}_t; t) - \epsilon) \right\|_2^2 \right] \quad (3.96)$$

$$= \frac{T}{2} \mathbb{E}_{\epsilon \sim \mathcal{N}(0, \mathbf{I}), i \sim U\{1, T\}} \left[\frac{\sigma_t^2}{\alpha_t^2} (\text{SNR}(s) - \text{SNR}(t)) \|\epsilon - \hat{\epsilon}_{\theta}(\mathbf{z}_t; t)\|_2^2 \right] \quad (3.97)$$

$$\begin{aligned} &= \frac{T}{2} \mathbb{E}_{\epsilon \sim \mathcal{N}(0, \mathbf{I}), i \sim U\{1, T\}} \left[\text{SNR}(t)^{-1} (\text{SNR}(s) - \text{SNR}(t)) \right. \\ &\quad \cdot \left. \|\epsilon - \hat{\epsilon}_{\theta}(\mathbf{z}_t; t)\|_2^2 \right] \quad (3.98) \end{aligned}$$

$$= \frac{T}{2} \mathbb{E}_{\epsilon \sim \mathcal{N}(0, \mathbf{I}), i \sim U\{1, T\}} \left[\left(\frac{\text{SNR}(s)}{\text{SNR}(t)} - 1 \right) \|\epsilon - \hat{\epsilon}_{\theta}(\mathbf{z}_t; t)\|_2^2 \right]. \quad (3.99)$$

For more details on the noise prediction parameterization please refer to Section 4. The above estimator of the loss can be made more stable in practice by re-expressing the constant term inside the expectation using numerically stable primitives. For details, please refer to Appendix A.3.1.

3.7.1 Ancestral Sampling

Once trained, to randomly sample from our generative diffusion model:

$$p(\mathbf{x} \mid \mathbf{z}_0) \prod_{i=1}^T p(\mathbf{z}_{s(i)} \mid \mathbf{z}_{t(i)}), \quad (3.100)$$

we can perform what's known as *ancestral sampling*. That is, we start with noise $\mathbf{z}_1 \sim \mathcal{N}(0, \mathbf{I})$ and follow the estimated reverse Markov Chain:

$$\mathbf{z}_1 \rightarrow \mathbf{z}_{(T-1)/T} \rightarrow \mathbf{z}_{(T-2)/T} \rightarrow \cdots \rightarrow \mathbf{z}_0 \rightarrow \mathbf{x}. \quad (3.101)$$

Since the forward process transitions are Markovian and linear Gaussian, the top-down posterior is tractable due to Gaussian conjugacy. Furthermore, our generative model is defined to be equal to the top-down posterior, that is, for time $s < t$:

$$p(\mathbf{z}_s \mid \mathbf{z}_t) = q(\mathbf{z}_s \mid \mathbf{z}_t, \mathbf{x} = \hat{\mathbf{x}}_{\theta}(\mathbf{z}_t; t)), \quad (3.102)$$

with a denoising model $\hat{\mathbf{x}}_{\theta}(\mathbf{z}_t; t)$ in place of \mathbf{x} . Thus, we can use our estimate of the posterior mean $\mu_{\theta}(\mathbf{z}_t; s, t)$ to sample from q in reverse order, according to the following update rule, for any $s < t$:

$$\mathbf{z}_s = \mu_{\theta}(\mathbf{z}_t; s, t) + \sigma_Q(s, t)\boldsymbol{\epsilon} \quad (3.103)$$

$$= \frac{\alpha_s}{\alpha_t} (\mathbf{z}_t - \sigma_t c \hat{\boldsymbol{\epsilon}}_{\theta}(\mathbf{z}_t; t)) + \sqrt{1 - \alpha_s^2 c} \boldsymbol{\epsilon}, \quad (3.104)$$

where $c = -\text{expm1}(\gamma_{\eta}(s) - \gamma_{\eta}(t))$, $\boldsymbol{\epsilon} \sim \mathcal{N}(0, \mathbf{I})$, and we used the fact that $\sigma_s = \sqrt{1 - \alpha_s^2}$ by definition in a variance-preserving diffusion process. For details on related derivations please see Appendix A.3.

3.8 Reverse Process: Continuous-Time Generative Model

A continuous-time variational diffusion model ($T \rightarrow \infty$) corresponds to the infinitely deep limit of a hierarchical VAE, when the diffusion process (noise schedule) is learned rather than fixed. As previously alluded to, the extension of diffusion models to continuous-time has been proven to be advantageous by various authors (Song et al., 2021b; Kingma et al., 2021; Huang et al., 2021; Vahdat et al., 2021).

In this section, we explain why using a continuous-time VLB is strictly preferable over a discrete-time version and provide detailed derivations of its estimator in terms of a denoising and noise-prediction model. Note that, due to the shared notation between discrete and continuous-time models introduced in Section 3.4, the various derivations and results therein (e.g. for $p(\mathbf{z}_s \mid \mathbf{z}_t)$) are equally applicable for the continuous-time version presented in this section.

3.9 On Infinite Depth

Kingma et al. (2021) showed that doubling the number of timesteps T always improves the diffusion loss, which suggests we should optimize a continuous-time VLB, with $T \rightarrow \infty$. This finding is straightforward to verify; we start by recalling that the discrete-time diffusion loss using T steps is given by: $\mathcal{L}_T(\mathbf{x})$

$$= \frac{1}{2} \mathbb{E}_{\epsilon \sim \mathcal{N}(0, \mathbf{I})} \left[\sum_{i=1}^T (\text{SNR}(s(i)) - \text{SNR}(t(i))) \left\| \mathbf{x} - \hat{\mathbf{x}}_{\theta}(\mathbf{z}_{t(i)}; t(i)) \right\|_2^2 \right], \quad (3.105)$$

where $s(i) = (i-1)/T$ and $t(i) = i/T$. To double the number of timesteps T , we can introduce a new symbol $t'(i)$ to represent an interpolation between $s(i)$ and $t(i)$, defined as:

$$t'(i) = \frac{s(i) + t(i)}{2} = \frac{1}{2} \left(\frac{i-1}{T} + \frac{i}{T} \right) = \frac{i-0.5}{T} = t(i) - \frac{0.5}{T}. \quad (3.106)$$

Using shorthand notation s , t and t' for $s(i)$, $t(i)$ and $t'(i)$; the diffusion loss with T timesteps can be written equivalently to Equation 3.105 as:

$$\begin{aligned} \mathcal{L}_T(\mathbf{x}) = \frac{1}{2} \mathbb{E}_{\epsilon \sim \mathcal{N}(0, \mathbf{I})} \left[\sum_{i=1}^T (\text{SNR}(s) - \text{SNR}(t') \right. \\ \left. + \text{SNR}(t') - \text{SNR}(t)) \left\| \mathbf{x} - \hat{\mathbf{x}}_{\theta}(\mathbf{z}_t; t) \right\|_2^2 \right], \quad (3.107) \end{aligned}$$

whereas the new diffusion loss with $2T$ timesteps is given by:

$$\mathcal{L}_{2T}(\mathbf{x}) = \frac{1}{2} \mathbb{E}_{\epsilon \sim \mathcal{N}(0, \mathbf{I})} \left[\sum_{i=1}^T (\text{SNR}(s) - \text{SNR}(t')) \right.$$

$$\cdot \|\mathbf{x} - \hat{\mathbf{x}}_{\theta}(\mathbf{z}_{t'}; t')\|_2^2 + (\text{SNR}(t') - \text{SNR}(t)) \|\mathbf{x} - \hat{\mathbf{x}}_{\theta}(\mathbf{z}_t; t)\|_2^2 \Big]. \quad (3.108)$$

If we then subtract the two losses and cancel out common terms we get the following:

$$\begin{aligned} \mathcal{L}_{2T}(\mathbf{x}) - \mathcal{L}_T(\mathbf{x}) &= \frac{1}{2} \mathbb{E}_{\epsilon \sim \mathcal{N}(0, \mathbf{I})} \Bigg[\\ &\sum_{i=1}^T \left\{ \text{SNR}(s) \|\mathbf{x} - \hat{\mathbf{x}}_{\theta}(\mathbf{z}_{t'}; t')\|_2^2 - \text{SNR}(t') \|\mathbf{x} - \hat{\mathbf{x}}_{\theta}(\mathbf{z}_{t'}; t')\|_2^2 \right. \\ &\quad \left. + \text{SNR}(t') \|\mathbf{x} - \hat{\mathbf{x}}_{\theta}(\mathbf{z}_t; t)\|_2^2 - \text{SNR}(t) \|\mathbf{x} - \hat{\mathbf{x}}_{\theta}(\mathbf{z}_t; t)\|_2^2 \right\} \\ &- \left(\sum_{i=1}^T \text{SNR}(s) \|\mathbf{x} - \hat{\mathbf{x}}_{\theta}(\mathbf{z}_t; t)\|_2^2 - \text{SNR}(t') \|\mathbf{x} - \hat{\mathbf{x}}_{\theta}(\mathbf{z}_t; t)\|_2^2 \right. \\ &\quad \left. + \text{SNR}(t') \|\mathbf{x} - \hat{\mathbf{x}}_{\theta}(\mathbf{z}_t; t)\|_2^2 - \text{SNR}(t) \|\mathbf{x} - \hat{\mathbf{x}}_{\theta}(\mathbf{z}_t; t)\|_2^2 \right) \Bigg] \end{aligned} \quad (3.109)$$

$$\begin{aligned} &= \frac{1}{2} \mathbb{E}_{\epsilon \sim \mathcal{N}(0, \mathbf{I})} \Bigg[\sum_{i=1}^T (\text{SNR}(s) - \text{SNR}(t')) \\ &\quad \cdot \left(\|\mathbf{x} - \hat{\mathbf{x}}_{\theta}(\mathbf{z}_{t'}; t')\|_2^2 - \|\mathbf{x} - \hat{\mathbf{x}}_{\theta}(\mathbf{z}_t; t)\|_2^2 \right) \Bigg]. \quad (3.110) \end{aligned}$$

We can use Equation 3.110 to justify optimizing a continuous-time objective. Since $t' < t$, the prediction error term with $\mathbf{z}_{t'}$ will be lower than the one with \mathbf{z}_t , as $\mathbf{z}_{t'}$ is a less noisy version of \mathbf{x} from earlier on in the diffusion process. In other words, it is always easier to predict \mathbf{x} from $\mathbf{z}_{t'}$ than from \mathbf{z}_t , given an adequately trained model. Formally, doubling the number of timesteps T always improves the VLB:

$$\mathcal{L}_{2T}(\mathbf{x}) - \mathcal{L}_T(\mathbf{x}) < 0 \implies \text{VLB}_{2T}(\mathbf{x}) > \text{VLB}_T(\mathbf{x}), \quad \forall T \in \mathbb{N}^+. \quad (3.111)$$

Thus it is strictly advantageous to optimize a continuous-time VLB, where $T \rightarrow \infty$ and time t is treated as continuous rather than discrete.

3.10 Estimator of the Continuous-Time Diffusion Loss

To arrive at an unbiased Monte Carlo estimator of the continuous-time diffusion loss $\mathcal{L}_\infty(\mathbf{x})$, we can first take the discrete-time version and substitute in the time segment width $\tau = 1/T$ to reveal:

$$\mathcal{L}_T(\mathbf{x}) =$$

$$= \frac{T}{2} \mathbb{E}_{\epsilon \sim \mathcal{N}(0, \mathbf{I}), i \sim U\{1, T\}} \left[(\text{SNR}(s) - \text{SNR}(t)) \|\mathbf{x} - \hat{\mathbf{x}}_\theta(\mathbf{z}_t; t)\|_2^2 \right] \quad (3.112)$$

$$= \frac{1}{2} \mathbb{E}_{\epsilon \sim \mathcal{N}(0, \mathbf{I}), i \sim U\{1, T\}} \left[\right. \quad (3.113)$$

$$\left. T \left(\text{SNR} \left(t - \frac{1}{T} \right) - \text{SNR}(t) \right) \|\mathbf{x} - \hat{\mathbf{x}}_\theta(\mathbf{z}_t; t)\|_2^2 \right] \quad (\text{since } s = (i-1)/T) \quad (3.114)$$

$$= \frac{1}{2} \mathbb{E}_{\epsilon \sim \mathcal{N}(0, \mathbf{I}), i \sim U\{1, T\}} \left[\frac{\text{SNR}(t - \tau) - \text{SNR}(t)}{\tau} \|\mathbf{x} - \hat{\mathbf{x}}_\theta(\mathbf{z}_t; t)\|_2^2 \right], \quad (\text{substitute } \tau = 1/T) \quad (3.115)$$

again using the shorthand notation s and t for $s(i) = (i-1)/T$ and $t(i) = i/T$, respectively.

The constant inside the expectation in Equation 3.115 is readily recognized as the (negative) *backward difference* numerical approximation to the derivative of $\text{SNR}(t)$ w.r.t t , since:

$$\frac{d \text{SNR}(t)}{dt} = \lim_{\tau \rightarrow 0} \frac{\text{SNR}(t + \tau) - \text{SNR}(t)}{\tau} \quad (\text{forward diff.}) \quad (3.116)$$

$$= \lim_{\tau \rightarrow 0} \frac{\text{SNR}(t) - \text{SNR}(t - \tau)}{\tau}, \quad (\text{backward diff.}) \quad (3.117)$$

and therefore

$$\lim_{\tau \rightarrow 0} \frac{\text{SNR}(t - \tau) - \text{SNR}(t)}{\tau} = \lim_{\tau \rightarrow 0} -\frac{\text{SNR}(t) - \text{SNR}(t - \tau)}{\tau} \quad (3.118)$$

$$= -\frac{d \text{SNR}(t)}{dt}. \quad (3.119)$$

Thus taking the limit as $T \rightarrow \infty$ of the discrete-time diffusion loss:

$$\mathcal{L}_\infty(\mathbf{x}) = \lim_{T \rightarrow \infty} \frac{1}{2} \mathbb{E}_{\epsilon \sim \mathcal{N}(0, \mathbf{I})} \left[\sum_{i=1}^T (\text{SNR}(s) - \text{SNR}(t)) \|\mathbf{x} - \hat{\mathbf{x}}_\theta(\mathbf{z}_t; t)\|_2^2 \right] \quad (3.120)$$

$$= \lim_{T \rightarrow \infty} \frac{1}{2} \mathbb{E}_{\epsilon \sim \mathcal{N}(0, \mathbf{I}), i \sim U\{1, T\}} \left[\frac{\text{SNR}(t - \tau) - \text{SNR}(t)}{\tau} \|\mathbf{x} - \hat{\mathbf{x}}_\theta(\mathbf{z}_t; t)\|_2^2 \right] \quad (3.121)$$

$$= \frac{1}{2} \mathbb{E}_{\epsilon \sim \mathcal{N}(0, \mathbf{I})} \left[\int_0^1 -\frac{d \text{SNR}(t)}{dt} \|\mathbf{x} - \hat{\mathbf{x}}_\theta(\mathbf{z}_t; t)\|_2^2 dt \right] \quad (3.122)$$

$$= -\frac{1}{2} \mathbb{E}_{\epsilon \sim \mathcal{N}(0, \mathbf{I}), t \sim \mathcal{U}(0, 1)} [\text{SNR}'(t) \|\mathbf{x} - \hat{\mathbf{x}}_\theta(\mathbf{z}_t; t)\|_2^2]. \quad (3.124)$$

We can express the above in terms of the noise-prediction model $\hat{\epsilon}_\theta(\mathbf{z}_t; t)$ as follows:

$$\text{SNR}'(t) \|\mathbf{x} - \hat{\mathbf{x}}_\theta(\mathbf{z}_t; t)\|_2^2 \quad (3.125)$$

$$= \text{SNR}'(t) \left\| \frac{\mathbf{z}_t - \sigma_t \epsilon}{\alpha_t} - \frac{\mathbf{z}_t - \sigma_t \hat{\epsilon}_\theta(\mathbf{z}_t; t)}{\alpha_t} \right\|_2^2 \quad (3.126)$$

$$= \text{SNR}'(t) \left\| \frac{\sigma_t}{\alpha_t} (\epsilon - \hat{\epsilon}_\theta(\mathbf{z}_t; t)) \right\|_2^2 \quad (\text{cancel } \mathbf{z}_t \text{ terms and factor}) \quad (3.127)$$

$$= \text{SNR}'(t) \cdot \frac{\sigma_t^2}{\alpha_t^2} \|\epsilon - \hat{\epsilon}_\theta(\mathbf{z}_t; t)\|_2^2 \quad (3.128)$$

$$= \text{SNR}'(t) \cdot \text{SNR}(t)^{-1} \|\epsilon - \hat{\epsilon}_\theta(\mathbf{z}_t; t)\|_2^2 \quad (\text{SNR}(t) = \alpha_t^2 / \sigma_t^2) \quad (3.129)$$

$$= \text{SNR}(t)^{-1} \cdot \frac{d}{dt} e^{-\gamma_\eta(t)} \|\epsilon - \hat{\epsilon}_\theta(\mathbf{z}_t; t)\|_2^2 \quad (3.130)$$

$$= \text{SNR}(t)^{-1} \cdot e^{-\gamma_\eta(t)} \cdot -\frac{d}{dt} \gamma_\eta(t) \|\epsilon - \hat{\epsilon}_\theta(\mathbf{z}_t; t)\|_2^2 \quad (\text{chain rule}) \quad (3.131)$$

$$= \frac{1}{e^{-\gamma_\eta(t)}} \cdot e^{-\gamma_\eta(t)} \cdot -\frac{d}{dt} \gamma_\eta(t) \|\epsilon - \hat{\epsilon}_\theta(\mathbf{z}_t; t)\|_2^2 \quad (\text{SNR}(t) = e^{-\gamma_\eta(t)}) \quad (3.132)$$

$$= -\gamma'_\eta(t) \|\epsilon - \hat{\epsilon}_\theta(\mathbf{z}_t; t)\|_2^2, \quad (3.133)$$

where the simplified form of $\text{SNR}(t) = \exp(-\gamma_\eta(t))$ derived in Equation A.14 was used to arrive at the final result. Plugging the final expression back into the expected loss in Equation 3.124 we get

$$\mathcal{L}_\infty(\mathbf{x}) = \frac{1}{2} \mathbb{E}_{\epsilon \sim \mathcal{N}(0, \mathbf{I}), t \sim \mathcal{U}(0, 1)} \left[\gamma'_\eta(t) \|\boldsymbol{\epsilon} - \hat{\boldsymbol{\epsilon}}_\theta(\mathbf{z}_t; t)\|_2^2 \right] \quad (3.134)$$

$$= \mathbb{E}_{q(\mathbf{z}_0 | \mathbf{x})} [\log p(\mathbf{x} | \mathbf{z}_0)] - D_{\text{KL}}(q(\mathbf{z}_1 | \mathbf{x}) \parallel p(\mathbf{z}_1)) - \text{VLB}(\mathbf{x}) \quad (3.135)$$

$$= -\text{VLB}(\mathbf{x}) + c, \quad (3.136)$$

where $c \approx 0$ is constant with respect to the model parameters of $\hat{\boldsymbol{\epsilon}}_\theta(\mathbf{z}_t; t)$. For more details on related aspects please refer to Appendix A.3.2.

In the next section, we explain why the continuous-time VLB derived in this section is invariant to the noise schedule of the forward diffusion process, except for at its endpoints. In other words, the VLB is unaffected by the shape of the signal-to-noise ratio function $\text{SNR}(t)$ between $t = 0$ and $t = 1$. We also explain how this invariance holds for models that optimize a *weighted* diffusion loss rather than the standard VLB, and connect the many weighted diffusion objectives used in practice to maximizing this principled variational lower bound.

4

Understanding Diffusion Objectives

In this section, we provide a deeper understanding of diffusion models. We start by covering many of the different diffusion losses and network output parameterizations commonly used in literature, namely:

- (i) Image Prediction ([Sohl-Dickstein et al., 2015; Kingma et al., 2021](#));
- (ii) Noise Prediction ([Ho et al., 2020](#));
- (iii) Score-based ([Song et al., 2021b,a](#));
- (iv) Energy-based ([Salimans and Ho, 2021; Du et al., 2023](#));
- (v) Velocity Prediction ([Salimans and Ho, 2022](#));
- (vi) Flow-based ([Lipman et al., 2023; Albergo and Vanden-Eijnden, 2023; Liu et al., 2023](#)).

We show in detail how all these parameterizations are equivalently valid, as each one can be expressed in terms of the others using a simple linear function. This implies that one can, for example, choose a parameterization for training and then reparameterize during inference. A common use case is to train a noise prediction model, then reparameterize it

back to image space at inference time to clip the predicted image to a valid range (e.g. $[-1, 1]$) at each denoising step. This has been shown to mitigate the accumulation of sampling errors in practice, thereby improving sample quality.

We then explain the close connection between *weighted* diffusion losses used in practice and maximizing the variational lower bound (i.e. the ELBO). Our exposition is designed to be instructive and consistent with VDM++ (Kingma and Gao, 2023), without departing too far from the material already covered and the notation already used. In Sections 3.4 and 3.8 we established that diffusion-based objectives correspond directly to the ELBO when the weighting function is uniform. However, the relationship between the non-uniform weighted diffusion objectives and the ELBO is less well understood, as they appear to optimize different things on the face of it. This has led to the widely held belief that the ELBO (i.e. maximum likelihood) may not be the correct objective for obtaining high-quality samples.

Although weighted diffusion model objectives *appear* markedly different from the ELBO, all commonly used diffusion objectives optimize a weighted integral of ELBOs over different noise levels (Kingma and Gao, 2023). Furthermore, if the weighting function is monotonic, then the diffusion objective equates to the ELBO under simple Gaussian noise-based data augmentation. Lastly, we will show how different diffusion objectives imply specific weighting functions $w(\cdot)$ of the noise schedule. To avoid unnecessary repetition, we refer the reader to Kingma and Gao (2023) for a detailed breakdown of the most commonly used diffusion loss functions in the literature and the respective derivations of their implied weighting functions.

Model	Posterior Mean $\mu_\theta(\mathbf{z}_t; s, t)$
Image Denoising $\hat{\mathbf{x}}_\theta(\mathbf{z}_t; t)$	$\frac{\alpha_{t s}\sigma_s^2}{\sigma_t^2}\mathbf{z}_t + \frac{\alpha_s\sigma_{t s}^2}{\sigma_t^2}\hat{\mathbf{x}}_\theta(\mathbf{z}_t; t)$
Noise Prediction $\hat{\mathbf{e}}_\theta(\mathbf{z}_t; t)$	$\frac{1}{\alpha_{t s}}\mathbf{z}_t - \frac{\sigma_{t s}^2}{\alpha_{t s}\sigma_t}\hat{\mathbf{e}}_\theta(\mathbf{z}_t; t)$
Score-based $\mathbf{s}_\theta(\mathbf{z}_t; t)$	$\frac{1}{\alpha_{t s}}\mathbf{z}_t + \frac{\sigma_{t s}^2}{\alpha_{t s}}\mathbf{s}_\theta(\mathbf{z}_t; t)$
Energy-based $E_\theta(\mathbf{z}_t; t)$	$\frac{1}{\alpha_{t s}}\mathbf{z}_t - \frac{\sigma_{t s}^2}{\alpha_{t s}}\nabla_{\mathbf{z}_t}E_\theta(\mathbf{z}_t; t)$
Velocity Prediction $\hat{\mathbf{v}}_\theta(\mathbf{z}_t; t)$	$\frac{1 - \sigma_{t s}^2}{\alpha_{t s}}\mathbf{z}_t - \frac{\sigma_{t s}^2\alpha_s}{\sigma_t}\hat{\mathbf{v}}_\theta(\mathbf{z}_t; t)$
Flow-based $\hat{\mathbf{u}}_\theta(\mathbf{z}_t; t)$	$\frac{\sigma_t - \sigma_{t s}^2}{\alpha_{t s}\sigma_t}\mathbf{z}_t - \frac{\sigma_{t s}^2\alpha_s}{\sigma_t}\hat{\mathbf{u}}_\theta(\mathbf{z}_t; t)$

Table 4.1: Equivalent ways of parameterizing a variational diffusion model. Here $\mu_\theta(\mathbf{z}_t; s, t)$ is our model estimate of the true mean $\mu_Q(\mathbf{z}_t, \mathbf{x}; s, t)$ of the top-down posterior distribution $q(\mathbf{z}_s \mid \mathbf{z}_t, \mathbf{x})$, at any time $s < t$ (c.f. Section 3.3).

4.1 Model Parameterizations

As previously mentioned, there are multiple ways of operationalizing a diffusion model in terms of what the neural network outputs in practice. In the following, we present the most commonly used parameterizations, show that they are equivalently valid, and derive the associated expression for the posterior mean estimate of a variational diffusion model $\mu_\theta(\mathbf{z}_t; s, t)$. The results are summarized in Tables 4.1 and 4.2.

Image Denoising model $\hat{\mathbf{x}}_\theta(\mathbf{z}_t; t)$:

$$\mu_\theta(\mathbf{z}_t; s, t) = \frac{\alpha_{t|s}\sigma_s^2}{\sigma_t^2}\mathbf{z}_t + \frac{\alpha_s\sigma_{t|s}^2}{\sigma_t^2}\hat{\mathbf{x}}_\theta(\mathbf{z}_t; t), \quad (4.1)$$

which as mentioned earlier, simply predicts \mathbf{x} from its noisy versions \mathbf{z}_t , i.e. performs image *denoising*. For a derivation, see Section 3.5.

Noise Prediction model $\hat{\epsilon}_{\theta}(\mathbf{z}_t; t)$:

$$\mu_{\theta}(\mathbf{z}_t; s, t) = \frac{1}{\alpha_{t|s}} \mathbf{z}_t - \frac{\sigma_{t|s}^2}{\alpha_{t|s} \sigma_t} \hat{\epsilon}_{\theta}(\mathbf{z}_t; t), \quad (4.2)$$

which we can derive in detail starting from the denoising model:

$$\mu_{\theta}(\mathbf{z}_t; s, t) = \frac{\alpha_{t|s} \sigma_s^2}{\sigma_t^2} \mathbf{z}_t + \frac{\alpha_s \sigma_{t|s}^2}{\sigma_t^2} \hat{\mathbf{x}}_{\theta}(\mathbf{z}_t; t) \quad (4.3)$$

$$= \frac{\alpha_{t|s} \sigma_s^2 \mathbf{z}_t}{\sigma_t^2} + \frac{\alpha_s \sigma_{t|s}^2 \left(\frac{\mathbf{z}_t - \sigma_t \hat{\epsilon}_{\theta}(\mathbf{z}_t; t)}{\alpha_t} \right)}{\sigma_t^2} \quad (\text{since } \mathbf{x} = (\mathbf{z}_t - \sigma_t \epsilon_t) / \alpha_t) \quad (4.4)$$

$$= \frac{\alpha_{t|s}}{\alpha_{t|s}} \cdot \frac{\alpha_{t|s} \sigma_s^2 \mathbf{z}_t + \frac{\alpha_s \sigma_{t|s}^2 \mathbf{z}_t}{\alpha_t} - \frac{\alpha_s \sigma_{t|s}^2 \sigma_t \hat{\epsilon}_{\theta}(\mathbf{z}_t; t)}{\alpha_t}}{\sigma_t^2} \quad (\text{recall that } \alpha_{t|s} = \frac{\alpha_t}{\alpha_s}) \quad (4.5)$$

$$= \frac{\frac{\alpha_t}{\alpha_s} \left(\alpha_{t|s} \sigma_s^2 \mathbf{z}_t + \frac{\alpha_s \sigma_{t|s}^2 \mathbf{z}_t}{\alpha_t} - \frac{\alpha_s \sigma_{t|s}^2 \sigma_t \hat{\epsilon}_{\theta}(\mathbf{z}_t; t)}{\alpha_t} \right)}{\alpha_{t|s} \sigma_t^2} \quad (\text{cancel common factors}) \quad (4.6)$$

$$= \frac{\alpha_{t|s}^2 \sigma_s^2 \mathbf{z}_t + \sigma_{t|s}^2 \mathbf{z}_t - \sigma_{t|s}^2 \sigma_t \hat{\epsilon}_{\theta}(\mathbf{z}_t; t)}{\alpha_{t|s} \sigma_t^2} \quad (4.7)$$

$$= \frac{\mathbf{z}_t \left(\sigma_t^2 - \alpha_{t|s}^2 \sigma_s^2 + \alpha_{t|s}^2 \sigma_s^2 \right)}{\alpha_{t|s} \sigma_t^2} - \frac{\sigma_{t|s}^2 \sigma_t \hat{\epsilon}_{\theta}(\mathbf{z}_t; t)}{\alpha_{t|s} \sigma_t^2} \quad (\text{recall that } \sigma_{t|s}^2 = \sigma_t^2 - \alpha_{t|s}^2 \sigma_s^2) \quad (4.8)$$

$$= \frac{\mathbf{z}_t \sigma_t^2}{\alpha_{t|s} \sigma_t^2} - \frac{\sigma_{t|s}^2 \hat{\epsilon}_{\theta}(\mathbf{z}_t; t)}{\alpha_{t|s} \sigma_t} \quad (4.9)$$

$$= \frac{1}{\alpha_{t|s}} \mathbf{z}_t - \frac{\sigma_{t|s}^2}{\alpha_{t|s} \sigma_t} \hat{\epsilon}_{\theta}(\mathbf{z}_t; t). \quad (4.10)$$

Ho et al. (2020) first introduced noise prediction, which remains widely used for its practical effectiveness and close connection to score-based models (Song et al., 2021b), as described next.

Model	$\hat{\mathbf{x}}_{\theta}(\mathbf{z}_t; t)$	$\hat{\epsilon}_{\theta}(\mathbf{z}_t; t)$	Equivalent Reparameterization		
Image Denoising $\hat{\mathbf{x}}_{\theta}(\mathbf{z}_t; t)$	$-\frac{\mathbf{z}_t - \sigma_t \hat{\epsilon}_{\theta}}{\alpha_t}$	$\frac{\mathbf{z}_t + \sigma_t^2 \mathbf{s}_{\theta}}{\alpha_t}$	$\mathbf{z}_t - \sigma_t \hat{\mathbf{v}}_{\theta}$	$\alpha_t \mathbf{z}_t - \sigma_t \hat{\mathbf{v}}_{\theta}$	$\hat{\mathbf{u}}_{\theta}(\mathbf{z}_t; t)$
Noise Prediction $\hat{\epsilon}_{\theta}(\mathbf{z}_t; t)$	$\frac{\mathbf{z}_t - \alpha_t \hat{\mathbf{x}}_{\theta}}{\sigma_t}$	$-$	$-\sigma_t \mathbf{s}_{\theta}$	$\sigma_t \mathbf{z}_t + \alpha_t \hat{\mathbf{v}}_{\theta}$	$\alpha_t \hat{\mathbf{u}}_{\theta} + \mathbf{z}_t$
Score-based $\mathbf{s}_{\theta}(\mathbf{z}_t; t)$	$\frac{\alpha_t \hat{\mathbf{x}}_{\theta} - \mathbf{z}_t}{\sigma_t^2}$	$\frac{-\hat{\epsilon}_{\theta}}{\sigma_t}$	$-$	$\frac{-\sigma_t \mathbf{z}_t + \alpha_t \hat{\mathbf{v}}_{\theta}}{\sigma_t}$	$\frac{-\alpha_t \hat{\mathbf{u}}_{\theta} + \mathbf{z}_t}{\sigma_t}$
Velocity Prediction $\hat{\mathbf{v}}_{\theta}(\mathbf{z}_t; t)$	$\frac{\alpha_t \mathbf{z}_t - \hat{\mathbf{x}}_{\theta}}{\sigma_t}$	$\frac{\hat{\epsilon}_{\theta} - \sigma_t \mathbf{z}_t}{\alpha_t}$	$-\frac{\sigma_t(\mathbf{z}_t + \mathbf{s}_{\theta})}{\alpha_t}$	$-$	$\hat{\mathbf{u}}_{\theta} - \mathbf{z}_t$
Flow-Based $\hat{\mathbf{u}}_{\theta}(\mathbf{z}_t; t)$	$\frac{\mathbf{z}_t - \hat{\mathbf{x}}_{\theta}}{\sigma_t}$	$\frac{\hat{\epsilon}_{\theta}(\alpha_t - \sigma_t) - \mathbf{z}_t}{\alpha_t}$	$\frac{\sigma_t \mathbf{s}_{\theta}(\sigma_t - \alpha_t) - \mathbf{z}_t}{\alpha_t}$	$\mathbf{z}_t + \hat{\mathbf{v}}_{\theta}$	$-$

Table 4.2: Equivalent reparameterizations of a variational diffusion model. For example, image prediction can be expressed in terms of velocity prediction as $\hat{\mathbf{x}}_{\theta}(\mathbf{z}_t; t) = \alpha_t \mathbf{z}_t - \sigma_t \hat{\mathbf{v}}_{\theta}(\mathbf{z}_t; t)$. As shown, all the translation operations are simple linear functions of each other because $\mathbf{z}_t = \alpha_t \mathbf{x} + \sigma_t \epsilon_t$ by the definition of the forward diffusion process. This implies that one can choose to parameterize the diffusion model using any of the mentioned methods during training and then re-parameterize it during inference. A common use case is to train a noise prediction model, then reparameterize back to image space at inference time to clip the predicted image to a valid range (e.g. $[-1, 1]$) at each denoising step t . Finally, noise and velocity prediction have sometimes demonstrated superior performance and numerical stability in practice.

Score-based model $\mathbf{s}_\theta(\mathbf{z}_t; t)$:

$$\boldsymbol{\mu}_\theta(\mathbf{z}_t; s, t) = \frac{1}{\alpha_{t|s}} \mathbf{z}_t + \frac{\sigma_{t|s}^2}{\alpha_{t|s}} \mathbf{s}_\theta(\mathbf{z}_t; t), \quad (4.11)$$

which approximates $\nabla_{\mathbf{z}_t} \log q(\mathbf{z}_t)$, and is closely related to noise-prediction in the following way:

$$\mathbf{s}_\theta(\mathbf{z}_t; t) \approx \nabla_{\mathbf{z}_t} \log q(\mathbf{z}_t) \quad (4.12)$$

$$= \mathbb{E}_{q(\mathbf{x})} [\nabla_{\mathbf{z}_t} \log q(\mathbf{z}_t \mid \mathbf{x})] \quad (\text{marginal of the data } q(\mathbf{x})) \quad (4.13)$$

$$= \mathbb{E}_{q(\mathbf{x})} [\nabla_{\mathbf{z}_t} \log \mathcal{N}(\mathbf{z}_t; \alpha_t \mathbf{x}, \sigma_t^2 \mathbf{I})] \quad (4.14)$$

$$= \mathbb{E}_{q(\mathbf{x})} \left[\nabla_{\mathbf{z}_t} \log \left(\prod_{i=1}^D \frac{1}{\sigma_t \sqrt{2\pi}} \exp \left\{ -\frac{1}{2\sigma_t^2} (\mathbf{z}_{t,i} - \alpha_t \mathbf{x}_i)^2 \right\} \right) \right] \quad (\text{isotropic covariance}) \quad (4.15)$$

$$= \mathbb{E}_{q(\mathbf{x})} \left[\nabla_{\mathbf{z}_t} \left(-\frac{D}{2} \log (2\pi\sigma_t^2) - \frac{1}{2\sigma_t^2} \sum_{i=1}^D (\mathbf{z}_{t,i} - \alpha_t \mathbf{x}_i)^2 \right) \right] \quad (4.16)$$

$$= \mathbb{E}_{q(\mathbf{x})} \left[-\frac{1}{\sigma_t^2} (\mathbf{z}_t - \alpha_t \mathbf{x}) \right] \quad (\text{expected gradient}) \quad (4.17)$$

$$= \mathbb{E}_{q(\mathbf{x})} \left[-\frac{1}{\sigma_t} \hat{\boldsymbol{\epsilon}}_\theta(\mathbf{z}_t; t) \right] \quad (\text{due to } \boldsymbol{\epsilon} = (\mathbf{z}_t - \alpha_t \mathbf{x})/\sigma_t) \quad (4.18)$$

$$= -\frac{1}{\sigma_t} \hat{\boldsymbol{\epsilon}}_\theta(\mathbf{z}_t; t). \quad (4.19)$$

The optimal score model (with parameters $\boldsymbol{\theta}^*$) is equal to the gradient of the log-probability density w.r.t. the data at each noise scale: $\mathbf{s}_{\boldsymbol{\theta}^*}(\mathbf{z}_t; t) = \nabla_{\mathbf{z}_t} \log q(\mathbf{z}_t)$, for any t . This stems from a Score Matching with Langevin Dynamics (SMLD) perspective on generative modelling (Song and Ermon, 2019; Song et al., 2021b). SMLD is closely related to probabilistic diffusion models (Ho et al., 2020). For continuous state spaces, diffusion models implicitly compute the score at each noise scale, so the two approaches can be categorized jointly as *score-based models*. For more details on score-based models, please refer to Song et al. (2021b).

Energy-based model $E_{\theta}(\mathbf{z}_t; t)$:

$$\boldsymbol{\mu}_{\theta}(\mathbf{z}_t; s, t) = \frac{1}{\alpha_{t|s}} \mathbf{z}_t - \frac{\sigma_{t|s}^2}{\alpha_{t|s}} \nabla_{\mathbf{z}_t} E_{\theta}(\mathbf{z}_t; t), \quad (4.20)$$

since the score model can be parameterized with the gradient of an energy-based model:

$$\mathbf{s}_{\theta}(\mathbf{z}_t; t) \approx \nabla_{\mathbf{z}_t} \log q(\mathbf{z}_t) \quad (4.21)$$

$$= \nabla_{\mathbf{z}_t} \log \left(\frac{1}{Z} \exp(-E_{\theta}(\mathbf{z}_t; t)) \right) \quad (\text{Boltzmann dist.}) \quad (4.22)$$

$$= \nabla_{\mathbf{z}_t} \left(-E_{\theta}(\mathbf{z}_t; t) - \log Z \right) \quad (\nabla_{\mathbf{z}_t} \log Z = 0) \quad (4.23)$$

$$= -\nabla_{\mathbf{z}_t} E_{\theta}(\mathbf{z}_t; t), \quad (4.24)$$

which we can use to substitute $\mathbf{s}_{\theta}(\mathbf{z}_t; t)$ in Equation 4.11 to get the new expression in Equation 4.20. [Du et al. \(2023\)](#) provide compelling arguments in favour of an energy-based parameterization as it enables the use of more sophisticated sampling schemes and forms of composition.

With that said, the energy-based parameterization of diffusion models remains comparatively underexplored to date. For a detailed review of energy-based models and their relationship with score-based models refer to [Song and Kingma \(2021\)](#) and [Salimans and Ho \(2021\)](#).

Velocity Prediction model $\hat{\mathbf{v}}_{\theta}(\mathbf{z}_t; t)$:

$$\boldsymbol{\mu}_{\theta}(\mathbf{z}_t; s, t) = \frac{1 - \sigma_{t|s}^2}{\alpha_{t|s}} \mathbf{z}_t - \frac{\sigma_{t|s}^2 \alpha_s}{\sigma_t} \hat{\mathbf{v}}_{\theta}(\mathbf{z}_t; t), \quad (4.25)$$

which represents the tangential velocity resulting from an angular parameterization $\phi_t = \arctan(\sigma_t/\alpha_t)$ of the latent variable \mathbf{z}_t specified as follows ([Salimans and Ho, 2022](#)):

$$\mathbf{z}_t = \cos(\phi_t) \mathbf{x} + \sin(\phi_t) \boldsymbol{\epsilon}, \quad (4.26)$$

$$\mathbf{v} := \frac{d\mathbf{z}_t}{d\phi_t} = \cos(\phi_t) \boldsymbol{\epsilon} - \sin(\phi_t) \mathbf{x}. \quad (4.27)$$

The velocity \mathbf{v} represents how the latent variable \mathbf{z}_t changes w.r.t. ϕ_t , and is analogous to the tangential velocity of a point moving on a circle.

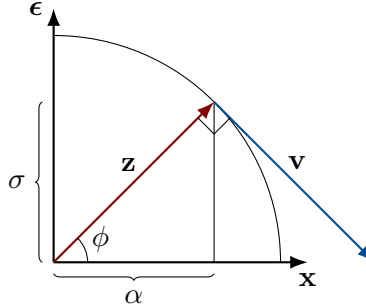


Figure 4.1: Illustrating the relationships between \mathbf{v} -prediction (i.e. the tangential velocity) and the noise schedule quantities involved in defining a diffusion process. Figure inspired by [Salimans and Ho \(2022\)](#).

This may be alternatively described as $\mathbf{v} = \|\mathbf{z}_t\| \frac{d\phi_t}{dt}$, where $\|\mathbf{z}_t\|$ is the radius of the circular path and $\frac{d\phi_t}{dt}$ is the angular velocity.

To derive our result in Equation 4.25, we can start by expressing ϵ in terms of \mathbf{v} :

$$\mathbf{v} = \cos(\phi_t)\epsilon - \sin(\phi_t)\mathbf{x} \quad (4.28)$$

$$:= \alpha_t \epsilon - \sigma_t \mathbf{x} \quad (4.29)$$

$$= \alpha_t \epsilon - \sigma_t \left(\frac{\mathbf{z}_t - \sigma_t \epsilon}{\alpha_t} \right) \quad (4.30)$$

$$\mathbf{v} + \frac{\sigma_t \mathbf{z}_t}{\alpha_t} = \epsilon \left(\frac{\alpha_t^2}{\alpha_t} + \frac{\sigma_t^2}{\alpha_t} \right) \quad (4.31)$$

$$\mathbf{v} + \frac{\sigma_t \mathbf{z}_t}{\alpha_t} = \epsilon \left(\frac{1 - \sigma_t^2 + \sigma_t^2}{\alpha_t} \right) \quad (\text{recall } \alpha^2 = 1 - \sigma_t^2) \quad (4.32)$$

$$\alpha_t \mathbf{v} + \sigma_t \mathbf{z}_t = \epsilon \quad (4.33)$$

$$\implies \hat{\epsilon}_\theta(\mathbf{z}_t; t) = \alpha_t \hat{\mathbf{v}}_\theta(\mathbf{z}_t; t) + \sigma_t \mathbf{z}_t. \quad (4.34)$$

Now recalling that $\mathbf{s}_\theta(\mathbf{z}_t; t) = -\hat{\epsilon}_\theta(\mathbf{z}_t; t)/\sigma_t$, and substituting the above into the score-based parameterization in Equation 4.11, we get:

$$\mu_\theta(\mathbf{z}_t; s, t) = \frac{\mathbf{z}_t}{\alpha_{t|s}} + \frac{\sigma_{t|s}^2}{\alpha_{t|s}} \cdot -\frac{1}{\sigma_t} (\alpha_t \hat{\mathbf{v}}_\theta(\mathbf{z}_t; t) + \sigma_t \mathbf{z}_t) \quad (4.35)$$

$$= \frac{\mathbf{z}_t}{\alpha_{t|s}} - \frac{\sigma_{t|s}^2 \mathbf{z}_t}{\alpha_{t|s}} - \frac{\sigma_{t|s}^2 \alpha_t}{\alpha_{t|s} \sigma_t} \hat{\mathbf{v}}_{\theta}(\mathbf{z}_t; t) \quad (4.36)$$

$$= \frac{1 - \sigma_{t|s}^2}{\alpha_{t|s}} \mathbf{z}_t - \frac{\sigma_{t|s}^2 \alpha_s}{\sigma_t} \hat{\mathbf{v}}_{\theta}(\mathbf{z}_t; t). \quad (4.37)$$

As we show next, there exists a close link between velocity prediction and Flow Matching (Lipman et al., 2023; Albergo and Vandenberg-Eijnden, 2023; Liu et al., 2023), which can be interpreted as a type of Gaussian diffusion. Kingma and Gao (2023) explore this relation under what they call **o**-prediction (c.f. Appendix D.3 in Kingma and Gao (2023)).

Flow-based model $\hat{\mathbf{u}}_{\theta}(\mathbf{z}_t; t)$:

$$\boldsymbol{\mu}_{\theta}(\mathbf{z}_t; s, t) = \frac{\sigma_t - \sigma_{t|s}^2}{\alpha_{t|s} \sigma_t} \mathbf{z}_t - \frac{\sigma_{t|s}^2 \alpha_s}{\sigma_t} \hat{\mathbf{u}}_{\theta}(\mathbf{z}_t; t), \quad (4.38)$$

where $\hat{\mathbf{u}}_{\theta}$ also represents a velocity field, but here the noise schedule of choice is a *linear interpolation* between data and noise over time. In our context, this translates to each latent variable \mathbf{z}_t being given by:

$$\mathbf{z}_t = \alpha_t \mathbf{x} + \sigma_t \boldsymbol{\epsilon} \quad (4.39)$$

$$= (1 - t) \mathbf{x} + t \boldsymbol{\epsilon}, \quad (4.40)$$

and the velocity field \mathbf{u} is obtained by differentiating w.r.t. time t :

$$\mathbf{u} := \frac{d\mathbf{z}_t}{dt} = \boldsymbol{\epsilon} - \mathbf{x}. \quad (4.41)$$

To derive our result in Equation 4.38, we first express $\boldsymbol{\epsilon}$ in terms of \mathbf{u} :

$$\boldsymbol{\epsilon} = \mathbf{u} + \mathbf{x} \quad (4.42)$$

$$= \mathbf{u} + \left(\frac{\mathbf{z}_t - t\boldsymbol{\epsilon}}{1 - t} \right) \quad (4.43)$$

$$\boldsymbol{\epsilon} \left(\frac{1}{1 - t} \right) = \mathbf{u} + \frac{\mathbf{z}_t}{1 - t} \quad (4.44)$$

$$\boldsymbol{\epsilon} = (1 - t) \mathbf{u} + \mathbf{z}_t \quad (4.45)$$

$$\implies \hat{\boldsymbol{\epsilon}}_{\theta}(\mathbf{z}_t; t) = \alpha_t \hat{\mathbf{u}}_{\theta}(\mathbf{z}_t; t) + \mathbf{z}_t. \quad (4.46)$$

Now we simply substitute the above into the noise prediction parameterization in Equation 4.2 and simplify:

$$\boldsymbol{\mu}_{\theta}(\mathbf{z}_t; s, t) = \frac{1}{\alpha_{t|s}} \mathbf{z}_t - \frac{\sigma_{t|s}^2}{\alpha_{t|s} \sigma_t} (\alpha_t \hat{\mathbf{u}}_{\theta}(\mathbf{z}_t; t) + \mathbf{z}_t) \quad (4.47)$$

$$= \frac{\mathbf{z}_t \sigma_t}{\alpha_{t|s} \sigma_t} - \frac{\sigma_{t|s}^2 \mathbf{z}_t}{\alpha_{t|s} \sigma_t} - \frac{\sigma_{t|s}^2 \alpha_t}{\alpha_{t|s} \sigma_t} \hat{\mathbf{u}}_{\theta}(\mathbf{z}_t; t) \quad (4.48)$$

$$= \frac{\sigma_t - \sigma_{t|s}^2}{\alpha_{t|s} \sigma_t} \mathbf{z}_t - \frac{\sigma_{t|s}^2 \alpha_t}{\sigma_t} \hat{\mathbf{u}}_{\theta}(\mathbf{z}_t; t). \quad (4.49)$$

The \mathbf{u} -prediction parameterization is best known as Flow Matching (FM) (Lipman et al., 2023), has many other flavours (Albergo and Vanden-Eijnden, 2023; Liu et al., 2023), and is reminiscent of velocity prediction (Salimans and Ho, 2022). As shown above, Gaussian FM is practically equivalent to (continuous-time) diffusion modelling but uses a particular neural network parameterization and noise schedule.

To conclude, one other parameterization not covered here but certainly worth learning about is \mathbf{F} -prediction (Karras et al., 2022).

Practical Advantages. Each aforementioned parameterization has its own strengths and weaknesses. For example, noise prediction $\hat{\epsilon}_{\theta}$ is stable at lower noise levels but can explode errors at high noise levels, as the *implied* image prediction $\hat{\mathbf{x}}_{\theta}$ approaches a division by zero:

$$\hat{\mathbf{x}}_{\theta} = \frac{\mathbf{z}_t - \sigma_t \hat{\epsilon}_{\theta}}{\alpha_t}, \quad \text{where} \quad \alpha_t \xrightarrow{t \rightarrow 1} 0. \quad (4.50)$$

The same is true for the score-based parameterization. In fact, any reparameterization formula that involves division by one of the noise schedule parameters is subject to this problem, and these can simply be read off Table 4.2. Importantly, both of the velocity prediction versions (i.e. $\hat{\mathbf{v}}_{\theta}$ and $\hat{\mathbf{u}}_{\theta}$) overcome this issue, as the corresponding image prediction formulas do *not* require any division by a noise schedule parameter. Direct image prediction overcomes the division by zero issue too but is subject to a more subtle problem: it provides a weak supervision signal at low noise levels. Collectively, these considerations make a compelling argument for adopting velocity-based parameterizations.

Loss	Image Denoising $\ \mathbf{x} - \hat{\mathbf{x}}_{\theta}(\mathbf{z}_t; t)\ _2^2$	Noise Prediction $\ \boldsymbol{\epsilon} - \hat{\boldsymbol{\epsilon}}_{\theta}(\mathbf{z}_t; t)\ _2^2$	Velocity Prediction $\ \mathbf{v} - \hat{\mathbf{v}}_{\theta}(\mathbf{z}_t; t)\ _2^2$
$\ \mathbf{x} - \hat{\mathbf{x}}_{\theta}(\mathbf{z}_t; t)\ _2^2$	1	σ_t^2 / α_t^2	σ_t^2
$\ \boldsymbol{\epsilon} - \hat{\boldsymbol{\epsilon}}_{\theta}(\mathbf{z}_t; t)\ _2^2$	α_t^2 / σ_t^2	1	$1 / \alpha_t^2$
$\ \mathbf{v} - \hat{\mathbf{v}}_{\theta}(\mathbf{z}_t; t)\ _2^2$	$\sigma_t^2 \left(\frac{\alpha_t^2}{\sigma_t^2} + 1 \right)^2$	$\alpha_t^2 \left(\frac{\sigma_t^2}{\alpha_t^2} + 1 \right)^2$	1

Table 4.3: Translating diffusion model loss parameterizations. Each loss on the LHS column can be rewritten in terms of the other parameterizations weighted by a specific constant. For example, the image prediction loss can be written in terms of noise prediction weighted by σ_t^2 / α_t^2 , that is: $\|\mathbf{x} - \hat{\mathbf{x}}_{\theta}(\mathbf{z}_t; t)\|_2^2 = \sigma_t^2 / \alpha_t^2 \|\boldsymbol{\epsilon} - \hat{\boldsymbol{\epsilon}}_{\theta}(\mathbf{z}_t; t)\|_2^2$, whereas the \mathbf{v} -prediction (Salimans and Ho, 2022) loss can be written in terms of image prediction by: $\|\mathbf{v} - \hat{\mathbf{v}}_{\theta}(\mathbf{z}_t; t)\|_2^2 = \sigma_t^2 \left(\alpha_t^2 / \sigma_t^2 + 1 \right)^2 \|\mathbf{x} - \hat{\mathbf{x}}_{\theta}(\mathbf{z}_t; t)\|_2^2$.

4.2 Translating Loss Parameterizations

Translating between different loss parameterizations is straightforward due to the linearity of the forward diffusion process $\mathbf{z}_t = \alpha_t \mathbf{x} + \sigma_t \boldsymbol{\epsilon}$. This will be particularly useful for analyzing diffusion loss objectives later on. For now, we provide the derivations of the most popular loss parameterizations and summarize the results in Table 4.3.

Image to Noise Prediction. Firstly, we rewrite the image prediction $\hat{\mathbf{x}}_{\theta}(\mathbf{z}_t; t)$ loss in terms of noise prediction $\hat{\boldsymbol{\epsilon}}_{\theta}(\mathbf{z}_t; t)$ by:

$$\|\mathbf{x} - \hat{\mathbf{x}}_{\theta}(\mathbf{z}_t; t)\|_2^2 = \left\| \frac{\mathbf{z}_t - \sigma_t \boldsymbol{\epsilon}}{\alpha_t} - \frac{\mathbf{z}_t - \sigma_t \hat{\boldsymbol{\epsilon}}_{\theta}(\mathbf{z}_t; t)}{\alpha_t} \right\|_2^2 \quad (\text{since } \mathbf{z}_t = \alpha_t \mathbf{x} + \sigma_t \boldsymbol{\epsilon}) \quad (4.51)$$

$$= \frac{\sigma_t^2}{\alpha_t^2} \|\boldsymbol{\epsilon} - \hat{\boldsymbol{\epsilon}}_{\theta}(\mathbf{z}_t; t)\|_2^2. \quad (\text{cancel terms and factor}) \quad (4.52)$$

Image to Velocity Prediction. Similarly, in terms of velocity prediction, we first review the definition:

$$\mathbf{v} := \alpha_t \boldsymbol{\epsilon} - \sigma_t \mathbf{x} \quad (\text{by definition}) \quad (4.53)$$

$$= \alpha_t \left(\frac{\mathbf{z}_t - \alpha_t \mathbf{x}}{\sigma_t} \right) - \sigma_t \mathbf{x}, \quad (\text{substitute } \boldsymbol{\epsilon} = (\mathbf{z}_t - \alpha_t \mathbf{x})/\sigma_t) \quad (4.54)$$

since $\alpha_t^2 = 1 - \sigma_t^2$ in a variance preserving process we then get:

$$\alpha_t \mathbf{z}_t - \sigma_t \mathbf{v} = (1 - \sigma_t^2) \mathbf{x} + \sigma_t^2 \mathbf{x} \quad (4.55)$$

$$\implies \mathbf{x} = \alpha_t \mathbf{z}_t - \sigma_t \mathbf{v}, \quad (4.56)$$

which we can now substitute into the image prediction loss, with a \mathbf{v} -prediction model $\hat{\mathbf{v}}_{\boldsymbol{\theta}}(\mathbf{z}_t; t)$:

$$\|\mathbf{x} - \hat{\mathbf{x}}_{\boldsymbol{\theta}}(\mathbf{z}_t; t)\|_2^2 = \|\alpha_t \mathbf{z}_t - \sigma_t \mathbf{v} - (\alpha_t \mathbf{z}_t - \sigma_t \hat{\mathbf{v}}_{\boldsymbol{\theta}}(\mathbf{z}_t; t))\|_2^2 \quad (4.57)$$

$$= \|\sigma_t \hat{\mathbf{v}}_{\boldsymbol{\theta}}(\mathbf{z}_t; t) - \sigma_t \mathbf{v}\|_2^2 \quad (\alpha_t \mathbf{z}_t \text{ terms cancel}) \quad (4.58)$$

$$= \sigma_t^2 \|\hat{\mathbf{v}}_{\boldsymbol{\theta}}(\mathbf{z}_t; t) - \mathbf{v}\|_2^2. \quad (\text{by factoring}) \quad (4.59)$$

Noise to Image Prediction. To rewrite the noise prediction loss in terms of image prediction we have:

$$\|\boldsymbol{\epsilon} - \hat{\boldsymbol{\epsilon}}_{\boldsymbol{\theta}}(\mathbf{z}_t; t)\|_2^2 = \left\| \frac{\mathbf{z}_t - \alpha_t \mathbf{x}}{\sigma_t} - \frac{\mathbf{z}_t - \alpha_t \hat{\mathbf{x}}_{\boldsymbol{\theta}}(\mathbf{z}_t; t)}{\sigma_t} \right\|_2^2 \quad (\text{recall that } \mathbf{z}_t = \alpha_t \mathbf{x} + \sigma_t \boldsymbol{\epsilon}) \quad (4.60)$$

$$= \left\| \frac{\alpha_t}{\sigma_t} (\hat{\mathbf{x}}_{\boldsymbol{\theta}}(\mathbf{z}_t; t) - \mathbf{x}) \right\|_2^2 \quad (\text{cancel } \mathbf{z}_t \text{ terms and factor}) \quad (4.61)$$

$$= \text{SNR}(t) \|\hat{\mathbf{x}}_{\boldsymbol{\theta}}(\mathbf{z}_t; t) - \mathbf{x}\|_2^2. \quad (\text{recall } \text{SNR}(t) = \alpha_t^2/\sigma_t^2) \quad (4.62)$$

Noise to Velocity Prediction. To express noise prediction in terms of velocity prediction we proceed as:

$$\|\boldsymbol{\epsilon} - \hat{\boldsymbol{\epsilon}}_{\boldsymbol{\theta}}(\mathbf{z}_t; t)\|_2^2 = \left\| \frac{\mathbf{v} + \sigma_t \mathbf{x}}{\alpha_t} - \frac{\hat{\mathbf{v}}_{\boldsymbol{\theta}}(\mathbf{z}_t; t) + \sigma_t \mathbf{x}}{\alpha_t} \right\|_2^2 \quad (\text{solving } \mathbf{v} = \alpha_t \boldsymbol{\epsilon} - \sigma_t \mathbf{x} \text{ for } \boldsymbol{\epsilon}) \quad (4.63)$$

$$= \left\| \frac{1}{\alpha_t} (\mathbf{v} - \hat{\mathbf{v}}_{\boldsymbol{\theta}}(\mathbf{z}_t; t)) \right\|_2^2 \quad (\text{cancel } \mathbf{x} \text{ terms and factor}) \quad (4.64)$$

$$= \frac{1}{\alpha_t^2} \|\mathbf{v} - \hat{\mathbf{v}}_{\theta}(\mathbf{z}_t; t)\|_2^2. \quad (4.65)$$

Velocity to Image Prediction. We can rewrite velocity prediction in terms of image prediction as follows:

$$\|\mathbf{v} - \hat{\mathbf{v}}_{\theta}(\mathbf{z}_t; t)\|_2^2 = \|\alpha_t \boldsymbol{\epsilon} - \sigma_t \mathbf{x} - (\alpha_t \hat{\boldsymbol{\epsilon}}_{\theta}(\mathbf{z}_t; t) - \sigma_t \hat{\mathbf{x}}_{\theta}(\mathbf{z}_t; t))\|_2^2 \quad (4.66)$$

$$= \left\| \alpha_t \left(\frac{\mathbf{z}_t - \alpha_t \mathbf{x}}{\sigma_t} \right) - \sigma_t \mathbf{x} - \alpha_t \left(\frac{\mathbf{z}_t - \alpha_t \hat{\mathbf{x}}_{\theta}(\mathbf{z}_t; t)}{\sigma_t} \right) + \sigma_t \hat{\mathbf{x}}_{\theta}(\mathbf{z}_t; t) \right\|_2^2 \quad (4.67)$$

$$= \left\| \frac{\alpha_t^2 \hat{\mathbf{x}}_{\theta}(\mathbf{z}_t; t)}{\sigma_t} + \sigma_t \hat{\mathbf{x}}_{\theta}(\mathbf{z}_t; t) - \frac{\alpha_t^2 \mathbf{x}}{\sigma_t} - \sigma_t \mathbf{x} \right\|_2^2 \quad (\text{cancel } \mathbf{z}_t \text{ terms and factor}) \quad (4.68)$$

$$= \left\| \left(\frac{\alpha_t^2}{\sigma_t} + \sigma_t \right) (\hat{\mathbf{x}}_{\theta}(\mathbf{z}_t; t) - \mathbf{x}) \right\|_2^2 \quad (4.69)$$

$$= \sigma_t^2 (\text{SNR}(t) + 1)^2 \|\hat{\mathbf{x}}_{\theta}(\mathbf{z}_t; t) - \mathbf{x}\|_2^2. \quad (\text{as } \text{SNR}(t) = \alpha_t^2 / \sigma_t^2) \quad (4.70)$$

Velocity to Noise Prediction. We proceed similarly to the above for noise prediction, but now substituting image-related terms to get:

$$\|\mathbf{v} - \hat{\mathbf{v}}_{\theta}(\mathbf{z}_t; t)\|_2^2 = \|\alpha_t \boldsymbol{\epsilon} - \sigma_t \mathbf{x} - (\alpha_t \hat{\boldsymbol{\epsilon}}_{\theta}(\mathbf{z}_t; t) - \sigma_t \hat{\mathbf{x}}_{\theta}(\mathbf{z}_t; t))\|_2^2 \quad (4.71)$$

$$= \left\| \alpha_t \boldsymbol{\epsilon} - \sigma_t \left(\frac{\mathbf{z}_t - \sigma_t \boldsymbol{\epsilon}}{\alpha_t} \right) - \alpha_t \hat{\boldsymbol{\epsilon}}_{\theta}(\mathbf{z}_t; t) + \sigma_t \left(\frac{\mathbf{z}_t - \sigma_t \hat{\boldsymbol{\epsilon}}_{\theta}(\mathbf{z}_t; t)}{\alpha_t} \right) \right\|_2^2 \quad (4.72)$$

$$= \left\| \left(\frac{\sigma_t^2}{\alpha_t} + \alpha_t \right) (\boldsymbol{\epsilon} - \hat{\boldsymbol{\epsilon}}_{\theta}(\mathbf{z}_t; t)) \right\|_2^2 \quad (\text{cancel } \mathbf{z}_t \text{ terms and factor}) \quad (4.73)$$

$$= \alpha_t^2 \left(\frac{\sigma_t^2}{\alpha_t^2} + 1 \right)^2 \|\boldsymbol{\epsilon} - \hat{\boldsymbol{\epsilon}}_{\theta}(\mathbf{z}_t; t)\|_2^2. \quad (4.74)$$

4.3 Invariance to the Noise Schedule

An important result established that the continuous-time VLB is invariant to the noise schedule of the forward diffusion process (Kingma et al., 2021). To explain this result, we begin by performing a change of variables; i.e. we transform the integral w.r.t time t in the diffusion loss (Equation 3.123) into an integral w.r.t the signal-to-noise ratio. Since the signal-to-noise ratio function $\text{SNR}(t) = \exp(-\gamma_\eta(t))$ is *monotonic*, it is invertible ($\text{SNR}(t)$ is entirely non-increasing in time t meaning: $\text{SNR}(t) < \text{SNR}(s)$, for any $t > s$; ref. Section A.2). Using this fact, we can re-express our loss in terms of a new variable $v \equiv \text{SNR}(t)$, such that time t is instead given by $t = \text{SNR}^{-1}(v)$. Let $\mathbf{z}_v = \alpha_v \mathbf{x} + \sigma_v \boldsymbol{\epsilon}$ denote the latent variable \mathbf{z}_v whose noise-schedule functions α_v and σ_v correspond to α_t and σ_t evaluated at $t = \text{SNR}^{-1}(v)$.

By applying the *integration by substitution* formula

$$\int_a^b f(g(t)) \cdot g'(t) dt = \int_{g(a)}^{g(b)} f(v) dv, \quad (4.75)$$

we can express the diffusion loss in terms of our new variable v as follows:

$$\mathcal{L}_\infty(\mathbf{x}) = -\frac{1}{2} \mathbb{E}_{\boldsymbol{\epsilon} \sim \mathcal{N}(0, \mathbf{I}), t \sim \mathcal{U}(0, 1)} \left[\text{SNR}'(t) \|\mathbf{x} - \hat{\mathbf{x}}_\theta(\mathbf{z}_t; t)\|_2^2 \right] \quad (4.76)$$

$$= -\frac{1}{2} \mathbb{E}_{\boldsymbol{\epsilon} \sim \mathcal{N}(0, \mathbf{I})} \left[\int_0^1 \left\| \mathbf{x} - \hat{\mathbf{x}}_\theta \left(\sigma_t \left(\mathbf{x} \sqrt{\text{SNR}(t)} + \boldsymbol{\epsilon} \right); t \right) \right\|_2^2 \cdot \text{SNR}'(t) dt \right] \quad (4.77)$$

$$= -\frac{1}{2} \mathbb{E}_{\boldsymbol{\epsilon} \sim \mathcal{N}(0, \mathbf{I})} \left[\int_{\text{SNR}(0)}^{\text{SNR}(1)} \|\mathbf{x} - \hat{\mathbf{x}}_\theta(\mathbf{z}_v; v)\|_2^2 dv \right] \quad (dv = \text{SNR}'(t) dt) \quad (4.78)$$

$$= \frac{1}{2} \mathbb{E}_{\boldsymbol{\epsilon} \sim \mathcal{N}(0, \mathbf{I})} \left[\int_{\text{SNR}(1)}^{\text{SNR}(0)} \|\mathbf{x} - \hat{\mathbf{x}}_\theta(\mathbf{z}_v; v)\|_2^2 dv \right] \quad (\text{swap limits}) \quad (4.79)$$

$$= \frac{1}{2} \mathbb{E}_{\boldsymbol{\epsilon} \sim \mathcal{N}(0, \mathbf{I})} \left[\int_{\text{SNR}_{\min}}^{\text{SNR}_{\max}} \|\mathbf{x} - \hat{\mathbf{x}}_\theta(\mathbf{z}_v; v)\|_2^2 dv \right], \quad (4.80)$$

where $\text{SNR}_{\max} = \text{SNR}(0)$ denotes the *highest* signal-to-noise ratio at time $t = 0$ resulting in the least noisy latent \mathbf{z}_0 at the start of the

diffusion process (i.e. essentially the same as \mathbf{x}). Conversely, $\text{SNR}_{\min} = \text{SNR}(1)$ denotes the *lowest* signal-to-noise ratio resulting in the noisiest latent \mathbf{z}_1 at time $t = 1$.

The above shows that the diffusion loss is determined by the endpoints SNR_{\min} and SNR_{\max} , and is invariant to the shape of $\text{SNR}(t)$ between $t = 0$ and $t = 1$. More precisely, the *noise schedule* function $\exp(-\gamma_{\eta}(t))$ which maps the time variable $t \in [0, 1]$ to the signal-to-noise ratio $\text{SNR}(t)$ does not influence the diffusion loss integral in Equation 4.80, except for at its endpoints SNR_{\max} and SNR_{\min} . Therefore, given v , the shape of the noise schedule function $\exp(-\gamma_{\eta}(t))$ does not affect the diffusion loss.

Another way to understand the above result is by realizing that to compute the diffusion loss integral, it suffices to evaluate the antiderivative F of the squared-error term at the endpoints SNR_{\min} and SNR_{\max} :

$$\mathcal{L}_{\infty}(\mathbf{x}) = \quad (4.81)$$

$$- \frac{1}{2} \mathbb{E}_{\epsilon \sim \mathcal{N}(0, \mathbf{I})} \left[\int_0^1 \left\| \mathbf{x} - \hat{\mathbf{x}}_{\theta} \left(\sigma_t \left(\mathbf{x} \sqrt{\text{SNR}(t)} + \epsilon \right); t \right) \right\|_2^2 \cdot \text{SNR}'(t) dt \right] \quad (4.82)$$

$$= - \frac{1}{2} \mathbb{E}_{\epsilon \sim \mathcal{N}(0, \mathbf{I})} \left[\int_0^1 F'(\text{SNR}(t)) \cdot \text{SNR}'(t) dt \right] \quad (4.83)$$

$$= - \frac{1}{2} \mathbb{E}_{\epsilon \sim \mathcal{N}(0, \mathbf{I})} \left[\int_0^1 (F \circ \text{SNR})'(t) dt \right] \quad (4.84)$$

$$= \frac{1}{2} \mathbb{E}_{\epsilon \sim \mathcal{N}(0, \mathbf{I})} [- (F(\text{SNR}(1)) - F(\text{SNR}(0)))] \quad (4.85)$$

$$= \frac{1}{2} \mathbb{E}_{\epsilon \sim \mathcal{N}(0, \mathbf{I})} [F(\text{SNR}_{\max}) - F(\text{SNR}_{\min})], \quad (4.86)$$

since every continuous function has an antiderivative. Furthermore, there are infinitely many antiderivatives of the mean-square-error term, each of which, G , differs from F by a only constant c :

$$G(v) := \int \|\mathbf{x} - \hat{\mathbf{x}}_{\theta}(\mathbf{z}_v; v)\|_2^2 dv = F(v) + c, \quad (4.87)$$

for all signal-to-noise ratio functions $v \equiv \text{SNR}(t)$.

4.4 Weighted Diffusion Loss

The diffusion objectives used in practice can be understood as a weighted version of the diffusion loss:

$$\mathcal{L}_\infty(\mathbf{x}, w) = \frac{1}{2} \int_{\text{SNR}_{\min}}^{\text{SNR}_{\max}} w(v) \mathbb{E}_{\epsilon \sim \mathcal{N}(0, \mathbf{I})} \left[\|\mathbf{x} - \hat{\mathbf{x}}_\theta(\mathbf{z}_v; v)\|_2^2 \right] dv, \quad (4.88)$$

$$= -\frac{1}{2} \mathbb{E}_{\epsilon \sim \mathcal{N}(0, \mathbf{I})} \left[\int_0^1 w(\text{SNR}(t)) \text{SNR}'(t) \|\mathbf{x} - \hat{\mathbf{x}}_\theta(\mathbf{z}_t; t)\|_2^2 dt \right],$$

(recall Eq. 3.124) (4.89)

where $w(v) = w(\text{SNR}(t))$ is a chosen weighting function of the noise schedule. In intuitive terms, the weighting function stipulates the relative importance of each noise level prescribed by the noise schedule. Ideally, we would like to be able to adjust the weighting function such that the model focuses on modelling perceptually important information and ignoring imperceptible bits. From a Fourier analysis perspective (Rissanen et al., 2023; Kreis et al., 2022), by encouraging our model to focus on some noise levels more than others using a weighting function, we are implicitly specifying a preference for modelling low, mid, and/or high-frequency details at different levels.

When $w(v) = 1$, the diffusion objective is equivalent to maximizing the variational lower bound in Section 3.6. As detailed later in Section 4, the invariance to the noise schedule property outlined in Section 4.3 still holds for weighted diffusion objectives.

In terms of noise prediction, following Equation 3.134, the weighted diffusion objective becomes:

$$\mathcal{L}_\infty(\mathbf{x}, w) = \frac{1}{2} \mathbb{E}_{\epsilon \sim \mathcal{N}(0, \mathbf{I})} \left[\int_0^1 w(\text{SNR}(t)) \gamma'_\eta(t) \|\epsilon - \hat{\epsilon}_\theta(\mathbf{z}_t; t)\|_2^2 dt \right], \quad (4.90)$$

where $w(\text{SNR}(t)) = w(\exp(-\gamma_\eta(t)))$, as per the definition of the (learned) noise schedule in Section A.2.

It turns out that the main difference between most diffusion model objectives boils down to the *implied* weighting function $w(\text{SNR}(t))$ being used (Kingma et al., 2021; Kingma and Gao, 2023). For instance, Ho et al. (2020); Song and Ermon (2019, 2020); Nichol and Dhariwal (2021)

choose to minimize a so-called *simple* objective of the form:

$$\mathcal{L}_{\infty\text{-simple}}(\mathbf{x}) := \mathbb{E}_{\epsilon \sim \mathcal{N}(0, \mathbf{I}), t \sim \mathcal{U}(0, 1)} \left[\|\boldsymbol{\epsilon} - \hat{\boldsymbol{\epsilon}}_{\boldsymbol{\theta}}(\mathbf{z}_t; t)\|_2^2 \right], \quad (4.91)$$

or the analogous discrete-time version

$$\mathcal{L}_{T\text{-simple}}(\mathbf{x}) := \mathbb{E}_{\epsilon \sim \mathcal{N}(0, \mathbf{I}), i \sim U\{1, T\}} \left[\left\| \boldsymbol{\epsilon} - \hat{\boldsymbol{\epsilon}}_{\boldsymbol{\theta}}(\mathbf{z}_{t(i)}; t(i)) \right\|_2^2 \right], \quad (4.92)$$

where $t(i) = i/T$ for T . Contrasting the above with Equation 4.90, we can deduce that the $\mathcal{L}_{\infty\text{-simple}}(\mathbf{x})$ objective above implies the following weighting function:

$$\begin{aligned} \mathcal{L}_{\infty}(\mathbf{x}, w) &= \frac{1}{2} \mathbb{E}_{\epsilon \sim \mathcal{N}(0, \mathbf{I}), t \sim \mathcal{U}(0, 1)} \left[w(\text{SNR}(t)) \gamma'_{\boldsymbol{\eta}}(t) \|\boldsymbol{\epsilon} - \hat{\boldsymbol{\epsilon}}_{\boldsymbol{\theta}}(\mathbf{z}_t; t)\|_2^2 \right] \\ &\quad (4.93) \end{aligned}$$

$$= \frac{1}{2} \mathbb{E}_{\epsilon \sim \mathcal{N}(0, \mathbf{I}), t \sim \mathcal{U}(0, 1)} \left[\frac{1}{\gamma'_{\boldsymbol{\eta}}(t)} \gamma'_{\boldsymbol{\eta}}(t) \|\boldsymbol{\epsilon} - \hat{\boldsymbol{\epsilon}}_{\boldsymbol{\theta}}(\mathbf{z}_t; t)\|_2^2 \right] \quad (4.94)$$

$$= \frac{1}{2} \mathcal{L}_{\infty\text{-simple}}(\mathbf{x}) \implies w(\text{SNR}(t)) = \frac{1}{\gamma'_{\boldsymbol{\eta}}(t)}. \quad (4.95)$$

It is worth restating that – in contrast to VDMs – the noise schedule specification in most commonly used diffusion models is fixed rather than learned from data, i.e. there are no learnable parameters $\boldsymbol{\eta}$.

Moreover, notice that Ho et al. (2020)’s popular noise prediction objective is an implicitly defined *weighted* objective in image space, where the weighting is a function of the signal-to-noise ratio:

$$\mathcal{L}_{\infty\text{-simple}}(\mathbf{x}) = \mathbb{E}_{\epsilon \sim \mathcal{N}(0, \mathbf{I}), t \sim \mathcal{U}(0, 1)} \left[\|\boldsymbol{\epsilon} - \hat{\boldsymbol{\epsilon}}_{\boldsymbol{\theta}}(\mathbf{z}_t; t)\|_2^2 \right] \quad (4.96)$$

$$\begin{aligned} &= \mathbb{E}_{\epsilon \sim \mathcal{N}(0, \mathbf{I}), t \sim \mathcal{U}(0, 1)} \left[\left\| \frac{\mathbf{z}_t - \alpha_t \mathbf{x}}{\sigma_t} - \frac{\mathbf{z}_t - \alpha_t \hat{\mathbf{x}}_{\boldsymbol{\theta}}(\mathbf{z}_t; t)}{\sigma_t} \right\|_2^2 \right] \\ &\quad (4.97) \end{aligned}$$

$$= \mathbb{E}_{\epsilon \sim \mathcal{N}(0, \mathbf{I}), t \sim \mathcal{U}(0, 1)} \left[\frac{\alpha_t^2}{\sigma_t^2} \|\mathbf{x} - \hat{\mathbf{x}}_{\boldsymbol{\theta}}(\mathbf{z}_t; t)\|_2^2 \right] \quad (4.98)$$

$$= \mathbb{E}_{\epsilon \sim \mathcal{N}(0, \mathbf{I}), t \sim \mathcal{U}(0, 1)} \left[w(\text{SNR}(t)) \|\mathbf{x} - \hat{\mathbf{x}}_{\boldsymbol{\theta}}(\mathbf{z}_t; t)\|_2^2 \right], \quad (4.99)$$

recalling that $\mathbf{z}_t = \alpha_t \mathbf{x} + \sigma_t \boldsymbol{\epsilon}$, $\boldsymbol{\epsilon} \sim \mathcal{N}(0, \mathbf{I})$ by definition (ref. Section 3.1). In this case, the implied weighting function of the noise schedule (in image space) is the identity: $w(\text{SNR}(t)) = \text{SNR}(t)$.

4.5 Noise Schedule Density

To remain consistent with Kingma and Gao (2023), let $\lambda = \log(\alpha_\lambda^2 / \sigma_\lambda^2)$ denote the logarithm of the signal-to-noise ratio function $\text{SNR}(t)$, where $\alpha_\lambda^2 = \text{sigmoid}(\lambda_t)$ and $\sigma_\lambda^2 = \text{sigmoid}(-\lambda_t)$, for a timestep t . Let $f_\lambda : [0, 1] \rightarrow \mathbb{R}$ denote the *noise schedule* function, which maps from time $t \in [0, 1]$ to the log-SNR λ , which we may explicitly denote by λ_t . Like before, the noise schedule function is monotonic thus invertible: $t = f_\lambda^{-1}(\lambda)$, and its endpoints are $\lambda_{\max} := f_\lambda(0)$ and $\lambda_{\min} := f_\lambda(1)$.

We can perform a *change of variables* to define a probability density over noise levels:

$$p(\lambda) = p_T(f_\lambda^{-1}(\lambda)) \left| \frac{df_\lambda^{-1}(\lambda)}{d\lambda} \right| \quad (4.100)$$

$$= 1 \cdot \left| \frac{dt}{d\lambda} \right| \quad (4.101)$$

$$= -\frac{dt}{d\lambda}, \quad (\text{as } f_\lambda \text{ is monotonic}) \quad (4.102)$$

where $p_T = \mathcal{U}(0, 1)$ is a (continuous) uniform distribution over time, which we sample from during training $t \sim p_T$ to compute the log-SNR $\lambda = f_\lambda(t)$. In intuitive terms, the density $p(\lambda)$ describes the relative importance that the model assigns to different noise levels. Note that it can sometimes be beneficial to use different noise schedules for training and sampling (Karras et al., 2022). Since f_λ is strictly monotonically decreasing in time and thus has negative slope, we can simplify the absolute value in Equation 4.101 with a negative sign to ensure the density $p(\lambda)$ remains positive.

Nothing that $\text{SNR}(t) = e^\lambda$, the weighted diffusion objective can be trivially expressed in terms of λ as:

$$\mathcal{L}_\infty(\mathbf{x}) = -\frac{1}{2} \mathbb{E}_{\epsilon \sim \mathcal{N}(0, \mathbf{I}), t \sim \mathcal{U}(0, 1)} \left[\text{SNR}'(t) \|\mathbf{x} - \hat{\mathbf{x}}_\theta(\mathbf{z}_t; t)\|_2^2 \right] \quad (4.103)$$

$$= -\frac{1}{2} \mathbb{E}_{\epsilon \sim \mathcal{N}(0, \mathbf{I}), t \sim \mathcal{U}(0, 1)} \left[e^\lambda \frac{d\lambda}{dt} \|\mathbf{x} - \hat{\mathbf{x}}_\theta(\mathbf{z}_t; t)\|_2^2 \right] \quad (\text{chain rule}) \quad (4.104)$$

$$= -\frac{1}{2} \mathbb{E}_{\epsilon \sim \mathcal{N}(0, \mathbf{I}), t \sim \mathcal{U}(0, 1)} \left[e^{\lambda} \frac{d\lambda}{dt} \left\| \frac{\mathbf{z}_t - \sigma_t \epsilon}{\alpha_t} - \frac{\mathbf{z}_t - \sigma_t \hat{\epsilon}_{\theta}(\mathbf{z}_t; t)}{\alpha_t} \right\|_2^2 \right] \quad (4.105)$$

$$= -\frac{1}{2} \mathbb{E}_{\epsilon \sim \mathcal{N}(0, \mathbf{I}), t \sim \mathcal{U}(0, 1)} \left[e^{\lambda} \frac{d\lambda}{dt} \frac{\sigma_t^2}{\alpha_t^2} \|\epsilon - \hat{\epsilon}_{\theta}(\mathbf{z}_t; \lambda_t)\|_2^2 \right] \quad (4.106)$$

$$= -\frac{1}{2} \mathbb{E}_{\epsilon \sim \mathcal{N}(0, \mathbf{I}), t \sim \mathcal{U}(0, 1)} \left[\frac{d\lambda}{dt} \|\epsilon - \hat{\epsilon}_{\theta}(\mathbf{z}_t; \lambda_t)\|_2^2 \right]. \quad (\text{since } e^{\lambda} = \alpha_t^2 / \sigma_t^2) \quad (4.107)$$

For complete clarity, the negative sign in front comes from the fact that $\lambda_t = -\gamma_{\eta}(t)$ in the previous parameterization; so the negative sign in front of the original denoising objective in Equation 3.124 no longer cancels out with the $-\gamma'_{\eta}(t)$ term from the noise-prediction derivation in Equation 3.133.

As in Section 4.3, we can perform a change of variables to transform our integral w.r.t. to time t into an integral w.r.t. our new variable λ – the *logarithm* of the signal-to-noise ratio:

$$\mathcal{L}_{\infty}(\mathbf{x}) = -\frac{1}{2} \mathbb{E}_{\epsilon \sim \mathcal{N}(0, \mathbf{I}), t \sim \mathcal{U}(0, 1)} \left[\frac{d\lambda}{dt} \|\epsilon - \hat{\epsilon}_{\theta}(\mathbf{z}_t; \lambda_t)\|_2^2 \right] \quad (4.108)$$

$$= -\frac{1}{2} \mathbb{E}_{\epsilon \sim \mathcal{N}(0, \mathbf{I})} \left[\int_0^1 \left\| \epsilon - \hat{\epsilon}_{\theta} \left(\sigma_t \left(\mathbf{x} \sqrt{\exp(\lambda_t)} + \epsilon \right); t \right) \right\|_2^2 \cdot \frac{d\lambda}{dt} dt \right] \quad (4.109)$$

$$= -\frac{1}{2} \mathbb{E}_{\epsilon \sim \mathcal{N}(0, \mathbf{I})} \left[\int_{f_{\lambda}(0)}^{f_{\lambda}(1)} \|\epsilon - \hat{\epsilon}_{\theta}(\mathbf{z}_{\lambda}; \lambda)\|_2^2 d\lambda \right] \quad (4.110)$$

$$= \frac{1}{2} \mathbb{E}_{\epsilon \sim \mathcal{N}(0, \mathbf{I})} \left[\int_{f_{\lambda}(1)}^{f_{\lambda}(0)} \|\epsilon - \hat{\epsilon}_{\theta}(\mathbf{z}_{\lambda}; \lambda)\|_2^2 d\lambda \right] \quad (\text{swap limits}) \quad (4.111)$$

$$= \frac{1}{2} \mathbb{E}_{\epsilon \sim \mathcal{N}(0, \mathbf{I})} \left[\int_{\lambda_{\min}}^{\lambda_{\max}} \|\epsilon - \hat{\epsilon}_{\theta}(\mathbf{z}_{\lambda}; \lambda)\|_2^2 d\lambda \right]. \quad (4.112)$$

The weighted version of the objective is then simply

$$\mathcal{L}_w(\mathbf{x}) = \frac{1}{2} \mathbb{E}_{\epsilon \sim \mathcal{N}(0, \mathbf{I})} \left[\int_{\lambda_{\min}}^{\lambda_{\max}} w(\lambda) \|\epsilon - \hat{\epsilon}_{\theta}(\mathbf{z}_{\lambda}; \lambda)\|_2^2 d\lambda \right], \quad (4.113)$$

which once again shows that the diffusion loss integral does *not* depend directly on the *noise schedule* function f_λ except for at its endpoints $\lambda_{\min}, \lambda_{\max}$; and through the choice of weighting function $w(\lambda)$. In other words, given the value of λ , the value of $t = f_\lambda^{-1}(\lambda)$ is simply irrelevant for evaluating the integral.

Therefore, the only meaningful difference between diffusion objectives is the choice of weighting function used (Kingma and Gao, 2023).

4.6 Importance Sampling Distribution

Although the invariance to the noise schedule still holds under different weighting functions $w(\lambda)$ in Equation 4.113, it does *not* hold for the Monte Carlo estimator we use during training (e.g. Equation 4.107), which is based on random samples from our distribution over the time variable $t \sim \mathcal{U}(0, 1)$, and Gaussian noise distribution $\epsilon \sim \mathcal{N}(0, \mathbf{I})$. Indeed, the choice of noise schedule affects the *variance* of the Monte Carlo estimator of the diffusion loss. To demonstrate this fact, we first briefly review Importance Sampling (IS); which is a set of Monte Carlo methods used to estimate expectations under a *target* distribution p using a weighted average of samples from an *importance* distribution q of our choosing.

Let $p(x)$ be a probability density for a random variable X , and $f(X)$ be some function we would like to compute the expectation of $\mu = \mathbb{E}_p [f(X)]$. The basic probability result of IS stipulates that whenever sampling from some target distribution $p(x)$ directly is inefficient or impossible (e.g. we only know $p(x)$ up to a normalizing constant), we can choose any density $q(x)$ to compute μ :

$$\mu = \int f(x)p(x) dx = \int f(x)p(x) \frac{q(x)}{q(x)} dx = \mathbb{E}_q \left[\frac{p(X)}{q(X)} f(X) \right], \quad (4.114)$$

as long as $q(x) > 0$ whenever $f(x)p(x) \neq 0$. Concretely, we can estimate μ using samples from q :

$$\hat{\mu} = \frac{1}{N} \sum_{i=1}^N \frac{p(X_i)}{q(X_i)} f(X_i), \quad X_1, \dots, X_N \stackrel{\text{iid}}{\sim} q, \quad (4.115)$$

where, by the weak law of large numbers, $\hat{\mu} \xrightarrow{P} \mu$ when $N \rightarrow \infty$.

Now, observe that it is possible to rewrite the weighted diffusion objective above (i.e. Equation 4.107) such that the noise schedule density $p(\lambda)$ is revealed to be an *importance sampling* distribution:

$$\mathcal{L}_w(\mathbf{x}) = \frac{1}{2} \mathbb{E}_{\epsilon \sim \mathcal{N}(0, \mathbf{I}), t \sim \mathcal{U}(0, 1)} \left[w(\lambda_t) \cdot -\frac{d\lambda}{dt} \cdot \|\boldsymbol{\epsilon} - \hat{\boldsymbol{\epsilon}}_{\boldsymbol{\theta}}(\mathbf{z}_t; \lambda)\|_2^2 \right] \quad (4.116)$$

$$= - \int_0^1 \left(\frac{1}{2} \int \|\boldsymbol{\epsilon} - \hat{\boldsymbol{\epsilon}}_{\boldsymbol{\theta}}(\mathbf{z}_t; \lambda)\|_2^2 p(\epsilon) d\epsilon \right) w(\lambda) \frac{d\lambda}{dt} dt \quad (4.117)$$

$$=: - \int_0^1 h(t; \mathbf{x}) w(\lambda) \frac{d\lambda}{dt} dt \quad (\text{define } h(\cdot) \text{ for brevity}) \quad (4.118)$$

$$= \int_{f_{\lambda}(1)}^{f_{\lambda}(0)} h(\lambda; \mathbf{x}) w(\lambda) d\lambda \quad (\text{change-of-variables}) \quad (4.119)$$

$$= \int_{f_{\lambda}(1)}^{f_{\lambda}(0)} h(\lambda; \mathbf{x}) w(\lambda) \frac{p(\lambda)}{p(\lambda)} d\lambda \quad (\text{introduce IS distribution}) \quad (4.120)$$

$$= \mathbb{E}_{\lambda \sim p(\lambda)} \left[\frac{w(\lambda)}{p(\lambda)} h(\lambda; \mathbf{x}) \right] \quad (4.121)$$

$$= \mathbb{E}_{\lambda \sim p(\lambda)} \left[\frac{w(\lambda)}{p(\lambda)} \mathbb{E}_{\epsilon \sim \mathcal{N}(0, \mathbf{I})} \left[\frac{1}{2} \|\boldsymbol{\epsilon} - \hat{\boldsymbol{\epsilon}}_{\boldsymbol{\theta}}(\mathbf{z}_{\lambda}; \lambda)\|_2^2 \right] \right] \quad (4.122)$$

$$= \frac{1}{2} \mathbb{E}_{\epsilon \sim \mathcal{N}(0, \mathbf{I}), \lambda \sim p(\lambda)} \left[\frac{w(\lambda)}{p(\lambda)} \|\boldsymbol{\epsilon} - \hat{\boldsymbol{\epsilon}}_{\boldsymbol{\theta}}(\mathbf{z}_{\lambda}; \lambda)\|_2^2 \right]. \quad (4.123)$$

It is clear then that different choices of the noise schedule affect the variance of the Monte Carlo estimator of the diffusion loss because the noise schedule density $p(\lambda)$ acts as an importance sampling distribution. Importantly, judicious choices of the importance distribution can substantially increase the efficiency of Monte Carlo algorithms for numerically evaluating integrals.

A natural question to ask at this stage is how one may select $p(\lambda)$, such that a variance reduction is obtained. Variance reduction is obtained if and only if the difference between the variance of the original estimator $h(\lambda; \mathbf{x})$ and the importance sampling estimator $\hat{h}(\lambda; \mathbf{x}) := h(\lambda; \mathbf{x})w(\lambda)/p(\lambda)$ is strictly positive. Formally, the following expression

should evaluate to a value greater than 0:

$$\begin{aligned} \mathbb{V}_w(h(\lambda; \mathbf{x})) - \mathbb{V}_p(\hat{h}(\lambda; \mathbf{x})) &= \\ &= \int h^2(\lambda; \mathbf{x})w(\lambda) d\lambda - \left(\int h(\lambda; \mathbf{x})w(\lambda) d\lambda \right)^2 \end{aligned} \quad (4.124)$$

$$- \left(\int \left(\frac{h(\lambda; \mathbf{x})w(\lambda)}{p(\lambda)} \right)^2 p(\lambda) d\lambda - \left(\int \frac{h(\lambda; \mathbf{x})w(\lambda)}{p(\lambda)} p(\lambda) d\lambda \right)^2 \right) \quad (4.125)$$

$$= \int h^2(\lambda; \mathbf{x})w(\lambda) d\lambda - \left(\int h(\lambda; \mathbf{x})w(\lambda) d\lambda \right)^2 \quad (4.126)$$

$$- \int \hat{h}^2(\lambda; \mathbf{x})p(\lambda) d\lambda + \left(\int h(\lambda; \mathbf{x})w(\lambda) d\lambda \right)^2 \quad (4.127)$$

$$= \int h^2(\lambda; \mathbf{x})w(\lambda) - \frac{h^2(\lambda; \mathbf{x})w^2(\lambda)}{p(\lambda)} d\lambda \quad (\text{substitute out } \hat{h}) \quad (4.128)$$

$$= \mathbb{E}_w \left[\left(1 - \frac{w(\lambda)}{p(\lambda)} \right) h^2(\lambda; \mathbf{x}) \right], \quad (4.129)$$

revealing a concise expression that may be useful for practical evaluation. It is a well-known result that the optimal IS distribution is of the form $p^*(\lambda) \propto |h(\lambda; \mathbf{x})|w(\lambda)$, since it minimizes the variance of the IS estimator (Wasserman, 2004). However, this result is mostly of theoretical interest rather than practical, as it requires knowledge of the integral we are aiming to estimate in the first place.

Furthermore, our current setting is somewhat different from the type of problem one would typically attack with importance sampling, as here we get to choose both distributions involved:

- (i) The weighting function $w(\lambda)$ acts as the *target* distribution. It stipulates the relative importance of each noise level and ensures the model is focusing on perceptually important information. However, $w(\lambda)$ may not be a valid probability density as the most commonly used (implied) weighting functions do not integrate to 1 over their support.
- (ii) The *importance* distribution is the noise schedule density $p(\lambda)$,

which specifies the noise schedule of the Gaussian diffusion process.

This means we technically ought to retune the noise schedule for different choices of weighting function. To avoid this, [Kingma and Gao \(2023\)](#) propose an adaptive noise schedule where:

$$p(\lambda) \propto \mathbb{E}_{\mathbf{x} \sim \mathcal{D}, \epsilon \sim \mathcal{N}(0, \mathbf{I})} \left[w(\lambda) \|\epsilon - \hat{\epsilon}_{\theta}(\mathbf{z}_{\lambda}; \lambda)\|_2^2 \right], \quad (4.130)$$

thereby ensuring that the magnitude of the loss (Equation 4.123) is approximately invariant to λ , and spread evenly across time t . This approach is often found to speed up optimization significantly. [Song et al. \(2021a\)](#); [Vahdat et al. \(2021\)](#) have also explored variance reduction techniques for diffusion models but from a score-based perspective.

Alternative Adaptive Weighting Methods. [Karras et al. \(2024\)](#) introduce a learning-based adaptation mechanism that balances gradient magnitudes, thereby changing the effective weighting of noise levels during training. Relatedly, [Dieleman et al. \(2022\)](#) propose a technique they call *time warping*, which uses a learnable function to convert loss values into an adaptive noise-level distribution that balances model capacity. [Mueller et al. \(2023\)](#) extend time warping to heterogenous data, learning different noise level distributions for different data types. All the above mechanisms, among others ([Santos and Lin, 2023](#); [Sabour et al., 2024](#)), represent different ways to adapt the noise level weighting, and this topic remains a fertile ground for future work.

4.7 ELBO with Data Augmentation

In this section, we dissect the main result presented by [Kingma and Gao \(2023\)](#); that when the weighting function of the diffusion loss is monotonic, the resulting objective is equivalent to the ELBO under simple data augmentation using Gaussian additive noise. We provide an instructive derivation of this result, discuss its implications, and discuss an extension to the setting of non-monotonic weighting functions.

The general goal is to inspect the behaviour of the weighted diffusion objective across time t , and manipulate the expression such that we end up with an expectation under a valid probability distribution specified

by the weighting function $w(\lambda)$. This then allows us to examine the integrand and reveal that it corresponds to the expected negative ELBO of noise-perturbed data.

To that end, let $q(\mathbf{z}_{t:1} \mid \mathbf{x}) := q(\mathbf{z}_t, \mathbf{z}_{t+dt}, \dots, \mathbf{z}_1 \mid \mathbf{x})$ denote the joint distribution of the posterior (forward process) for a subset of timesteps: $\{t, t + dt, \dots, 1\}$, where $t > 0$ and dt denotes an infinitesimal change in time. Analogously, let $p(\mathbf{z}_{t:1})$ denote the prior (generative model) for the same subset of timesteps.

The KL divergence of the joint posterior $q(\mathbf{z}_{t:1} \mid \mathbf{x})$ from the joint prior $p(\mathbf{z}_{t:1})$ is given by

$$\mathcal{L}(t; \mathbf{x}) := D_{\text{KL}}(q(\mathbf{z}_{t:1} \mid \mathbf{x}) \parallel p(\mathbf{z}_{t:1})) \quad (4.131)$$

$$= \frac{1}{2} \mathbb{E}_{\boldsymbol{\epsilon} \sim \mathcal{N}(0, \mathbf{I})} \left[- \int_{f_\lambda(t)}^{f_\lambda(1)} \|\boldsymbol{\epsilon} - \hat{\boldsymbol{\epsilon}}_{\boldsymbol{\theta}}(\mathbf{z}_\lambda; \lambda)\|_2^2 d\lambda \right].$$

(from Eq. 4.112) (4.132)

Next, we rearrange and differentiate under the integral sign w.r.t. time t to give:

$$\frac{d\mathcal{L}(t; \mathbf{x})}{dt} = \frac{d}{dt} \left(\int_{f_\lambda(t)}^{f_\lambda(1)} -\frac{1}{2} \mathbb{E}_{\boldsymbol{\epsilon} \sim \mathcal{N}(0, \mathbf{I})} [\|\boldsymbol{\epsilon} - \hat{\boldsymbol{\epsilon}}_{\boldsymbol{\theta}}(\mathbf{z}_\lambda; \lambda)\|_2^2] d\lambda \right) \quad (4.133)$$

$$=: \frac{d}{dt} \left(\int_{f_\lambda(t)}^{f_\lambda(1)} h(\lambda; \mathbf{x}) d\lambda \right) \quad (4.134)$$

$$= \frac{d}{dt} [F(f_\lambda(1)) - F(f_\lambda(t))] \quad (F \text{ is an antiderivative of } h) \quad (4.135)$$

$$= 0 - F'(f_\lambda(t)) \cdot f'_\lambda(t) \quad (\text{chain rule}) \quad (4.136)$$

$$= -F'(\lambda) \cdot \frac{d\lambda}{dt} \quad (\text{recall } \lambda = f_\lambda(t)) \quad (4.137)$$

$$= \frac{1}{2} \frac{d\lambda}{dt} \mathbb{E}_{\boldsymbol{\epsilon} \sim \mathcal{N}(0, \mathbf{I})} [\|\boldsymbol{\epsilon} - \hat{\boldsymbol{\epsilon}}_{\boldsymbol{\theta}}(\mathbf{z}_\lambda; \lambda)\|_2^2],$$

(since $F'(\lambda) = h(\lambda; \mathbf{x})$) (4.138)

which allows us to rewrite the weighted diffusion objective by substitut-

ing in the above result:

$$\mathcal{L}_w(\mathbf{x}) = -\frac{1}{2} \mathbb{E}_{\epsilon \sim \mathcal{N}(0, \mathbf{I}), t \sim \mathcal{U}(0, 1)} \left[w(\lambda_t) \cdot \frac{d\lambda}{dt} \cdot \|\epsilon - \hat{\epsilon}_\theta(\mathbf{z}_t; \lambda)\|_2^2 \right] \quad (4.139)$$

$$= \mathbb{E}_{t \sim \mathcal{U}(0, 1)} \left[w(\lambda_t) \cdot -\frac{1}{2} \frac{d\lambda}{dt} \mathbb{E}_{\epsilon \sim \mathcal{N}(0, \mathbf{I})} \left[\|\epsilon - \hat{\epsilon}_\theta(\mathbf{z}_t; \lambda)\|_2^2 \right] \right] \quad (4.140)$$

$$= \mathbb{E}_{t \sim \mathcal{U}(0, 1)} \left[-\frac{d\mathcal{L}(t; \mathbf{x})}{dt} w(\lambda_t) \right]. \quad (\text{time derivative}) \quad (4.141)$$

After some simple manipulation, we can see that the resulting expression is an expectation of the time derivative of the joint KL divergence $\mathcal{L}(t; \mathbf{x})$, weighted by the weighting function $w(\lambda_t)$. This result is not particularly interesting or surprising by itself, but it enables the next step; using integration by parts to turn the above expression into an expectation under a valid probability distribution specified by the weighting function. Recall that the formula for integration by parts is given by:

$$\int_a^b u(t)v'(t) dt = u(b)v(b) - u(a)v(a) - \int_a^b u'(t)v(t) dt. \quad (4.142)$$

Setting $u(t) = w(\lambda_t)$ and $v'(t) = d/dt \mathcal{L}(t; \mathbf{x})$ then gives:

$$\mathcal{L}_w(\mathbf{x}) = \int_0^1 -\frac{d\mathcal{L}(t; \mathbf{x})}{dt} w(\lambda_t) dt \quad (4.143)$$

$$= - \left(w(\lambda_1)\mathcal{L}(1; \mathbf{x}) - w(\lambda_0)\mathcal{L}(0; \mathbf{x}) - \int_0^1 \frac{dw(\lambda_t)}{dt} \mathcal{L}(t; \mathbf{x}) dt \right) \quad (4.144)$$

$$= \int_0^1 \frac{dw(\lambda_t)}{dt} \mathcal{L}(t; \mathbf{x}) dt + w(\lambda_0)\mathcal{L}(0; \mathbf{x}) - w(\lambda_1)\mathcal{L}(1; \mathbf{x}) \quad (4.145)$$

$$= \int_0^1 \frac{dw(\lambda_t)}{dt} \mathcal{L}(t; \mathbf{x}) dt + c, \quad (\text{absorb constants into } c) \quad (4.146)$$

where c is a small constant for two simple reasons:

- (i) $w(\lambda_0)\mathcal{L}(0; \mathbf{x}) = w(\lambda_{\max})D_{\text{KL}}(q(\mathbf{z}_{0:1} \mid \mathbf{x}) \parallel p(\mathbf{z}_{0:1}))$ is small due to the weighting function acting on λ_{\max} always being very small by construction (Kingma and Gao, 2023);
- (ii) $-w(\lambda_1)\mathcal{L}(1; \mathbf{x}) = -w(\lambda_{\min})D_{\text{KL}}(q(\mathbf{z}_1 \mid \mathbf{x}) \parallel p(\mathbf{z}_1))$ includes the KL between the posterior of the noisiest latent \mathbf{z}_1 and the prior,

which is both independent of the parameters $\boldsymbol{\theta}$ of the model $\hat{e}_{\boldsymbol{\theta}}(\mathbf{z}_t; \lambda)$, and very close to 0 for a well-specified forward diffusion process.

The astute reader may notice that the derivative term $d/dt w(\lambda_t)$ in Equation 4.146 is a valid probability density function (PDF) specified by the weighting function, so long as $w(\lambda_t)$ is monotonically increasing w.r.t. time t , and $w(\lambda_{t=1}) = 1$. The proof is straightforward: by the Fundamental Theorem of Calculus, the PDF $f(x)$ of a random variable X is obtained by differentiating the cumulative distribution function (CDF) $F(x)$, that is: $f(x) = d/dx F(x)$, where $F : \mathbb{R} \rightarrow [0, 1]$, $\lim_{x \rightarrow -\infty} F(x) = 0$ and $\lim_{x \rightarrow \infty} F(x) = 1$.

Therefore, in our context, w is a valid CDF if it satisfies the following three standard conditions:

$$(i) \quad w : \mathbb{R} \rightarrow [0, 1] \quad (4.147)$$

$$(ii) \quad t > t - dt \implies w(\lambda_t) \geq w(\lambda_{t-dt}), \quad \forall t \in [0, 1] \quad (4.148)$$

$$(iii) \quad \lim_{t \rightarrow 0} w(\lambda_t) = 0, \text{ and } \lim_{t \rightarrow 1} w(\lambda_t) = 1. \quad (4.149)$$

In words, w must: (i) map the real line to $[0, 1]$, (ii) be non-decreasing w.r.t. time t , and (iii) be normalized w.r.t. time t .

If the above conditions hold, we can define a valid probability distribution $p_w(t)$ specified by the weighting function:

$$p_w(t) := \frac{dw(\lambda_t)}{dt}, \quad \text{where} \quad w(\lambda_t) = \int_0^{\lambda_t} p_w(t) dt, \quad (4.150)$$

with support on the range $[0, 1]$, thus $\int_0^1 p_w(t) dt = 1$.

This then permits us to rewrite the diffusion loss as an expectation under $p_w(t)$ by substituting:

$$\mathcal{L}_w(\mathbf{x}) = \int_0^1 \frac{dw(\lambda_t)}{dt} \mathcal{L}(t; \mathbf{x}) dt + c \quad (\text{from Eq. 4.146}) \quad (4.151)$$

$$= \mathbb{E}_{t \sim p_w(t)} [\mathcal{L}(t; \mathbf{x})] + c. \quad (4.152)$$

The final move is to show that the joint KL divergence $\mathcal{L}(t; \mathbf{x})$ for any subset of timesteps $\{t, t + dt, \dots, 1\}$ decomposes into the expected negative ELBO of noisy data $\mathbf{z}_t \sim q(\mathbf{z}_t | \mathbf{x})$ at any timestep t :

$$\mathcal{L}(t; \mathbf{x}) = D_{\text{KL}}(q(\mathbf{z}_{t:1} | \mathbf{x}) \parallel p(\mathbf{z}_{t:1})) \quad (4.153)$$

$$= \int q(\mathbf{z}_{t:1} \mid \mathbf{x}) \log \frac{q(\mathbf{z}_{t:1} \mid \mathbf{x})}{p(\mathbf{z}_{t:1})} d\mathbf{z}_{t:1} \quad (4.154)$$

$$= \int q(\mathbf{z}_t \mid \mathbf{x}) q(\mathbf{z}_{t+dt:1} \mid \mathbf{x}) \log \frac{q(\mathbf{z}_t \mid \mathbf{x}) q(\mathbf{z}_{t+dt:1} \mid \mathbf{x})}{p(\mathbf{z}_t \mid \mathbf{z}_{t+dt}) p(\mathbf{z}_{t+dt:1})} d\mathbf{z}_{t:1} \quad (4.155)$$

$$\begin{aligned} &= \mathbb{E}_{q(\mathbf{z}_t \mid \mathbf{x})} \left[\mathbb{E}_{q(\mathbf{z}_{t+dt:1} \mid \mathbf{x})} \left[\log \frac{q(\mathbf{z}_{t+dt:1} \mid \mathbf{x})}{p(\mathbf{z}_{t+dt:1})} - \log p(\mathbf{z}_t \mid \mathbf{z}_{t+dt}) \right] \right] \\ &\quad + \mathbb{E}_{q(\mathbf{z}_t \mid \mathbf{x})} [\log q(\mathbf{z}_t \mid \mathbf{x})] \quad (\text{constant entropy term } \mathcal{H}(\cdot)) \end{aligned} \quad (4.156)$$

$$\begin{aligned} &= \mathbb{E}_{q(\mathbf{z}_t \mid \mathbf{x})} \left[\mathbb{E}_{q(\mathbf{z}_{t+dt} \mid \mathbf{x})} [-\log p(\mathbf{z}_t \mid \mathbf{z}_{t+dt})] \right. \\ &\quad \left. + D_{\text{KL}}(q(\mathbf{z}_{t+dt:1} \mid \mathbf{x}) \parallel p(\mathbf{z}_{t+dt:1})) \right] - \mathcal{H}(q(\mathbf{z}_t \mid \mathbf{x})) \end{aligned} \quad (4.157)$$

$$= \mathbb{E}_{q(\mathbf{z}_t \mid \mathbf{x})} [-\text{ELBO}_t(\mathbf{z}_t)] - \mathcal{H}(q(\mathbf{z}_t \mid \mathbf{x})). \quad (4.158)$$

As shown, factoring the joint distributions into infinitesimal transitions between \mathbf{z}_t and \mathbf{z}_{t+dt} reveals an expected variational free energy term (negative ELBO), which is an upper bound on the negative log-likelihood of noisy data: $-\text{ELBO}_t(\mathbf{z}_t) \geq -\log p(\mathbf{z}_t)$, where $\mathbf{z}_t \sim q(\mathbf{z}_t \mid \mathbf{x})$ for any timestep t . The entropy term $\mathcal{H}(q(\mathbf{z}_t \mid \mathbf{x}))$ is constant since our forward process is fixed, i.e. it is a Gaussian diffusion.

Finally, substituting the above result into the (expected) weighted diffusion loss gives

$$\mathcal{L}_w(\mathbf{x}) = \mathbb{E}_{p_w(t)} [\mathcal{L}(t; \mathbf{x})] + c \quad (\text{from Equation 4.152}) \quad (4.159)$$

$$\begin{aligned} &= \mathbb{E}_{p_w(t)} \left[\mathbb{E}_{q(\mathbf{z}_t \mid \mathbf{x})} [-\text{ELBO}_t(\mathbf{z}_t)] - \mathcal{H}(q(\mathbf{z}_t \mid \mathbf{x})) \right] + c \\ &\quad (\text{substitute}) \end{aligned} \quad (4.160)$$

$$\begin{aligned} &= -\mathbb{E}_{p_w(t), q(\mathbf{z}_t \mid \mathbf{x})} [\text{ELBO}_t(\mathbf{z}_t)] + c \\ &\quad (\text{absorb entropy constant}) \end{aligned} \quad (4.161)$$

$$\begin{aligned} &\geq -\mathbb{E}_{p_w(t), q(\mathbf{z}_t \mid \mathbf{x})} [\log p(\mathbf{z}_t)] + c, \\ &\quad (\text{noisy data log-likelihood}) \end{aligned} \quad (4.162)$$

which proves that when the weighting function $w(\lambda_t)$ is monotonically increasing w.r.t. time t , diffusion objectives are equivalent to the ELBO under simple data augmentation using Gaussian additive noise. To be

clear, the Gaussian additive noise comes from the fact that the forward diffusion specification is linear Gaussian, and as such, each $\mathbf{z}_t \sim q(\mathbf{z}_t \mid \mathbf{x})$ is simply a noisy version of the data \mathbf{x} . The distribution $p_w(t)$ acts as a sort of data augmentation kernel, specifying the importance of different noise levels. It is worth noting that this type of data augmentation setup resembles distribution augmentation (DistAug) and distribution smoothing methods (Meng et al., 2020; Jun et al., 2020), which have previously been shown to improve the sample quality of autoregressive generative models.

Now going back to Equation 4.146, we see that the diffusion loss is a weighted integral of ELBOs:

$$\mathcal{L}_w(\mathbf{x}) = \int_0^1 \mathcal{L}(t; \mathbf{x}) \frac{dw(\lambda_t)}{dt} dt + c \quad (4.163)$$

$$= \int_0^1 \mathbb{E}_{q(\mathbf{z}_t \mid \mathbf{x})} [-\text{ELBO}_t(\mathbf{z}_t)] dw(\lambda_t) + c, \quad (4.164)$$

since $\mathcal{L}(t; \mathbf{x})$ equates to the expected negative ELBO for noise-perturbed data $\mathbf{z}_t \sim q(\mathbf{z}_t \mid \mathbf{x})$ as explained above, and the $dw(\lambda_t)$ term simply weights the ELBO at each noise level.

4.7.1 Non-monotonic Weighting Functions

Several works have observed impressive synthesis results when using non-monotonic weighting functions (Nichol and Dhariwal, 2021; Karras et al., 2022; Choi et al., 2022; Hang et al., 2023). What are the theoretical implications of using such weighting functions?

Looking again at Equation 4.164, we observe that regardless of the weighting function, diffusion objectives boil down to a weighted integral of ELBOs. However, if the weighting function is non-monotonic (thus w is not a valid CDF) then the derivative term $d/dt w(\lambda_t)$ will be negative for some points in time, meaning we end up *minimizing* the ELBO at those noise levels rather than maximizing it! This is somewhat inconvenient in light of the practical success of non-monotonic weighting functions and seems to reaffirm the widespread belief that maximum likelihood may not be the appropriate objective for generating high-quality samples. One sensible explanation for this success is that the

non-monotonic weighting functions sacrifice some modes of the likelihood in exchange for better perceptual synthesis. Indeed, the majority of bits in images are allocated to imperceptible details and can, therefore, be largely ignored if what we care about is perceptual quality. This aspect was briefly touched upon by [Ho et al. \(2020\)](#); they found that although their diffusion models were not competitive with the state-of-the-art likelihood-based models in terms of lossless codelengths, the samples were of high quality, nonetheless.

With that said, [Kingma and Gao \(2023\)](#) showed that contrary to popular belief, likelihood maximization (i.e. maximizing the ELBO) and high-quality image synthesis are not mutually exclusive in diffusion models. They were able to achieve state-of-the-art FID ([Heusel et al., 2017](#))/Inception ([Salimans et al., 2016](#)) scores on the high-resolution ImageNet benchmark using *monotonic* weighting functions and some practical/architectural improvements proposed by [Hoogeboom et al. \(2023\)](#). For a more detailed characterisation of commonly used weighting functions and whether they are monotonic we encourage the reader to refer to [Kingma and Gao \(2023\)](#) and [Hoogeboom et al. \(2024\)](#). To conclude, as we have learned, optimizing the weighted diffusion loss with a monotonic weighting function is equivalent to maximizing the ELBO under simple data augmentation using Gaussian additive noise.

5

Discussion & Outlook

Despite the growing interest in diffusion models, gaining a deep understanding of the model class remained somewhat elusive for the uninitiated in non-equilibrium statistical physics. With that in mind, we have synthesized a holistic view of diffusion models using only directed graphical modelling and variational inference principles, which is simple and imposes relatively fewer prerequisites on the reader.

The Top-down Perspective. We began by reviewing hierarchical latent variable models and established a unifying graphical modelling-based perspective on their connection with diffusion models. We showed that diffusion models share a specific *top-down* latent variable hierarchy structure with ladder networks (Valpola, 2015) and top-down inference HVAEs (Sønderby et al., 2016), which explains why they share optimization objectives. Although introducing additional latent variables significantly improves the flexibility of both the inference and generative models, it comes with additional challenges. We highlighted the difficulties with using purely *bottom-up* inference procedures in deep latent variable hierarchies, including *posterior collapse* for instance, whereby the posterior distribution (of the top-most layer, say) may collapse to a

standard Gaussian prior, failing to learn meaningful representations and deactivating latent variables. [Burda et al. \(2015\)](#); [Sohl-Dickstein et al. \(2015\)](#) point to the asymmetry between the generative and inference models in bottom-up HVAEs as a source of difficulty in training the inference model efficiently, as there is no way to express each term in the VLB as an expectation under a distribution over a single variable. [Luo \(2022\)](#); [Bishop and Bishop \(2023\)](#) echo similar efficiency-based arguments against optimizing the VLB under bottom-up inference in hierarchical latent variable models.

We showed that efficiency-based perspectives paint an incomplete picture; the main reason one ought to avoid bottom-up inference in hierarchical latent variable models is the lack of direct *feedback* from the generative model. We showed that since the purpose of the inference model is to perform *Bayesian inference* at any given layer in the hierarchy, interleaving feedback from each transition in the generative model into each respective transition in the inference model makes both procedures more accurate. Although this may not benefit diffusion models to the same extent as HVAEs, as the inference model of the former is fixed, the top-down hierarchy structure is nonetheless ubiquitous.

In diffusion models the Markovian transitions between latent states $q(\mathbf{z}_t | \mathbf{z}_{t-1})$ are chosen to be linear Gaussian with isotropic covariances, thus the top-down posterior $q(\mathbf{z}_{t-1} | \mathbf{z}_t, \mathbf{x})$ is tractable through Gaussian conjugacy and the KL divergence terms in the VLB simplify significantly to squared-error terms (Section 3.6.1). Since the Gaussian diffusion process can be defined directly in terms of the conditionals $q(\mathbf{z}_t | \mathbf{x})$ (Section 3.1), it is possible to: (i) train any level of the latent variable hierarchy independently; (ii) share the same denoising model across the whole hierarchy. These are critical advantages over ladder networks and top-down HVAEs, as they both induce hierarchical dependencies between the latent states, preventing the training of individual layers independently. This advantage is particularly salient for infinitely deep latent variable hierarchies induced by diffusion as detailed in Section 3.

In summary, the top-down perspective offers an intuitive understanding of diffusion models as a specific instantiation of ladder networks and hierarchical VAEs with top-down inference models.

Addressing the W[H]ole Problem with VAEs. We highlight that a major problem with (hierarchical) VAEs, which is *not* present in diffusion models, is the *hole problem*. The hole problem refers to the mismatch between the aggregate posterior and the prior. As shown in Figure 2.4, there can be regions with high probability density under the prior which have low probability density under the aggregate posterior. This affects the quality of generated samples, as the decoder may receive latents sampled from regions not covered by the training data. Furthermore, the higher the dimensionality of our data, the less likely it is that our finite dataset covers the entirety of the input space. The manifold hypothesis posits that high-dimensional datasets lie along a much lower-dimensional latent manifold. However, since providing latent variable identifiability guarantees is challenging for most problems (Hyvärinen et al., 2024), in practice, we often resort to unfalsifiable assumptions about both the functional form and dimensionality of the latent space.

Diffusion models cleverly circumvent both of the aforementioned issues by: (i) defining the aggregate posterior to be equal to the prior by construction; and (ii) sacrificing the ability to learn *representations* by fixing the posterior distribution to follow a pre-determined noise schedule. Point (i) ensures a smooth transition between the prior $p(\mathbf{z}_T)$ and the model $p(\mathbf{x} \mid \mathbf{z}_1)$, thereby avoiding drift at inference time. Point (ii) entails defining the latent variables $\mathbf{z}_{1:T}$ as simple noisy versions of the input rather than learnable representations. The added noise can be interpreted as a kind of data augmentation technique, which helps smooth out the data density landscape and connect distant modes of the underlying data distribution.

An Inductive Bias for Perceptual Quality. As explained in Section 3.1, the noise schedule is specified by parameters α_t , σ_t^2 and in combination with a weighting function $w(\alpha_t^2/\sigma_t^2)$, stipulates the relative importance of each noise level in the diffusion objective (Section 4.4). *It turns out that the main difference between most diffusion model objectives boils down to the implied weighting function being used* (Kingma and Gao, 2023). If the primary goal is high-quality synthesis, it suffices to adjust the noise schedule and weighting function such that the model focuses on perceptually important information. Indeed, the majority

of bits in images are allocated to imperceptible details which can in principle be ignored. Moreover, by encouraging the model to focus on some noise levels more than others, we are implicitly prescribing a preference for modelling low, mid, and/or high-frequency details at different noise levels. Relatedly, Ho et al. (2020) found that although their diffusion models were not competitive with state-of-the-art likelihood-based models in terms of lossless codelengths (i.e. compression ability), the samples generated were of high quality nonetheless. *This demonstrates that diffusion models possess excellent inductive biases for image data.*

Why Diffusion Works. We argue that the success of diffusion models can be partly attributed to an additional reduction in *degrees-of-freedom* compared to top-down HVAEs. In VAEs, several simplifying assumptions are needed to make the inference problem tractable and scalable: (i) amortized posterior; (ii) mean-field variational family; (iii) parametric assumptions on $p(\mathbf{x}, \mathbf{z})$; (iv) a Monte Carlo estimator of the VLB. Under the top-down perspective established in Section 3, it is easy to see that diffusion models constitute yet another simplifying assumption by fixing the inference distribution. This transforms the learning problem from minimizing the *reverse* KL divergence to improve our posterior approximation q where the prior p may be fixed:

$$\arg \min_{q \in \mathcal{Q}} D_{\text{KL}}(q(\mathbf{z}_{1:T} \mid \mathbf{x}) \parallel p(\mathbf{z}_{1:T})), \quad (5.1)$$

to minimizing the *forward* KL where the posterior q is fixed:

$$\arg \min_{p \in \mathcal{P}} D_{\text{KL}}(q(\mathbf{z}_{1:T} \mid \mathbf{x}) \parallel p(\mathbf{z}_{1:T})) \quad (5.2)$$

$$= \arg \min_{p \in \mathcal{P}} \mathbb{E}_{q(\mathbf{z}_{1:T} \mid \mathbf{x})} \left[-\log p(\mathbf{z}_{1:T}) \right] - \overbrace{\mathcal{H}(q(\mathbf{z}_{1:T} \mid \mathbf{x}))}^{\text{constant}}, \quad (5.3)$$

which amounts to a *supervised learning* problem under noise-augmented data, optimized via maximum likelihood. Unsupervised learning tries to represent *all* the information about $p(\mathbf{x})$, which includes imperceptible details and complicates the learning problem. Conversely, supervised learning is effective at filtering out unnecessary information for the task at hand, which in combination with carefully weighted diffusion objectives, helps explain how/why diffusion models are capable of high-quality

image synthesis that better aligns with human perception. Generally speaking, having a learnable posterior q can destabilize HLVM training by creating asynchronous learning dynamics with the prior/model p , often leading to posterior collapse due to a constantly shifting target. Diffusion models avoid this by simply holding q fixed, thereby providing a fixed target for p to match during training. Relatedly, the scalability of simple $L2$ -like diffusion objectives also plays a role in its current practical success compared to other HLVM objectives.

In summary, when one’s goal is merely high-quality synthesis, it is generally advantageous to sacrifice representation learning ability by fixing the posterior q and leveraging the tried-and-tested machinery of supervised learning to train a good generative model. *Interestingly, this supervised learning rationale was the motivation behind ladder networks (Valpola, 2015), and we argue that it provides an intuitive perspective on the success of diffusion models.*

Is Maximum Likelihood the Right Objective? In Section 4, we provided a thorough explanation of the various weighted diffusion objectives in the literature. By analyzing weighted diffusion objectives, it is possible to show that they are equivalent to the ELBO under simple data augmentation using Gaussian additive noise (Kingma and Gao, 2023), so long as the weighting function $w(\lambda_t)$ is *monotonically* increasing w.r.t. time t . In Section 4 we provide an instructive derivation of this result and show that it holds if w is a valid CDF. Multiple recent works report impressive image synthesis results using *non-monotonic* weighting functions (Nichol and Dhariwal, 2021; Karras et al., 2022), which somewhat peculiarly implies that the ELBO is being *minimized* at certain noise levels. This seems to reaffirm the widespread belief that maximum likelihood may *not* be the right objective to use for high-quality image synthesis. However, Kingma and Gao (2023) suggest that likelihood maximization needs *not* be intrinsically at odds with high-quality image synthesis, as they were able to achieve state-of-the-art FID scores on the high-resolution ImageNet benchmark by optimizing the ELBO under simple data augmentation.

In light of these results, we further stress that studying the connection between weighted diffusion objectives and maximum likelihood (i.e. the ELBO) is particularly important. This is because we know from Shannon’s *source coding theorem* that the average codelength of the optimal compression scheme is the entropy of the data $\mathcal{H}(X) = \mathbb{E}[-\log p(\mathbf{x})]$, and as long as we are minimizing codelengths given by the information content $-\log p_{\theta}(\mathbf{x})$ defined by a probabilistic model p_{θ} (e.g. by maximizing likelihood w.r.t. θ), then the resulting average codelength $\mathbb{E}[-\log p_{\theta}(\mathbf{x})]$ approaches the entropy of the true data distribution. *This is the fundamental goal of both generative modelling and compression, a goal with which maximum likelihood learning is well aligned.*

Closing Remarks. The success of diffusion models is arguably as much a product of collective engineering effort and scale as it is a product of algorithmic and theoretical insight. Nonetheless, identifying analogies between model classes undoubtedly aids in understanding, and recognizing the unique properties of specific models helps refine our intuitions about what may or may not work in the future. Fertile ground for future work includes: (i) enabling diffusion models to learn meaningful representations, perhaps with inspiration from predecessors like ladder networks (Valpola, 2015) and denoising autoencoders (Vincent et al., 2008); (ii) expanding the family of forward diffusion processes beyond linear Gaussian transitions with isotropic covariances, as this should tighten the VLB; and (iii) studying the identifiability guarantees provided by deterministic diffusion modelling (e.g. probability flow ODEs (Song et al., 2021b)) for causal representation learning.

Acknowledgements

We would like to thank Charles Jones, Rajat Rasal and Avinash Kori for fruitful discussions and valuable feedback. The authors were supported by funding from the ERC under the EU’s Horizon 2020 research and innovation programme (Project MIRA, grant No. 757173), and acknowledge support from EPSRC for the Causality in Healthcare AI Hub (grant number EP/Y028856/1).

Appendices

A

Notation & Extras

A.1 Notation

SYMBOL	DESCRIPTION	SECTION
\mathbf{x}	Observed datapoint, e.g. input image	§1
t	Time index variable $t \in \{1, 2, \dots, T\}$, or $t \in [0, 1]$ for continuous-time	§2.2
\mathbf{z}_t	Latent variable at time t	§2.2
$\mathbf{z}_{1:T}$	Finite set of latent variables representing $\mathbf{z}_1, \mathbf{z}_2, \dots, \mathbf{z}_T$	§2.2
$\mathbf{z}_{0:1}$	Set of latent variables in continuous-time from $t = 0$ to $t = 1$	§3.1
α_t	Noise schedule coefficient $\alpha_t \in (0, 1)$	§3.1
σ_t^2	Noise schedule variance $\sigma_t^2 \in (0, 1)$	§3.1
$\boldsymbol{\epsilon}_t$	Isotropic random noise, $\boldsymbol{\epsilon}_t \sim \mathcal{N}(0, \mathbf{I})$	§1

$\text{SNR}(t)$	Signal-to-noise ratio (SNR) function at time t , defined as α_t^2/σ_t^2	§A.2
$q(\mathbf{z}_t \mid \mathbf{x})$	Latent variable distribution given \mathbf{x}	§3.1
$q(\mathbf{z}_t \mid \mathbf{z}_s)$	Transition distribution from time s to time t , where $s < t$	§3.2
$\alpha_{t s}$	Transition coefficient from time s to t	§3.2
$\sigma_{t s}^2$	Variance of transition distribution	§3.2
$q(\mathbf{z}_s \mid \mathbf{z}_t, \mathbf{x})$	Top-down posterior distribution at time s	§2.4
$\boldsymbol{\mu}_Q(\mathbf{z}_t, \mathbf{x}; s, t)$	Mean of top-down posterior distribution at time s ; $\boldsymbol{\mu}_Q$ for short	§3.3
$\sigma_Q^2(s, t)$	Variance of top-down posterior distribution; σ_Q^2 for short	§3.3
$p(\mathbf{z}_s \mid \mathbf{z}_t)$	Generative transition distribution defined as $q(\mathbf{z}_s \mid \mathbf{z}_t, \mathbf{x} = \hat{\mathbf{x}}_\theta(\mathbf{z}_t, t))$	§3.4
$p(\mathbf{x} \mid \mathbf{z}_0)$	Observation likelihood (e.g. input image), analogous to $p(\mathbf{x} \mid \mathbf{z}_1)$ in discrete-time	§3.4
$\boldsymbol{\phi}$	Variational parameters related to q_ϕ	§1
$\boldsymbol{\theta}$	Model parameters pertaining to p_θ	§1
$\hat{\mathbf{x}}_\theta(\mathbf{z}_t, t)$	Denoising model mapping any \mathbf{z}_t to \mathbf{x}	§3.5
$\hat{\boldsymbol{\epsilon}}_\theta(\mathbf{z}_t, t)$	Noise prediction model, which approximates $\nabla_{\mathbf{z}_t} \log q(\mathbf{z}_t)$	§3.5
$\hat{s}_\theta(\mathbf{z}_t, t)$	Score prediction model, equivalent to $-\hat{\boldsymbol{\epsilon}}_\theta(\mathbf{z}_t, t)/\sigma_t$	§3.5
$\boldsymbol{\mu}_\theta(\mathbf{z}_t; s, t)$	Predicted posterior mean at time $s < t$	§3.5
$\text{VLB}(\mathbf{x})$	Single-datapoint variational lower bound; also denoted as $\text{ELBO}(\mathbf{x})$	§1
$\mathcal{L}_T(\mathbf{x})$	Discrete-time diffusion loss	§3.6
$\mathcal{L}_\infty(\mathbf{x})$	Continuous-time diffusion loss	§3.9

$\mathcal{L}_w(\mathbf{x})$	Weighted diffusion loss; also $\mathcal{L}_\infty(\mathbf{x}, w)$	§4.4
$\gamma_\eta(t)$	Neural network with parameters η for learning the noise schedule	§A.2
$w(\cdot)$	Noise level weighting function	§4.4
λ	Logarithm of $\text{SNR}(t)$; also λ_t	§4.5
$f_\lambda(t)$	Noise schedule function, mapping t to λ	§4.5
λ_{\min}	Lowest log SNR given by $f_\lambda(t = 1)$	§4.5
λ_{\max}	Highest log SNR given by $f_\lambda(t = 0)$	§4.5
$p(\lambda)$	Density over noise levels	§4.5
$\mathcal{L}(t; \mathbf{x})$	Joint KL divergence up to time t	§4.7
$p_w(t)$	Augmentation kernel specified by $w(\cdot)$	§4.7

To remain consistent with prior work and avoid notational clutter, we may use the same symbols to denote random variables and their outcomes whenever our intentions can be clearly understood from context.

A.2 Learning the Noise Schedule

Perturbing data with multiple noise scales and choosing an appropriate *noise schedule* is instrumental to the success of diffusion models. The noise schedule of the forward process is typically pre-specified and has no learnable parameters, however, VDMs learn the noise schedule via the parameterization:

$$\sigma_t^2 = \text{sigmoid}(\gamma_{\eta}(t)), \quad (\text{A.1})$$

where $\gamma_{\eta}(t)$ is a *monotonic* neural network comprised of linear layers with weights η restricted to be positive. A monotonic function is a function defined on a subset of the real numbers which is either entirely non-increasing or entirely non-decreasing. As explained later, the noise schedule can be conveniently parameterized in terms of the signal-to-noise ratio. The signal-to-noise ratio (SNR) is defined as $\text{SNR}(t) = \alpha_t^2/\sigma_t^2$, and since \mathbf{z}_t grow noisier over time we have that: $\text{SNR}(t) < \text{SNR}(s)$ for any $t > s$.

For now, we provide some straightforward derivations of the expressions for α_t^2 and $\text{SNR}(t)$ as a function of $\gamma_{\eta}(t)$. Recall that in a variance-preserving diffusion process $\alpha_t^2 = 1 - \sigma_t^2$, therefore:

$$\alpha_t^2 = 1 - \sigma_t^2 \quad (\text{A.2})$$

$$= 1 - \text{sigmoid}(\gamma_{\eta}(t)) \quad (\text{A.3})$$

$$\implies \alpha_t^2 = \text{sigmoid}(-\gamma_{\eta}(t)), \quad (\text{A.4})$$

as for an input $x \in \mathbb{R}$ the following holds

$$1 - \text{sigmoid}(x) = 1 - \frac{1}{1 + e^{-x}} \quad (\text{A.5})$$

$$= \frac{1 + e^{-x}}{1 + e^{-x}} - \frac{1}{1 + e^{-x}} \quad (\text{A.6})$$

$$= \frac{e^{-x}}{1 + e^{-x}} \cdot \frac{e^x}{e^x} \quad (\text{A.7})$$

$$= \text{sigmoid}(-x). \quad (\text{A.8})$$

To derive $\text{SNR}(t)$ as a function of $\gamma_{\eta}(t)$, we simply substitute in the above equations and simplify:

$$\text{SNR}(t) = \frac{\alpha_t^2}{\sigma_t^2} = \frac{\text{sigmoid}(-\gamma_{\eta}(t))}{\text{sigmoid}(\gamma_{\eta}(t))} \quad (\text{by definition}) \quad (\text{A.9})$$

$$= \frac{(1 + e^{\gamma_{\eta}(t)})^{-1}}{(1 + e^{-\gamma_{\eta}(t)})^{-1}} \quad (\text{A.10})$$

$$= \frac{1 + e^{-\gamma_{\eta}(t)}}{1 + e^{\gamma_{\eta}(t)}} \quad (\text{A.11})$$

$$= \frac{\frac{e^{\gamma_{\eta}(t)}}{e^{\gamma_{\eta}(t)}} + \frac{1}{e^{\gamma_{\eta}(t)}}}{1 + e^{\gamma_{\eta}(t)}} \cdot \frac{e^{\gamma_{\eta}(t)}}{e^{\gamma_{\eta}(t)}} \quad (\text{A.12})$$

$$= \frac{e^{\gamma_{\eta}(t)} + 1}{e^{\gamma_{\eta}(t)}(1 + e^{\gamma_{\eta}(t)})} \quad (\text{A.13})$$

$$= \frac{1}{e^{\gamma_{\eta}(t)}}, \quad (\text{A.14})$$

which is equivalently expressed as $\text{SNR}(t) = \exp(-\gamma_{\eta}(t))$.

A.3 Numerically Stable Primitives

The closed-form expressions for the mean and variance of $p(\mathbf{z}_s \mid \mathbf{z}_t)$ can be further simplified to include more numerically stable functions like $\text{expm1}(\cdot) = \exp(\cdot) - 1$, which are available in standard numerical packages. The resulting simplified expressions – which we derive in detail next – enable more numerically stable implementations as highlighted by Kingma et al. (2021).

Recall from Section A.2 that the noise schedule parameters are given by: $\sigma_t^2 = \text{sigmoid}(\gamma_{\eta}(t))$, and $\alpha_t^2 = \text{sigmoid}(-\gamma_{\eta}(t))$, for any t . For brevity, let s and t be shorthand notation for $\gamma_{\eta}(s)$ and $\gamma_{\eta}(t)$ respectively. The posterior variance simplifies to:

$$\sigma_Q^2(s, t) = \frac{\sigma_{t|s}^2 \sigma_s^2}{\sigma_t^2} = \frac{\sigma_s^2 \left(\sigma_t^2 - \frac{\alpha_t^2}{\sigma_s^2} \sigma_s^2 \right)}{\sigma_t^2} \quad (\text{A.15})$$

$$= \frac{\frac{1}{1+e^{-s}} \cdot \left(\frac{1}{1+e^{-t}} - \frac{(1+e^t)^{-1}}{(1+e^s)^{-1}} \cdot \frac{1}{1+e^{-s}} \right)}{\frac{1}{1+e^{-t}}} \quad (\text{cancel denominator}) \quad (\text{A.16})$$

$$= (1 + e^{-t}) \cdot \frac{1}{1 + e^{-s}} \cdot \left(\frac{1}{1 + e^{-t}} - \frac{1 + e^s}{1 + e^t} \cdot \frac{1}{1 + e^{-s}} \right) \quad (\text{distribute } 1 + e^{-t}) \quad (\text{A.17})$$

$$= \frac{1}{1 + e^{-s}} \cdot \left(1 - \frac{1 + e^s}{1 + e^t} \cdot \frac{1 + e^{-t}}{1 + e^{-s}} \right) \quad (\text{A.18})$$

$$= \frac{1}{1 + e^{-s}} \cdot \left(1 - \frac{e^s (1 + e^{-s})}{1 + e^t} \cdot \frac{e^{-t} (1 + e^t)}{1 + e^{-s}} \right) \quad (\text{cancel common factors}) \quad (\text{A.19})$$

$$= \frac{1}{1 + e^{-s}} \cdot \left(1 - e^{s-t} \right) \quad (\text{A.20})$$

$$= \sigma_s^2 \cdot (-\text{expm1}(\gamma_{\theta}(s) - \gamma_{\theta}(t))) . \quad (\text{expm1}(\cdot) = \exp(\cdot) - 1) \quad (\text{A.21})$$

The posterior mean – under a noise-prediction model $\hat{\epsilon}_{\theta}(\mathbf{z}_t; t)$ – simplifies in a similar fashion to:

$$\mu_{\theta}(\mathbf{z}_t; s, t) = \frac{1}{\alpha_{t|s}} \mathbf{z}_t - \frac{\sigma_{t|s}^2}{\alpha_{t|s} \sigma_t} \hat{\epsilon}_{\theta}(\mathbf{z}_t; t) \quad (\text{A.22})$$

$$= \frac{\alpha_s}{\alpha_t} \left(\mathbf{z}_t - \frac{\sigma_{t|s}^2}{\sigma_t} \hat{\epsilon}_{\theta}(\mathbf{z}_t; t) \right) \quad (\text{A.23})$$

$$= \frac{\alpha_s}{\alpha_t} \left(\mathbf{z}_t - \frac{\sigma_t^2 - \frac{\alpha_t^2}{\alpha_s^2} \sigma_s^2}{\sigma_t} \hat{\epsilon}_{\theta}(\mathbf{z}_t; t) \right) \quad (\text{substituting } \sigma_{t|s}^2 = \sigma_t^2 - \alpha_{t|s}^2 \sigma_s^2) \quad (\text{A.24})$$

$$= \frac{\alpha_s}{\alpha_t} \left(\mathbf{z}_t - \frac{\frac{1}{1+e^{-t}} - \frac{1+e^s}{1+e^t} \cdot \frac{1}{1+e^{-s}}}{\sqrt{\frac{1}{1+e^{-t}}}} \hat{\epsilon}_{\theta}(\mathbf{z}_t; t) \right) \quad (\text{A.25})$$

$$= \frac{\alpha_s}{\alpha_t} \left(\mathbf{z}_t - (1 + e^{-t}) \cdot \sqrt{\frac{1}{1 + e^{-t}}} \right) \quad (\text{A.26})$$

$$\cdot \left(\frac{1}{1+e^{-t}} - \frac{1+e^s}{1+e^t} \cdot \frac{1}{1+e^{-s}} \right) \hat{\epsilon}_{\theta}(\mathbf{z}_t; t) \right) \quad (\text{A.27})$$

$$= \frac{\alpha_s}{\alpha_t} \left(\mathbf{z}_t - \sigma_t \left(1 - e^{s-t} \right) \hat{\epsilon}_{\theta}(\mathbf{z}_t; t) \right) \quad (\text{A.28})$$

$$= \frac{\alpha_s}{\alpha_t} \left(\mathbf{z}_t + \sigma_t \text{expm1}(\gamma_{\eta}(s) - \gamma_{\eta}(t)) \hat{\epsilon}_{\theta}(\mathbf{z}_t; t) \right), \quad (\text{A.29})$$

where Equation A.27 simplifies significantly via the same logical steps in Equations A.17-A.20 above.

A.3.1 Numerically Stable Loss Estimator

The estimator of the discrete-time diffusion loss can be made more numerically stable in practice by re-expressing the constant term inside the expectation using more numerically stable primitives. Specifically:

$$\frac{\text{SNR}(s)}{\text{SNR}(t)} - 1 = \frac{\alpha_s^2}{\sigma_s^2} \div \frac{\alpha_t^2}{\sigma_t^2} - 1 \quad (\text{A.30})$$

$$= \frac{\alpha_s^2 \sigma_t^2}{\alpha_t^2 \sigma_s^2} - 1 \quad (\text{A.31})$$

$$= \frac{\text{sigmoid}(-\gamma_{\eta}(s)) \cdot \text{sigmoid}(\gamma_{\eta}(t))}{\text{sigmoid}(-\gamma_{\eta}(t)) \cdot \text{sigmoid}(\gamma_{\eta}(s))} - 1, \quad (\text{A.32})$$

letting s and t denote $\gamma_{\eta}(s)$ and $\gamma_{\eta}(t)$ for brevity we have:

$$\frac{\frac{1}{1+e^s} \cdot \frac{1}{1+e^{-t}}}{\frac{1}{1+e^t} \cdot \frac{1}{1+e^{-s}}} - 1 = \frac{(1+e^t)(1+e^{-s})}{(1+e^s)(1+e^{-t})} - 1 \quad (\text{A.33})$$

$$= \frac{e^t (1+e^{-t}) e^{-s} (1+e^s)}{(1+e^s)(1+e^{-t})} - 1 \quad (\text{A.34})$$

$$= e^t e^{-s} - 1 \quad (\text{A.35})$$

$$= \text{expm1}(\gamma_{\eta}(t) - \gamma_{\eta}(s)). \quad (\text{A.36})$$

Substituting the above back into the (noise-prediction-based) diffusion loss estimator gives:

$$\mathcal{L}_T(\mathbf{x}) = \frac{T}{2} \mathbb{E}_{\epsilon \sim \mathcal{N}(0, \mathbf{I}), i \sim U\{1, T\}} \left[\quad (\text{A.37}) \right.$$

$$\expm1(\gamma_{\boldsymbol{\eta}}(t) - \gamma_{\boldsymbol{\eta}}(s)) \|\boldsymbol{\epsilon} - \hat{\boldsymbol{\epsilon}}_{\boldsymbol{\theta}}(\mathbf{z}_t; t)\|_2^2 \Big], \quad (\text{A.38})$$

which is the final form of the objective we wanted to show.

A.3.2 Dealing with Edge Effects

There is an edge effect at diffusion time $t = 0$, possibly causing numerical issues (Sohl-Dickstein et al., 2015; Song et al., 2021a), which we can avoid by setting the likelihood term to:

$$p(\mathbf{x} \mid \mathbf{z}_1) = \frac{q(\mathbf{z}_1 \mid \mathbf{x})p(\mathbf{x})}{p(\mathbf{z}_1)}, \quad (\text{A.39})$$

and removing it from the variational lower bound. In discrete-time, this looks like:

$$\text{VLB} = \mathbb{E}_{q(\mathbf{z}_{1:T}, \mathbf{x})} \left[\log \frac{p(\mathbf{x} \mid \mathbf{z}_1)}{q(\mathbf{z}_1 \mid \mathbf{x})} + \log p(\mathbf{z}_T) + \sum_{t=2}^T \log \frac{p(\mathbf{z}_{t-1} \mid \mathbf{z}_t)}{q(\mathbf{z}_t \mid \mathbf{z}_{t-1})} \right] \quad (\text{A.40})$$

$$= \mathbb{E}_{q(\mathbf{z}_1, \mathbf{x})} \left[\log \frac{q(\mathbf{z}_1 \mid \mathbf{x})p(\mathbf{x})}{q(\mathbf{z}_1 \mid \mathbf{x})p(\mathbf{z}_1)} \right] \quad (\text{A.41})$$

$$+ \mathbb{E}_{q(\mathbf{z}_{1:T}, \mathbf{x})} \left[\log p(\mathbf{z}_T) + \sum_{t=2}^T \log \frac{p(\mathbf{z}_{t-1} \mid \mathbf{z}_t)}{q(\mathbf{z}_t \mid \mathbf{z}_{t-1})} \right]. \quad (\text{A.42})$$

The left-hand side (LHS) term above cancels out as the $\text{SNR} \rightarrow \infty$ (i.e. $\alpha_1 \rightarrow 1$ and $\sigma_1 \rightarrow 0$) since the least noisy latent variable $\mathbf{z}_1 = \alpha_1 \mathbf{x} + \sigma_1 \boldsymbol{\epsilon}$ approaches \mathbf{x} , meaning $p(\mathbf{z}_1) \approx p(\mathbf{x})$. Note that p in $p(\mathbf{z}_1)$ and $p(\mathbf{x})$ above refers to the (tractable) prior distribution of choice.

For continuous-time diffusion where $T \rightarrow \infty$ and $t \in [0, 1]$, we have that learning a model $p(\mathbf{z}_0)$ is practically equivalent to learning a model $p(\mathbf{x})$ since \mathbf{z}_0 (the least noisy latent variable) is almost identical to \mathbf{x} in the limit given large enough $\log\text{SNR} = \log(\alpha_0^2/\sigma_0^2)$. However, if one chooses to learn the noise schedule rather than fixing it, the $p(\mathbf{x} \mid \mathbf{z}_0)$ term may need to be incorporated back into the VLB objective, representing a final discrete step from latent space to image space. This manifests as some variation of a decoding step in both VDMs (Kingma et al., 2021) and score-based diffusion models (Song et al., 2021a).

A.4 Equivalence of Diffusion Specifications

Kingma et al. (2021) elaborate on the equivalence of diffusion noise-schedule specifications using the following straightforward example. Firstly, the change of variables we used implies that σ_v is given by:

$$v = \frac{\alpha_v^2}{\sigma_v^2} \implies \sqrt{v} = \frac{\alpha_v}{\sigma_v} \implies \sigma_v = \frac{\alpha_v}{\sqrt{v}}, \quad (\text{A.43})$$

therefore, \mathbf{z}_v can be equivalently expressed as

$$\mathbf{z}_v = \alpha_v \mathbf{x} + \sigma_v \boldsymbol{\epsilon} = \alpha_v \mathbf{x} + \frac{\alpha_v}{\sqrt{v}} \boldsymbol{\epsilon} = \alpha_v \left(\mathbf{x} + \frac{\boldsymbol{\epsilon}}{\sqrt{v}} \right), \quad (\text{A.44})$$

which holds for any diffusion specification (forward process) by definition. Now, consider two distinct diffusion specifications denoted as $\{\alpha_v^A, \sigma_v^A, \tilde{\mathbf{x}}_\theta^A\}$ and $\{\alpha_v^B, \sigma_v^B, \tilde{\mathbf{x}}_\theta^B\}$. Due to Equation A.44, any two diffusion specifications produce equivalent latents, up to element-wise rescaling:

$$\mathbf{z}_v^A = \frac{\alpha_v^A}{\alpha_v^B} \mathbf{z}_v^B \quad (\text{A.45})$$

$$\alpha_v^A \left(\mathbf{x} + \frac{\boldsymbol{\epsilon}}{\sqrt{v}} \right) = \frac{\alpha_v^A}{\alpha_v^B} \alpha_v^B \left(\mathbf{x} + \frac{\boldsymbol{\epsilon}}{\sqrt{v}} \right). \quad (\text{A.46})$$

This implies that we can denoise from any latent \mathbf{z}_v^B using a model $\tilde{\mathbf{x}}_\theta^A$ trained under a different noise specification, by trivially rescaling the latent \mathbf{z}_v^B such that it'd be equivalent to denoising from \mathbf{z}_v^A :

$$\tilde{\mathbf{x}}_\theta^B \left(\mathbf{z}_v^B, v \right) \equiv \tilde{\mathbf{x}}_\theta^A \left(\frac{\alpha_v^A}{\alpha_v^B} \mathbf{z}_v^B, v \right). \quad (\text{A.47})$$

Furthermore, when two diffusion specifications have equal SNR_{\min} and SNR_{\max} , then the marginal distributions $p^A(\mathbf{x})$ and $p^B(\mathbf{x})$ defined by the two generative models are equal:

$$\tilde{\mathbf{x}}_\theta^B \left(\mathbf{z}_v^B, v \right) \equiv \tilde{\mathbf{x}}_\theta^A \left(\frac{\alpha_v^A}{\alpha_v^B} \mathbf{z}_v^B, v \right) \implies p^A(\mathbf{x}) = p^B(\mathbf{x}), \quad (\text{A.48})$$

and both specifications yield identical diffusion loss in continuous time: $\mathcal{L}_\infty^A(\mathbf{x}) = \mathcal{L}_\infty^B(\mathbf{x})$, due to Equation 4.80. Importantly, this does *not* mean

that training under different noise specifications will result in the same model. To be clear, the $\tilde{\mathbf{x}}_{\theta}^B$ model is fully determined by the $\tilde{\mathbf{x}}_{\theta}^A$ model and the rescaling operation α_v^A/α_v^B . Furthermore, this invariance to the noise schedule does not hold for the Monte Carlo estimator of the diffusion loss, as the noise schedule affects the *variance* of the estimator and therefore affects optimization efficiency.

References

Michael Samuel Albergo and Eric Vanden-Eijnden. Building normalizing flows with stochastic interpolants. In *The Eleventh International Conference on Learning Representations*, 2023. 42, 50, 51

Brian DO Anderson. Reverse-time diffusion equation models. *Stochastic Processes and their Applications*, 12(3):313–326, 1982. 17

Christopher M Bishop and Hugh Bishop. *Deep Learning: Foundations and Concepts*. Springer, 2023. 10, 72

David M Blei, Alp Kucukelbir, and Jon D McAuliffe. Variational inference: A review for statisticians. *Journal of the American statistical Association*, 112(518):859–877, 2017. 7

Yuri Burda, Roger Grosse, and Ruslan Salakhutdinov. Importance weighted autoencoders. *arXiv preprint arXiv:1509.00519*, 2015. 3, 10, 72

Rewon Child. Very deep vaes generalize autoregressive models and can outperform them on images. In *International Conference on Learning Representations*, 2020. 13

Jooyoung Choi, Jungbeom Lee, Chaehun Shin, Sungwon Kim, Hyunwoo Kim, and Sungroh Yoon. Perception prioritized training of diffusion models. In *Proceedings of the IEEE/CVF Conference on Computer Vision and Pattern Recognition*, pages 11472–11481, 2022. 69

Fabio De Sousa Ribeiro, Tian Xia, Miguel Monteiro, Nick Pawlowski, and Ben Glocker. High fidelity image counterfactuals with probabilistic causal models. In *Proceedings of the 40th International Conference on Machine Learning*, pages 7390–7425. PMLR, 2023. [13](#)

Prafulla Dhariwal and Alexander Nichol. Diffusion models beat gans on image synthesis. *Advances in neural information processing systems*, 34:8780–8794, 2021. [17](#)

Sander Dieleman, Laurent Sartran, Arman Roshannai, Nikolay Savinov, Yaroslav Ganin, Pierre H Richemond, Arnaud Doucet, Robin Strudel, Chris Dyer, Conor Durkan, et al. Continuous diffusion for categorical data. *arXiv preprint arXiv:2211.15089*, 2022. [64](#)

Yilun Du, Conor Durkan, Robin Strudel, Joshua B Tenenbaum, Sander Dieleman, Rob Fergus, Jascha Sohl-Dickstein, Arnaud Doucet, and Will Sussman Grathwohl. Reduce, reuse, recycle: Compositional generation with energy-based diffusion models and mcmc. In *International conference on machine learning*, pages 8489–8510. PMLR, 2023. [42](#), [48](#)

Tiankai Hang, Shuyang Gu, Chen Li, Jianmin Bao, Dong Chen, Han Hu, Xin Geng, and Baining Guo. Efficient diffusion training via min-smr weighting strategy. *arXiv preprint arXiv:2303.09556*, 2023. [69](#)

Martin Heusel, Hubert Ramsauer, Thomas Unterthiner, Bernhard Nessler, and Sepp Hochreiter. Gans trained by a two time-scale update rule converge to a local nash equilibrium. *Advances in neural information processing systems*, 30, 2017. [70](#)

Jonathan Ho, Ajay Jain, and Pieter Abbeel. Denoising diffusion probabilistic models. *Advances in neural information processing systems*, 33:6840–6851, 2020. [2](#), [17](#), [28](#), [35](#), [42](#), [45](#), [47](#), [57](#), [58](#), [70](#), [74](#)

Jonathan Ho, Chitwan Saharia, William Chan, David J Fleet, Mohammad Norouzi, and Tim Salimans. Cascaded diffusion models for high fidelity image generation. *The Journal of Machine Learning Research*, 23(1):2249–2281, 2022. [17](#)

Matthew D Hoffman and Matthew J Johnson. Elbo surgery: yet another way to carve up the variational evidence lower bound. In *Workshop in Advances in Approximate Bayesian Inference, NIPS*, volume 1, 2016. [14](#), [15](#), [20](#)

Matthew D Hoffman, David M Blei, Chong Wang, and John Paisley. Stochastic variational inference. *Journal of Machine Learning Research*, 2013. 7

Emiel Hoogeboom, Victor Garcia Satorras, Clément Vignac, and Max Welling. Equivariant diffusion for molecule generation in 3d. In *International conference on machine learning*, pages 8867–8887. PMLR, 2022. 17

Emiel Hoogeboom, Jonathan Heek, and Tim Salimans. simple diffusion: End-to-end diffusion for high resolution images. In *Proceedings of the 40th International Conference on Machine Learning*, volume 202 of *Proceedings of Machine Learning Research*, pages 13213–13232. PMLR, 2023. 70

Emiel Hoogeboom, Thomas Mensink, Jonathan Heek, Kay Lamerigts, Ruiqi Gao, and Tim Salimans. Simpler diffusion (sid2): 1.5 fid on imagenet512 with pixel-space diffusion. *arXiv preprint arXiv:2410.19324*, 2024. 70

Chin-Wei Huang, Jae Hyun Lim, and Aaron C Courville. A variational perspective on diffusion-based generative models and score matching. *Advances in Neural Information Processing Systems*, 34:22863–22876, 2021. 3, 17, 36

Aapo Hyvärinen and Peter Dayan. Estimation of non-normalized statistical models by score matching. *Journal of Machine Learning Research*, 6(4), 2005. 17

Aapo Hyvärinen, Ilyes Khemakhem, and Ricardo Monti. Identifiability of latent-variable and structural-equation models: from linear to nonlinear. *Annals of the Institute of Statistical Mathematics*, 76(1):1–33, 2024. 73

Michael I Jordan, Zoubin Ghahramani, Tommi S Jaakkola, and Lawrence K Saul. An introduction to variational methods for graphical models. *Machine learning*, 37:183–233, 1999. 6

Heewoo Jun, Rewon Child, Mark Chen, John Schulman, Aditya Ramesh, Alec Radford, and Ilya Sutskever. Distribution augmentation for generative modeling. In *International Conference on Machine Learning*, pages 5006–5019. PMLR, 2020. 69

Tero Karras, Miika Aittala, Timo Aila, and Samuli Laine. Elucidating the design space of diffusion-based generative models. *Advances in Neural Information Processing Systems*, 35:26565–26577, 2022. 20, 51, 59, 69, 75

Tero Karras, Miika Aittala, Jaakko Lehtinen, Janne Hellsten, Timo Aila, and Samuli Laine. Analyzing and improving the training dynamics of diffusion models. In *Proceedings of the IEEE/CVF Conference on Computer Vision and Pattern Recognition*, pages 24174–24184, 2024. 64

Diederik Kingma, Tim Salimans, Ben Poole, and Jonathan Ho. Variational diffusion models. *Advances in neural information processing systems*, 34: 21696–21707, 2021. 3, 17, 28, 31, 36, 37, 42, 55, 57, 83, 86, 87

Diederik P Kingma and Ruiqi Gao. Understanding the diffusion objective as a weighted integral of elbos. *arXiv preprint arXiv:2303.00848*, 2023. 3, 17, 43, 50, 57, 59, 61, 64, 66, 70, 73, 75

Diederik P Kingma and Max Welling. Auto-encoding variational bayes. *arXiv preprint arXiv:1312.6114*, 2013. 3, 5, 7, 34

Diederik P Kingma, Max Welling, et al. An introduction to variational autoencoders. *Foundations and Trends® in Machine Learning*, 12(4):307–392, 2019. 7

Durk P Kingma, Tim Salimans, Rafal Jozefowicz, Xi Chen, Ilya Sutskever, and Max Welling. Improved variational inference with inverse autoregressive flow. *Advances in neural information processing systems*, 29, 2016. 3, 11, 12, 14

Karsten Kreis, Ruiqi Gao, and Arash Vahdat. Tutorial on denoising diffusion-based generative modeling: Foundations and applications, 2022. Tutorial presented at CVPR 2022. 57

Yaron Lipman, Ricky T. Q. Chen, Heli Ben-Hamu, Maximilian Nickel, and Matthew Le. Flow matching for generative modeling. In *The Eleventh International Conference on Learning Representations*, 2023. 42, 50, 51

Xingchao Liu, Chengyue Gong, and qiang liu. Flow straight and fast: Learning to generate and transfer data with rectified flow. In *The Eleventh International Conference on Learning Representations*, 2023. 42, 50, 51

Calvin Luo. Understanding diffusion models: A unified perspective. *arXiv preprint arXiv:2208.11970*, 2022. 3, 10, 72

Lars Maaløe, Casper Kaae Sønderby, Søren Kaae Sønderby, and Ole Winther. Auxiliary deep generative models. In *International conference on machine learning*, pages 1445–1453. PMLR, 2016. 8

Lars Maaløe, Marco Fraccaro, Valentin Liévin, and Ole Winther. Biva: A very deep hierarchy of latent variables for generative modeling. *Advances in neural information processing systems*, 32, 2019. [13](#)

Alireza Makhzani, Jonathon Shlens, Navdeep Jaitly, Ian Goodfellow, and Brendan Frey. Adversarial autoencoders. *arXiv preprint arXiv:1511.05644*, 2015. [15](#)

Chenlin Meng, Jiaming Song, Yang Song, Shengjia Zhao, and Stefano Ermon. Improved autoregressive modeling with distribution smoothing. In *International Conference on Learning Representations*, 2020. [69](#)

Miguel Monteiro, Fabio De Sousa Ribeiro, Nick Pawlowski, Daniel C Castro, and Ben Glocker. Measuring axiomatic soundness of counterfactual image models. In *The Eleventh International Conference on Learning Representations*, 2022. [13](#)

Markus Mueller, Kathrin Gruber, and Dennis Fok. Continuous diffusion for mixed-type tabular data. *arXiv preprint arXiv:2312.10431*, 2023. [64](#)

Alexander Quinn Nichol and Prafulla Dhariwal. Improved denoising diffusion probabilistic models. In *International Conference on Machine Learning*, pages 8162–8171. PMLR, 2021. [17](#), [20](#), [57](#), [69](#), [75](#)

Alexander Quinn Nichol, Prafulla Dhariwal, Aditya Ramesh, Pranav Shyam, Pamela Mishkin, Bob McGrew, Ilya Sutskever, and Mark Chen. Glide: Towards photorealistic image generation and editing with text-guided diffusion models. In *International Conference on Machine Learning*, pages 16784–16804. PMLR, 2022. [17](#)

Rajesh Ranganath, Dustin Tran, and David Blei. Hierarchical variational models. In *International conference on machine learning*, pages 324–333. PMLR, 2016. [8](#)

Antti Rasmus, Mathias Berglund, Mikko Honkala, Harri Valpola, and Tapani Raiko. Semi-supervised learning with ladder networks. *Advances in neural information processing systems*, 28, 2015. [11](#)

Danilo J. Rezende. Short notes on divergence measures. <https://danilorezende.com/wp-content/uploads/2018/07/divergences.pdf>, 2018. Accessed: 03-09-2024. [7](#)

Danilo Jimenez Rezende and Fabio Viola. Taming vaes. *arXiv preprint arXiv:1810.00597*, 2018. 15

Danilo Jimenez Rezende, Shakir Mohamed, and Daan Wierstra. Stochastic backpropagation and approximate inference in deep generative models. In *International conference on machine learning*, pages 1278–1286. PMLR, 2014. 3, 7, 34

Severi Rissanen, Markus Heinonen, and Arno Solin. Generative modelling with inverse heat dissipation. In *The Eleventh International Conference on Learning Representations*, 2023. 57

Robin Rombach, Andreas Blattmann, Dominik Lorenz, Patrick Esser, and Björn Ommer. High-resolution image synthesis with latent diffusion models. In *Proceedings of the IEEE/CVF conference on computer vision and pattern recognition*, pages 10684–10695, 2022. 17

Amirmojtaba Sabour, Sanja Fidler, and Karsten Kreis. Align your steps: Optimizing sampling schedules in diffusion models. *arXiv preprint arXiv:2404.14507*, 2024. 64

Chitwan Saharia, William Chan, Saurabh Saxena, Lala Li, Jay Whang, Emily L Denton, Kamyar Ghasemipour, Raphael Gontijo Lopes, Burcu Karagol Ayan, Tim Salimans, et al. Photorealistic text-to-image diffusion models with deep language understanding. *Advances in Neural Information Processing Systems*, 35:36479–36494, 2022. 17

Tim Salimans and Jonathan Ho. Should EBMs model the energy or the score? In *Energy Based Models Workshop - ICLR 2021*, 2021. 42, 48

Tim Salimans and Jonathan Ho. Progressive distillation for fast sampling of diffusion models. In *International Conference on Learning Representations*, 2022. 42, 48, 49, 51, 52

Tim Salimans, Diederik Kingma, and Max Welling. Markov chain monte carlo and variational inference: Bridging the gap. In *International conference on machine learning*, pages 1218–1226. PMLR, 2015. 3, 8

Tim Salimans, Ian Goodfellow, Wojciech Zaremba, Vicki Cheung, Alec Radford, and Xi Chen. Improved techniques for training gans. *Advances in neural information processing systems*, 29, 2016. 70

Javier E Santos and Yen Ting Lin. Using ornstein-uhlenbeck process to understand denoising diffusion probabilistic model and its noise schedules. *arXiv preprint arXiv:2311.17673*, 2023. 64

Rui Shu and Stefano Ermon. Bit prioritization in variational autoencoders via progressive coding. In *International Conference on Machine Learning*, pages 20141–20155. PMLR, 2022. 13

Jascha Sohl-Dickstein, Eric Weiss, Niru Maheswaranathan, and Surya Ganguli. Deep unsupervised learning using nonequilibrium thermodynamics. In *International conference on machine learning*, pages 2256–2265. PMLR, 2015. 2, 3, 10, 16, 28, 42, 72, 86

Casper Kaae Sønderby, Tapani Raiko, Lars Maaløe, Søren Kaae Sønderby, and Ole Winther. Ladder variational autoencoders. *Advances in neural information processing systems*, 29, 2016. 3, 10, 11, 12, 71

Yang Song and Stefano Ermon. Generative modeling by estimating gradients of the data distribution. *Advances in neural information processing systems*, 32, 2019. 17, 47, 57

Yang Song and Stefano Ermon. Improved techniques for training score-based generative models. *Advances in neural information processing systems*, 33: 12438–12448, 2020. 57

Yang Song and Diederik P Kingma. How to train your energy-based models. *arXiv preprint arXiv:2101.03288*, 2021. 48

Yang Song, Conor Durkan, Iain Murray, and Stefano Ermon. Maximum likelihood training of score-based diffusion models. *Advances in Neural Information Processing Systems*, 34:1415–1428, 2021a. 3, 42, 64, 86

Yang Song, Jascha Sohl-Dickstein, Diederik P Kingma, Abhishek Kumar, Stefano Ermon, and Ben Poole. Score-based generative modeling through stochastic differential equations. In *International Conference on Learning Representations*, 2021b. 3, 17, 21, 36, 42, 45, 47, 76

Jakub Tomczak and Max Welling. Vae with a vampprior. In *International Conference on Artificial Intelligence and Statistics*, pages 1214–1223. PMLR, 2018. 14

Arash Vahdat and Jan Kautz. Nvae: A deep hierarchical variational autoencoder. *Advances in Neural Information Processing Systems*, 33:19667–19679, 2020. [13](#)

Arash Vahdat, Karsten Kreis, and Jan Kautz. Score-based generative modeling in latent space. *Advances in Neural Information Processing Systems*, 34: 11287–11302, 2021. [3](#), [17](#), [36](#), [64](#)

Harri Valpola. From neural pca to deep unsupervised learning. In *Advances in independent component analysis and learning machines*, pages 143–171. Elsevier, 2015. [3](#), [11](#), [71](#), [75](#), [76](#)

Pascal Vincent. A connection between score matching and denoising autoencoders. *Neural computation*, 23(7):1661–1674, 2011. [17](#)

Pascal Vincent, Hugo Larochelle, Yoshua Bengio, and Pierre-Antoine Manzagol. Extracting and composing robust features with denoising autoencoders. In *Proceedings of the 25th international conference on Machine learning*, pages 1096–1103, 2008. [76](#)

Larry Wasserman. *All of statistics: a concise course in statistical inference*, volume 26. Springer, 2004. [63](#)